REGULATION OF SPONTANEOUS GLUTAMATE RELEASE BY EXTRACELLULAR CALCIUM

by

Nicholas Patrick Vyleta

A DISSERTATION

Presented to the Neuroscience Graduate Program and the Oregon Health and Science University School of Medicine

In partial fulfillment of the requirements for the degree of

Doctor of Philosophy

October 26, 2010

School of Medicine
Oregon Health & Science University

CERTIFICATE OF APPROVAL

This is to certify that the Ph.D. dissertation of
NICHOLAS VYLETA
has been approved on October 26, 2010

Advisor, Stephen Smith, PhD

Member and Chair, Gary Westbrook, PhD

Member, Michael Andresen, PhD

Member, Henrique vonGersdroff, PhD

Member, David Jacoby, MD

TABLE OF CONTENTS

LIST OF FIGURES

CHAPTER 1

CHAPTER 2

CHAPTER 3

ACKNOWLEDGEMENTS

I would first like to thank my mentor Dr. Stephen Smith for his countless hours of one-on-one interaction with me. He has taught me more than I can write here, either directly by explaining concepts at length, or indirectly by requiring me to look and think deeper myself. I have certainly not always been an easy graduate student, but Dr. Smith's ability to be persistent when I was not following, push me when I was being lazy, or leave me alone when I was on a roll and wanted freedom is in large part responsible for my success as a developing scientist.

I would like to also thank my thesis advisory committee members: Dr. Gary Westbrook, Dr. Henrique von Gersdorff, and Dr. Michael Andresen for their helpful advice and support throughout the process of my degree, from detailed critique of my experiments in our meetings, to private conversations about scientific philosophy. All of this help has been tremendously appreciated and certainly crucially beneficial to my development as a scientist. I would also like to thank Dr. David Jacoby who will serve on my committee for my thesis defense, and who has provided me with helpful comments on multiple occasions through our weekly research seminars in the Division of Pulmonary and Critical Care Medicine.

Thank you to my wife Meghan. She is truly my teammate in all aspects of life, and her support has undoubtedly produced in me not only a better scientist, but a better person.

ABSTRACT

Synaptic vesicles fuse with nerve terminal plasma membrane not only in response to an action potential, but also spontaneously. Such spontaneous events contribute to neuronal baseline noise, maintain synaptic strength, and can induce and modulate action potential firing in inhibitory neurons. The mechanisms controlling this mode of synaptic transmission remain largely unknown. *The overall objective of these studies was to determine mechanisms controlling spontaneous vesicle fusion.* The rate of spontaneous exocytosis is enhanced by extracellular calcium, however the mechanisms are not understood. Our data indicate that extracellular calcium does not catalyze spontaneous vesicle fusion by influx through voltage-gated calcium channels and increases in the concentration of intracellular calcium ($[Ca^{2+}]_i$). These data suggest that extracellular calcium catalyzes spontaneous neurotransmitter release by a distinct mechanism from that of action potential-evoked release. We hypothesized that a G-protein coupled receptor (GPCR) that is activated by extracellular divalent cations, the calcium-sensing receptor (CaSR), could transduce changes in synaptic cleft $[Ca^{2+}]$ to changes in spontaneous exocytosis. Using pharmacological and genetic approaches, we find that CaSR plays a role in controlling spontaneous glutamate release from neocortical nerve terminals.

We also examined how intracellular signaling controls synaptic vesicle fusion. CaSR couples to the G_q family of GPCRs in both expression systems and native tissue. G_q activates phospholipase C (PLC) and the metabolism of

phosphatidylinositol-(4,5)-bisphosphate (PIP_2), resulting in the production of diacylglycerol (DAG) and inositol triphosphate. DAG analogues are potent modulators of both spontaneous and action potential-evoked glutamate release. We hypothesized that PLC activation increases neurotransmitter release. In our experiments, PLC inhibition decreased spontaneous glutamate release and the size of the readily releasable pool of synaptic vesicles, suggesting that PLC activity may maintain synaptic vesicle exocytosis.

We also hypothesized that extracellular calcium could stimulate spontaneous glutamate release by inducing calcium-induced calcium release (CICR) from ryanodine receptors (RyRs) on intracellular calcium stores. CICR has been reported to produce presynaptic calcium transients and spontaneous release in hippocampal boutons, and large-amplitude miniature inhibitory postsynaptic currents in cerebellar neurons. To determine the role of RyR-mediated Ca^{2+} release in spontaneous glutamate release in neocortical neurons, we measured miniature excitatory postsynaptic currents (mEPSCs) upon application of caffeine. We confirmed that caffeine increases spontaneous release in neocortical neurons, but observed that caffeine also produced a robust decrease in mEPSC amplitude. Caffeine inhibited postsynaptic non-NMDA type glutamate receptors, thus explaining the decrease in mEPSC amplitude. However, CICR did not appear to account for the dependence of spontaneous release rate on $[Ca^{2+}]_o$, because Ca^{2+} enhancement of spontaneous release was insensitive to buffering of intracellular Ca^{2+} by BAPTA.

INTRODUCTION

Spontaneous vesicle fusion is an important mode of neurotransmission

Spontaneous release was originally described at the frog neuromuscular junction (Fatt and Katz, 1950), with events identified as small, subthreshold depolarizations in the postsynaptic muscle cell membrane. They had shapes and time courses similar to full end-plate potentials evoked by electrical stimulation of the presynaptic motor nerve, but were ~ 100 times smaller in amplitude (1 mV compared to over 100 mV) and did not propagate beyond the immediate region of the synapse (Fatt and Katz, 1952). Although stimulus evoked end-plate potentials easily spread to more distal regions of the muscle membrane, spontaneous events could only be recorded directly at the end plate. It was difficult then to envision how such small, seemingly random events could be physiologically relevant.

It is now understood that spontaneous release in the central nervous system can perform important physiological functions. Mostly, physiological consequences of spontaneous events at the postsynaptic cell are becoming increasingly understood. The mechanisms regulating spontaneous release presynaptically, however, remain relatively unknown and will be important to elucidate to more fully understand synaptic transmission between central neurons.

During classical action potential-evoked neurotransmission, an action potential travels down the presynaptic axon and invades the nerve terminal. The

resulting depolarization of the nerve terminal plasma membrane causes voltage-activated calcium channels (VACCs) to open, allowing calcium ions to enter the terminal from the extracellular space (Llinas et al., 1976). This produces a transient increase in the concentration of intracellular Ca^{2+} ($[Ca^{2+}]_i$) nearby those open VACCs (Augustine et al., 1991). Calcium can then bind to a calcium sensor for exocytosis, and this can result in the fusion of synaptic vesicle membrane with nerve terminal plasma membrane and release of vesicular neurotransmitter into the synaptic cleft (for review see (Neher and Sakaba, 2008)). Spontaneous release occurs when a single synaptic vesicle fuses with the presynaptic membrane in the absence of an action potential, releasing a single packet or "quantum" of neurotransmitter onto a postsynaptic cell. The ion channel current activated by these neurotransmitter molecules can be recorded in the postsynaptic cell as a miniature synaptic event. The intracellular mechanisms controlling spontaneous vesicle fusion continue to be intensely studied and even controversial. For example, fundamental questions that remain unanswered include: what vesicle fusion machinery catalyzes spontaneous fusion? What is the dependence of spontaneous fusion on intracellular calcium? What is the source of calcium evoking spontaneous fusion? And, finally, are these properties of spontaneous release the same as for action-potential mediated release, or are there important mechanistic differences between the two release modes?

Excitatory forms of spontaneous release events, termed miniature excitatory postsynaptic currents (mEPSCs), were originally dismissed as probably unimportant because of their small size relative to action potential-

induced excitatory postsynaptic currents (EPSCs). Furthermore, spontaneous fusion occurs at a low rate – we estimate that in cultured neocortical neurons at room temperature vesicles fuse spontaneously once every ~ 100 seconds per nerve terminal. However, postsynaptic neurons receive several hundred presynaptic contacts, resulting in approximately three spontaneous events per second acting on the postsynaptic neuron. It is thus plausible that these events have physiological significance at the postsynaptic neuron. Evidence in support of this conclusion has been provided by several important investigations (McKinney et al., 1999; Carter and Regehr, 2002; Sutton et al., 2004).

It is now understood that in the central nervous system, mEPSCs can be similar in size to action potential-induced EPSCs (Carter and Regehr, 2002). Furthermore, two cortical neurons may be connected by only a single synapse with one release site (Stevens and Wang, 1995). With single release site connectivity, a single spontaneous release event is predicted to have equal effect on the postsynaptic neuron as synaptic release activated by a presynaptic action potential. The full physiological significance of spontaneous release has been difficult to elucidate due to the inability to selectively block spontaneous neurotransmitter release while leaving action potential-induced transmission intact. Several reports, however, have provided compelling evidence for the significance of spontaneous transmitter release to neuronal activity.

Single quantal events are potent modulators of firing frequency of cerebellar inhibitory interneurons, and can even elicit action potentials in these cells (Carter and Regehr, 2002). This result supports the idea that spontaneous

release of neurotransmitter is an important effector of the activity of small neurons with high input resistance. Importantly, neurons with high input resistance have long membrane time constants and thus an increased window over which temporal summation of events can occur. The authors showed that small numbers of coincident excitatory quantal inputs reliably produced action potentials in these cells. The authors also showed that the average amplitude of mEPSCs in these cells is quite large, at approximately 100 pA. This emphasizes that spontaneous events and action potential induced events can be similar in size. Because spontaneous release can modulate action potential activity, a mechanism by which spontaneous release frequency is modulated could ultimately affect the firing patterns of entire networks of neurons. This idea is further supported by the demonstration that activation of nicotinic acetylcholine receptors on cortical nerve terminals and subsequent stimulation of intracellular-calcium release-mediated spontaneous exocytosis can stimulate action potential firing in postsynaptic CA3 pyramidal cells in the hippocampus (Sharma and Vijayaraghavan, 2003).

Spontaneous neurotransmitter release also can impact network activity by regulating strength of individual synapses. Synaptic strength increases profoundly following only a few hours of synaptic blockade (O'Brien et al., 1998; Thiagarajan et al., 2005), but spontaneous release alone is sufficient to maintain synaptic strength (Sutton et al., 2004). Thus spontaneous release has an important homeostatic role preventing synaptic potentiation at times of reduced action potential evoked activity. This result highlights both the physiological

significance of spontaneous transmission and a differential role of spontaneous release from action potential evoked release of glutamate. Spontaneous release has attracted more attention with recent reports that synaptic vesicles that fuse spontaneously are distinct from those that fuse in response to depolarization and calcium influx ((Sara et al., 2005; Fredj and Burrone, 2009) but see (Groemer and Klingauf, 2007)).

Taken together, these results demonstrate that spontaneous release of glutamate is physiologically important. Particularly, the postsynaptic consequences of spontaneous transmission are now well appreciated. Elucidating the mechanisms that evoke and regulate spontaneous neurotransmitter release is a crucial next step towards understanding this mode of neurotransmission and is the focus of this thesis work.

The dependence of spontaneous exocytosis on $[Ca^{2+}]_o$

A key determinant of spontaneous release rate is the concentration of extracellular calcium ($[Ca^{2+}]_o$) (Yamasaki et al., 2006; Xu et al., 2009b; Groffen et al., 2010). Extracellular Ca^{2+} stimulates spontaneous release of glutamate; however, the mechanisms coupling Ca^{2+} in the synaptic cleft to spontaneous exocytosis remain unknown. Extracellular Ca^{2+} has been used to provide information about the “calcium dependence” of spontaneous release, with the assumption made that changes in $[Ca^{2+}]_o$ produce changes in $[Ca^{2+}]_i$ and therefore spontaneous vesicle fusion rate (Xu et al., 2009a). It has been assumed that mechanisms of spontaneous exocytosis are similar or identical to

those responsible for action potential-mediated exocytosis. During action potential-mediated exocytosis, Ca^{2+} enters the nerve terminal through VACCs, and binds to a member of the synaptotagmin family of proteins, triggering soluble N-ethylmaleimide-sensitive-factor attachment protein receptor (SNARE) protein-mediated vesicle fusion (Geppert et al., 1994; Chicka et al., 2008). Because all voltage-activated ion channels have some open probability at the resting membrane potential, stochastic openings of VACCs could occur. In theory, if one or more calcium channel opened at rest and allowed Ca^{2+} influx, a synaptic vesicle could undergo exocytosis in the absence of presynaptic action potential. This idea is supported by the demonstration at multiple types of synapses that exocytosis can result from the opening of a small number of VACCs (Augustine et al., 1991; Bucurenciu et al., 2010). Importantly, the likelihood of stochastic channel opening resulting in vesicle exocytosis would be greater with increased driving force for Ca^{2+} influx after elevation of $[Ca^{2+}]_o$. The involvement of VACC-mediated Ca^{2+} influx in the spontaneous release of glutamate from central neurons has yet to be thoroughly evaluated.

The relationship between action potential-induced postsynaptic potential size and $[Ca^{2+}]_o$ has a slope of approximately four on a log-log plot, indicating a binding of ≥ four Ca^{2+} to catalyze the fusion of each vesicle (Dodge and Rahamimoff, 1967; Rozov et al., 2001). An intriguing observation is that the relationship between spontaneous exocytosis rate and $[Ca^{2+}]_o$ during action potential blockade is less steep (Xu et al., 2009b; Groffen et al., 2010). Additionally, it was recently demonstrated that spontaneous release utilizes a

distinct, relatively high-affinity intracellular calcium sensor for triggering exocytosis (Groffen et al., 2010). These data suggest that extracellular Ca^{2+} may promote the spontaneous fusion of vesicles by a pathway distinct from that of action potential-induced vesicle fusion.

$[Ca^{2+}]_o$ changes with neuronal activity

The stimulation of spontaneous glutamate release by extracellular Ca^{2+} could have important physiological significance, as the concentration of Ca^{2+} in the synaptic cleft is predicted to vary with neuronal activity. The thin disk-like geometry of the synaptic cleft with a high surface-area to volume ratio could support significant removal of extracellular Ca^{2+} if Ca^{2+} enters pre- and postsynaptic cells during electrical activity (Smith, 1992). Furthermore, diffusion is slowed up to five-fold in the extracellular space compared with free solution (Kullmann et al., 1999). In support of these predictions, $[Ca^{2+}]_o$ measured at the surface of the brain with Ca^{2+}-selective electrodes decreased by 28% with normal electrical activity and up to 90% following focal brain trauma (Nilsson et al., 1996). These changes persisted for tens of seconds. Importantly, if the driving force for Ca^{2+} depletion at the surface of the brain is depletion of Ca^{2+} from the synaptic cleft, then decreases in $[Ca^{2+}]_o$ at the synapse must be larger than decreases measured at the brain's surface (due to relatively smaller volume of synaptic cleft). Simultaneous pre and postsynaptic electrical recordings revealed a decrease in Ca^{2+} or Ba^{2+} currents upon depolarization of either the pre or postsynaptic cell, consistent with depletion of cleft [divalent] by approximately

one-third (Borst and Sakmann, 1999). These findings support the prediction that $[Ca^{2+}]_o$ varies as a function of neuronal activity. Because spontaneous neurotransmitter release has physiological function and is dependent on $[Ca^{2+}]_o$, changes in $[Ca^{2+}]_o$ could have important implications on synapse function. It is thus desirable to understand the mechanisms that transduce changes in synaptic cleft $[Ca^{2+}]$ to changes in the rate of spontaneous exocytosis.

G-protein coupled receptors and spontaneous release

The activity of several G-protein coupled receptors (GPCRs) has been shown to be sensitive to $[Ca^{2+}]_o$. Among these are the calcium-sensing receptor (CaSR) and members of the metabotropic glutamate receptor (mGluR) family. CaSR is activated by extracellular Ca^{2+}. In the parathyroid, CaSR has a vital role in the regulation of serum $[Ca^{2+}]$ (Brown et al., 1993). CaSR has also been localized to nerve terminals in the brain (Ruat et al., 1995), and has been proposed to impact synaptic transmission by modulating a nonselective cation channel in response to changes in $[Ca^{2+}]_o$ (Smith et al., 2004). Synaptic transmission between cortical neurons was inhibited by the CaSR agonist spermidine, and excitatory post-synaptic currents (EPSCs) in CaSR loss-of-function mutant neurons were larger than in WT controls (Phillips et al., 2008). CaSR has also been reported to be important in neuronal development. CaSR activation increased neurite outgrowth and synapse formation in developing sympathetic neurons (Vizard et al., 2008). These data support the notion that CaSR is active in neurons and could transduce changes in synaptic cleft $[Ca^{2+}]$ to changes in nerve terminal function.

Physiological levels of extracellular Ca^{2+} activated mGluR signaling in central neurons, and augmented the sensitivity of those receptors to glutamate (Tabata and Kano, 2004). Interestingly, a type-I mGluR agonist increased mEPSC frequency in neocortical neurons (Simkus and Stricker, 2002). In nerve terminals both CaSR and mGluR activity could have the properties of both baseline activation and the ability to respond to physiological stimuli. CaSR is activated by physiological $[Ca^{2+}]_o$ (1.1 mM), and can respond to changes in $[Ca^{2+}]_o$ consistent with those induced by neuronal activity (Pi et al., 2005). In addition to being sensitive to physiological $[Ca^{2+}]_o$, mGluRs serve autoreceptor functions in nerve terminals by binding to released glutamate (Billups et al., 2005). We thus predicted that activation of presynaptic GPCR signaling by extracellular Ca^{2+} could modulate spontaneous exocytosis rate. In this thesis I tested the hypothesis that CaSR activation enhances spontaneous glutamate release.

Phospholipase C, PIP_2, and diacylglycerol and synaptic vesicle exocytosis

Evidence suggests that activation of nerve terminal GPCRs can enhance the spontaneous fusion of glutamate-filled synaptic vesicles ((Simkus and Stricker, 2002), Chapter 1 of this thesis). An important next question is: what possible downstream signaling mechanisms couple plasma-membrane GPCR activation to exocytosis? One candidate signaling pathway is the activation of phospholipase-C (PLC) by the G_q family of G-proteins and production of inositol-1,4,5-triphosphate (IP_3) and diacylglycerol (DAG) upon hydrolysis of phosphatidylinositol-(4,5)-bisphosphate (PIP_2) (for review see (Rhee, 2001)).

DAG is a potent modulator of synaptic vesicle fusion. Exogenously applied DAG analogues increase the rate of spontaneous exocytosis (Weirda et al., 2007; Lou et al., 2008) and the size of the readily releasable pool (RRP) of vesicles in central neurons (Stevens and Sullivan, 1998). DAG analogues including phorbol esters bind to proteins containing a C1-domain including protein kinase C (PKC) and Munc13s, a family of presynaptic vesicle priming proteins. Phorbol ester-induced enhancement of spontaneous exocytosis was sensitive to PKC inhibition at the Calyx of Held (Lou et al., 2008). PKC phosphorylation of Munc18-1, a vesicle fusion protein, was necessary for phorbol ester-induced potentiation of spontaneous fusion in hippocampal neurons (Weirda et al., 2007). In addition to PKC activation, there is evidence that DAG acts directly on Munc13-1 to increase exocytosis rate. Loss-of-function mutation in Munc13-1 renders neurons less sensitive to potentiation by phorbol esters than control neurons, indicating a direct role for Munc13-1 in DAG-induced potentiation of synaptic transmission (Rhee et al., 2002; Lou et al., 2008). Thus, DAG analogues act through both PKC and Munc13-1 activation to potentiate synaptic transmission. Importantly, DAG analogues increased the sensitivity of vesicle fusion to basal $[Ca^{2+}]_i$ (Lou et al., 2005), demonstrating a powerful effect of DAG on the nerve terminal vesicle fusion machinery.

PLC catalyzes the hydrolysis of PIP_2 to IP_3 and DAG. PLC is activated by GPCRs which couple to the G_q family of G-proteins. Our data supports the conclusion that CaSR activation stimulates spontaneous release. It is currently unknown what G-proteins CaSR couples to in nerve terminals in the brain.

However, in parathyroid cells CaSR activates PLC through G_q (Brown and MacLeod, 2001). Based on this evidence we hypothesized that CaSR activation increases PLC activity, and that PLC transduces changes in $[Ca^{2+}]_o$ in the synaptic cleft to changes in vesicle fusion and neurotransmitter release.

PIP_2 has recently been identified as a key molecule involved in the endocytosis of synaptic membrane after vesicle exocytosis, with PIP_2 hydrolysis being necessary for vesicle scission from the plasma membrane (Liu et al., 2009). Because endocytosis and exocytosis are functionally coupled and successful endocytosis is necessary for exocytosis (Hosoi et al., 2009), activation of CaSR and PLC-mediated PIP_2 hydrolysis may help maintain a pool of recycling synaptic vesicles. PIP_2 also helps localize synaptotagmin, the Ca^{2+} sensor for action potential-evoked exocytosis, to presynaptic release sites and increases the rate of Ca^{2+}/synaptotagmin-catalyzed synaptic vesicle fusion (Bai et al., 2004). PIP_2 also enhanced the ability of Doc2b, the proposed intracellular Ca^{2+} sensor for spontaneous exocytosis, to catalyze vesicle fusion (Groffen et al., 2010). Thus, PLC activity could have important affects on synaptic transmission independently of DAG, by directly controlling PIP_2 levels in the nerve terminal plasma membrane.

In this thesis I describe investigations of the mechanisms coupling extracellular Ca^{2+} to spontaneous glutamate release in cultured neocortical neurons. My results indicate that extracellular Ca^{2+} couples to spontaneous release differently than it does to action potential-evoked release. I provide evidence that activation

of CaSR stimulates spontaneous glutamate release. I also investigated which downstream signaling pathways could be activated by CaSR and other presynaptic GPCRs and lead to spontaneous vesicle fusion. I show that inhibition of PLC reduces spontaneous release in some neurons, and the size of the readily-releasable pool of synaptic vesicles in all neurons tested. Finally, I show that caffeine increases spontaneous glutamate release, consistent with intracellular calcium release promoting spontaneous vesicle fusion, but that caffeine also inhibited mEPSC amplitude by AMPA receptor blockade.

CHAPTER 1

Extracellular calcium stimulates spontaneous glutamate release independent of voltage-activated calcium channels or intracellular calcium rises, and involves activation of calcium-sensing receptor

CHAPTER 1

Extracellular calcium stimulates spontaneous glutamate release independent of voltage-activated calcium channels or intracellular calcium rises, and involves activation of calcium-sensing receptor

Nicholas P. Vyleta and Stephen M. Smith.

Division of Pulmonary & Critical Care Medicine, Oregon Health & Science University, Portland, OR 97239.

Thank you to Dr. Xiaohua Wang for genotyping of CaSR mutant mice. NPV performed all experiments and analyses. NPV wrote the manuscript with revisions by SMS.

ABSTRACT

Spontaneous release of glutamate is important for maintaining synaptic strength and neuronal firing in the brain. Mechanisms regulating spontaneous exocytosis of synaptic vesicles remain poorly understood. Extracellular calcium is a pivotal determinant of action potential-evoked vesicle fusion via entry through voltage-activated calcium channels (VACCs). Extracellular calcium also enhances spontaneous release; however the mechanisms remain relatively unknown. Here we report that external calcium triggers spontaneous glutamate release in neocortical neurons with lower cooperativity than expected for calcium influx-dependent vesicle fusion. Blockade of VACCs had no effect on spontaneous release rate or its dependence on extracellular calcium. Furthermore, the enhancement of spontaneous release by extracellular calcium was insensitive to chelation of intracellular calcium by BAPTA-AM. Blockade of sodium/calcium exchange increased spontaneous release rate, but did not prevent further enhancement by increased extracellular calcium. We tested whether activation of the calcium-sensing receptor (CaSR), a G-protein coupled receptor present in cortical nerve terminals, stimulated spontaneous glutamate release. CaSR activation by specific agonists increased spontaneous glutamate release and the dependence of spontaneous release on extracellular calcium was different in CaSR mutant neurons. These results indicate that extracellular calcium does not enhance spontaneous glutamate release by calcium influx but can promote exocytosis by activation of CaSR.

INTRODUCTION

Neurotransmitter release from a single vesicle activates a small postsynaptic voltage change and comprises the elementary unit of synaptic communication (Fatt and Katz, 1950; Del Castillo and Katz, 1954). Action potentials evoke vesicle fusion by triggering calcium entry through presynaptic VACCs. However, exocytosis may also occur spontaneously in the absence of an action potential (Elmqvist and Feldman, 1965a; Llinas et al., 1976). Mechanisms controlling action potential-evoked and spontaneous exocytosis have been considered equal, with the intracellular [Ca^{2+}] ($[Ca^{2+}]_i$) determining the rate of vesicle release (Del Castillo and Katz, 1954; Lou et al., 2005). However, evidence suggests that two mechanistically distinct forms of release may exist. At central synapses, evoked and spontaneous release have been distinguished by differences in vesicle pools used, intracellular Ca^{2+} sensors for exocytosis, sensitivity to phorbol esters, the spatial separation of the postsynaptic receptors that they target, and by the mechanism by which endocytosis occurs (Sara et al., 2005; Virmani et al., 2005; Atasoy et al., 2008; Fredj and Burrone, 2009; Chung et al., 2010; Groffen et al., 2010). The central role of calcium as a trigger for exocytosis and the mounting number of differences between evoked and spontaneous release raised the question: are both forms of release regulated similarly by external calcium?

Evoked and spontaneous vesicle fusion are both sensitive to changes in extracellular [Ca^{2+}] ($[Ca^{2+}]_o$) (Elmqvist and Feldman, 1965b; Katz and Miledi,

1965). Evoked release is steeply dependent on $[Ca^{2+}]_o$ at many synapses (Dodge and Rahamimoff, 1967; Augustine and Charlton, 1986; Borst and Sakmann, 1996; Reid et al., 1998; Rozov et al., 2001; Ikeda et al., 2008) and is triggered by Ca^{2+} entry via N-, P/Q- or R-type VACCs (Wheeler et al., 1994; Jun et al., 1999). Spontaneous release is also enhanced by extracellular Ca^{2+} (Yamasaki et al., 2006; Xu et al., 2009a; Groffen et al., 2010), and was recently shown to exhibit a high-order dependence on $[Ca^{2+}]_o$ (Xu et al., 2009a) raising the possibility that Ca^{2+} entry through VACC also mediates the Ca^{2+}- dependence of spontaneous fusion. Following an action potential, a short-lived microdomain of increased $[Ca^{2+}]_i$ (Neher and Sakaba, 2008) results from the synchronized activation of at least 60 VACCs to evoke the fusion of a single vesicle at the calyx of Held (Borst and Sakmann, 1996). How the infrequent, random openings of VACCs could cooperate sufficiently to trigger spontaneous release at the resting membrane potential remains unclear. However, at some synapses release can be triggered by only 1 or 2 VACCs per vesicle (Augustine et al., 1991; Stanley, 1993; Shahrezaei et al., 2006; Bucurenciu et al., 2010), providing a mechanism by which stochastic activation of VACC could trigger spontaneous release.

We explored the mechanism by which changes in $[Ca^{2+}]_o$ mediate changes in spontaneous release by measuring miniature excitatory post synaptic currents (mEPSCs) in cultured neocortical neurons. Enhancement of mEPSC frequency by extracellular Ca^{2+} was not mediated by VACC activity or reversal of the Na^+-Ca^{2+} exchanger (NCX). Optical recordings of nerve terminal $[Ca^{2+}]_i$ revealed that increases in $[Ca^{2+}]_o$ produced small increases in $[Ca^{2+}]_i$ in a subset

of neurons. However, enhancement of mEPSC frequency by extracellular Ca^{2+} was insensitive to intracellular Ca^{2+} chelation by the exogenous buffer BAPTA. Moreover mEPSC frequency had a relatively low-order dependence on $[Ca^{2+}]_o$ and surprisingly, was enhanced by extracellular Mg^{2+}. Stimulation of a G-protein coupled receptor (GPCR), the calcium-sensing receptor (CaSR) with specific agonists increased mEPSC frequency, and CaSR loss-of-function mutant neurons had fewer spontaneous events over the physiological range of $[Ca^{2+}]_o$. These data indicate that extracellular Ca^{2+} does not enhance spontaneous glutamate release via Ca^{2+} influx, and suggest that Ca^{2+} in the synaptic cleft can promote spontaneous exocytosis by activation of a presynaptic GPCR.

RESULTS

Extracellular Ca^{2+} enhances spontaneous vesicle fusion

We made whole-cell patch clamp recordings from neocortical neurons voltage-clamped at -70 mV. To investigate the effect of varying $[Ca^{2+}]_o$ on the spontaneous vesicle fusion rate, we measured mEPSCs when neuronal firing was blocked with tetrodotoxin (1 µM). Bicuculline methiodide (10 µM) was present in all external solutions to block $GABA_A$ receptor mediated post-synaptic currents. Extracellular Ca^{2+} dose-dependently and reversibly increased mEPSC (Fig. 1.1A,B). Surprisingly the concentration-effect relationship for mEPSC frequency versus $[Ca^{2+}]_o$ did not saturate even when $[Ca^{2+}]_o$ was increased to 20 mM (Fig. 1.1C). Furthermore, the relationship was approximately linear on a double logarithmic plot with a slope of 0.63, which is substantially lower than slopes of 3-5 for evoked transmission (Dodge and Rahamimoff, 1967; Augustine and Charlton, 1986; Borst and Sakmann, 1996; Reid et al., 1998; Rozov et al., 2001; Ikeda et al., 2008). One possibility is that the sustained application of high Ca^{2+} concentrations caused desensitization of the spontaneous release process and reduced the steepness of the concentration-effect relationship (Fig. 1.1). We examined for any evidence of desensitization by making single step changes in $[Ca^{2+}]_o$ from a common value. As expected a step change in $[Ca^{2+}]_o$ from 1.1 to 6 mM increased mEPSC frequency (Fig. 1.2A). The time courses of the changes in mEPSC frequency were described by single exponential functions following step changes in $[Ca^{2+}]_o$ from 1.1 mM to the range 0.2-20 mM (Fig. 1.2C). The

concentration-effect curve for mEPSC frequency versus $[Ca^{2+}]_o$ generated following single step changes in $[Ca^{2+}]_o$ was unchanged compared to the stepwise protocol over the lower part of the range (Fig. 1.2D, solid circles). However, the relationship was steeper at high Ca^{2+} concentrations, rising to 1.1 between $[Ca^{2+}]_o$ of 2 -20 mM, suggesting that $[Ca^{2+}]_o \geq 6$ mM produced desensitization of spontaneous release (Fig. 1.2C). These data also support the conclusion that the relationship between mEPSC frequency and $[Ca^{2+}]_o$ does not saturate over the range of $[Ca^{2+}]_o$ used (see also (Groffen et al., 2010)). Furthermore, the concentration-effect relationships for both protocols were much less steep than for evoked release (Dodge and Rahamimoff, 1967; Augustine and Charlton, 1986; Borst and Sakmann, 1996; Reid et al., 1998; Rozov et al., 2001; Ikeda et al., 2008) suggesting that external Ca^{2+} regulates spontaneous and evoked release by distinct mechanisms.

Amplitude histograms of mEPSCs showed that increasing $[Ca^{2+}]_o$ from 1.1 to 6 mM resulted in a small amplitude decrease (Fig. 1.2B).This was confirmed by the plot of mEPSC amplitude and $[Ca^{2+}]_o$ (Fig. 1.2E) and presumably resulted at least in part from the substitution of extracellular Na^+ for Ca^{2+} (to normalize osmolarity), which reduced the driving force for Na+ influx through ionotropic glutamate receptors.

It is well recognized that divalent cations screen surface charges, shift ion channel gating, and thereby reduce membrane excitability (Hille, 2001). We hypothesized that elevation of $[Ca^{2+}]_o$ reduced channel activation, and thereby increased input resistance and extended the space-clamp, enhancing mEPSC

detection from distal sites. However, input resistance and time constants for membrane capacitance were unchanged upon elevation of $[Ca^{2+}]_o$ from 1.1 to 6 mM (Fig. 1.3). Moreover the rise and decay times for the mEPSCs were slightly decreased rather than prolonged as expected if they had arisen from distant sites. Thus, the changes in mEPSC frequency that accompanied the change in bath $[Ca^{2+}]$ were not explained by surface charge screening of the neurons and altered detection of postsynaptic events.

VACC-mediated Ca^{2+} influx does not mediate extracellular Ca^{2+} enhancement of spontaneous fusion

Previous investigations have used extracellular Ca^{2+} to investigate the Ca^{2+} dependence of spontaneous release, assuming that changes in $[Ca^{2+}]_o$ produce changes in $[Ca^{2+}]_i$ and thus the rate of exocytosis (Xu et al., 2009a). An allosteric model of vesicle fusion rate versus $[Ca^{2+}]_i$ predicts that spontaneous release is a normal consequence of intracellular Ca^{2+} binding to the Ca^{2+}-sensor for calcium-influx mediated exocytosis, and that this relationship has a low cooperativity over the range of resting $[Ca^{2+}]_i$ (Lou et al., 2005). We hypothesized that stochastic activation of VACCs produced increases in $[Ca^{2+}]_i$, and that these events resulted in spontaneous exocytosis more frequently when the driving force for Ca^{2+}-influx was increased by elevation of $[Ca^{2+}]_o$. The low-order dependence of mEPSC frequency on $[Ca^{2+}]_o$ did not rule out a role for VACC in spontaneous release because it has been demonstrated that minimal VACC activity can influence resting $[Ca^{2+}]_i$ and release (Awatramani et al., 2005). To test the hypothesis that

extracellular Ca^{2+} stimulates spontaneous vesicle fusion via VACC-mediated Ca^{2+} influx, we measured the extracellular Ca^{2+}-dependence of mEPSC frequency in the presence of the VACC blocker cadmium (Cd^{2+}, 100 μM) (Carbone et al., 1997; Chen et al., 2007). Cd^{2+} did not decrease mEPSC frequency at baseline (1.1 mM) or elevated (6 mM) $[Ca^{2+}]_o$ (Figs. 1.4A,B). Elevation of $[Ca^{2+}]_o$ to 6 mM also increased mEPSC frequency after pretreatment with Cd^{2+} (Fig. 1.4C). Both the magnitude and time course of mEPSC frequency enhancement by extracellular Ca^{2+} were unchanged by Cd^{2+} (Fig. 1.4D,E; see also (Abenavoli et al., 2002)). We recorded VACC currents in response to a ramp depolarization and confirmed that Cd^{2+} blocked VACC currents in the cultured neocortical neurons studied here (Fig. 1.4F). Application of MVIIC (5 μM), which blocks N- and P/Q-type VACCs in cortical neurons (Hillyard et al., 1992; Rozov et al., 2001) also had no effect on the enhancement of mEPSC frequency by elevation of extracellular Ca^{2+} (8.0 ± 3.2 fold enhancement, n = 2, data not shown). Together these data strongly indicate that VACC-mediated Ca^{2+} influx is not a primary determinant of spontaneous vesicle fusion at baseline $[Ca^{2+}]_o$ or of enhanced spontaneous fusion at elevated $[Ca^{2+}]_o$.

Na^+/Ca^{2+} Exchange maintains baseline spontaneous release but does not mediate extracellular Ca^{2+}-enhancement

Next we tested if other mechanisms could link extracellular Ca^{2+} and vesicle fusion. Na+-Ca^{2+} exchange has been shown to play a prominent role in the removal of Ca^{2+} from nerve terminals (Nachshen et al., 1986; Sanchez-Armass

and Blaustein, 1987; Fontana et al., 1995). We hypothesized that if extracellular Ca^{2+} enhanced spontaneous fusion by promoting reverse-mode NCX activity (Na^{+} efflux, Ca^{2+} influx), then direct inhibition of NCX-mediated Ca^{2+} transport should block the enhancement of spontaneous fusion by elevation of $[Ca^{2+}]_o$. KB-R7943 inhibits forward- and reverse-mode NCX currents (Watano et al., 1996; Kimura et al., 1999). Basal mEPSC frequency was substantially increased by KB-R7943 (5 μM, 10 minute application; Fig. 1.5A, top and middle traces) consistent with the hypothesis that NCX modulates basal $[Ca^{2+}]_i$ and spontaneous fusion. To test if NCX is part of the pathway by which extracellular Ca^{2+} enhances spontaneous vesicle fusion, we elevated $[Ca^{2+}]_o$ after NCX inhibition. Increasing $[Ca^{2+}]_o$ from 1.1 to 6 mM still produced a large increase in spontaneous fusion rate after KB-R7943 application (Fig. 1.5A,B). On average, KB-R7943 elevated mEPSC frequency to 9.8 ± 1.9 times baseline and increasing $[Ca^{2+}]_o$ following NCX inhibition further enhanced mEPSC frequency to 16.8 ± 4.1 times that of baseline (Fig. 1.5B,C, $p = 0.03$). Interestingly, single-exponential fits of the extracellular Ca^{2+}-induced mEPSC frequency increases revealed that enhancement of spontaneous release by extracellular Ca^{2+} was faster when NCX was blocked. Time constants of mEPSC frequency increases were 17 and 9 seconds before and after NCX inhibition, respectively.

Taken together these data indicate that NCX activity maintains baseline spontaneous fusion rate but that reversal of NCX does not mediate extracellular Ca^{2+}-enhancement of spontaneous vesicle fusion. Furthermore, increasing

baseline spontaneous vesicle fusion by inhibition of NCX enhanced the rate of facilitation of spontaneous release by elevation of $[Ca^{2+}]_o$.

Increases in extracellular $[Ca^{2+}]$ produce small increases in nerve terminal intracellular $[Ca^{2+}]$ in a subset of neurons

We next tested directly whether changes in $[Ca^{2+}]_o$ produce changes in $[Ca^{2+}]_i$. We first measured Fluo-4 fluorescence changes at putative nerve terminals (Fig. 1.6A) in response to elevation of $[Ca^{2+}]_o$ from 1.1 to 6 mM. Increasing $[Ca^{2+}]_o$ did not produce a measurable increase in Fluo-4 signal, although a robust response to high external potassium (K^+, 90 mM) was measured in the same boutons (Fig 1.6B). We hypothesized that Fluo-4, which has a Kd for Ca^{2+} of ~ 345 nM (Takahashi et al., 1999) was not sensitive enough to respond to extracellular Ca^{2+}-induced changes in $[Ca^{2+}]_i$. We next performed experiments using the higher-affinity Ca^{2+} indicator Oregon Green BAPTA-1 (Kd ~ 170 nM). Experiments were performed in the presence of tetrodotoxin (TTX) and bicuculline (Bic) as during mEPSC recordings. Interestingly, application of TTX and Bic produced a marked reduction in OGB1 fluorescence to ~ 62% of baseline (Fig. 1.6C). These results indicate that active processes contribute to nerve terminal $[Ca^{2+}]_i$ in control conditions. Upon elevation of $[Ca^{2+}]_o$, we observed two types of responses: in some neurons, nerve terminal $[Ca^{2+}]_i$ appeared to be insensitive to elevation of $[Ca^{2+}]_o$ (Fig. 1.6D, left). Nerve terminals from other neurons displayed increases in OGB1 fluorescence upon elevation of $[Ca^{2+}]_o$ (Fig. 1.6D, right). All recordings showed robust responses to high

extracellular [K^+]. Combining the data from both responding and non-responding cells showed that, on average, $[Ca^{2+}]_o$ elevation produced a relatively small increase in nerve terminal $[Ca^{2+}]_i$. Importantly, however, our results are consistent with the conclusion that heterogeneity exists among neocortical neurons with regards to sensitivity of nerve terminal $[Ca^{2+}]_i$ to $[Ca^{2+}]_o$.

Enhancement of spontaneous release by extracellular Ca^{2+} is insensitive to intracellular Ca^{2+} chelation by BAPTA-AM

We next tested directly if the enhancement of spontaneous release by extracellular Ca^{2+} required increases in $[Ca^{2+}]_i$. In mammalian cells, intracellular BAPTA binds Ca^{2+} with a Kd of ~ 220 nM and with rapid kinetics (Pethig et al., 1989; Naraghi and Neher, 1997; Bucurenciu et al., 2008), and hence reduces action-potential evoked increases in $[Ca^{2+}]_i$ and exocytosis (Adler et al., 1991; Rozov et al., 2001). The membrane permeable form of BAPTA, BAPTA-AM, contains an acetoxylmethyl ester moiety that is cleaved by endogenous intracellular esterases, producing active BAPTA (Ouanounou et al., 1996). BAPTA-AM produces robust inhibition of action-potential evoked neurotransmitter release in hippocampal cells (Ouanounou et al., 1999; Abenavoli et al., 2002).

To test directly whether chelation of intracellular Ca^{2+} inhibited spontaneous release of glutamate, mEPSCs were recorded while $[Ca^{2+}]_o$ was increased from 1.1 to 6 mM both before and after a 10 minute application of BAPTA-AM (100 μM). Surprisingly, BAPTA-AM did not decrease spontaneous

release rate at baseline $[Ca^{2+}]_o$ or the enhancement of spontaneous release by elevation of $[Ca^{2+}]_o$ (Figs. 1.7A,B). Average baseline mEPSC frequency was 2.1 ± 0.54 events per second and increased to 5.0 ± 1.5 for $[Ca^{2+}]_o$ = 6 mM. mEPSC frequency in BAPTA-AM and control $[Ca^{2+}]_o$ was 3.3 ± 1.0 events per second, measured as the average frequency during the last 100 seconds of a 600 second BAPTA-AM application (p = 0.06 compared with control baseline). Importantly, elevation of $[Ca^{2+}]_o$ in the presence of intracellular BAPTA increased mEPSC frequency to 7.2 ± 2.4 events per second (p = 0.04 compared to BAPTA-AM alone). Thus, enhancement of spontaneous glutamate release by extracellular Ca^{2+} was insensitive to chelation of intracellular Ca^{2+} by BAPTA.

We confirmed that perfusion with BAPTA-AM decreased synaptic transmission in our cultured neocortical neurons by recording EPSCs evoked with an extracellular stimulating electrode. Extracellular stimulation produced currents in the postsynaptic neuron with brief latency that were blocked by the AMPA/kainate receptor antagonist CNQX (Fig 1.7C, left). Evoked synaptic transmission recovered after wash of CNQX and was completely abolished after 400 seconds of BAPTA-AM perfusion (Fig. 1.7C, right). On average, BAPTA-AM inhibited stimulus-evoked charge transfer by 93% (Fig. 1.7E). The average EPSC integral was 1.15 ± 0.46 pC before and 0.080 ± 0.028 pC after BAPTA-AM and decayed with an average time constant of 67 ± 20 s (n = 5). The inhibition of stimulus-evoked excitatory synaptic transmission was not reversible over the time course measured here, consistent with low membrane permeability of BAPTA.

Extracellular Mg^{2+} stimulates spontaneous vesicle fusion

Extracellular Mg^{2+} decreases VACC currents and so inhibits spike evoked synaptic transmission (Dodge and Rahamimoff, 1967; Carbone et al., 1997; Ikeda et al., 2008). In contrast to this antagonistic effect, Mg^{2+} and Ca^{2+} both act similarly at other sites. In particular these two divalent cations have qualitatively similar actions on CaSR, both acting as agonists although Mg^{2+} is ~ 3-fold less potent (Brown et al., 1993).

To further characterize the mechanism by which extracellular Ca^{2+} regulates spontaneous vesicle fusion we recorded mEPSCs while varying $[Mg^{2+}]_o$. Removing extracellular Ca^{2+} and decreasing extracellular Mg^{2+} markedly reduced mEPSC frequency (Fig. 1.8A, upper and middle traces). Elevating $[Mg^{2+}]_o$ to 6 mM increased mEPSC frequency to approximately baseline levels (bottom trace). The concentration-effect relationship for mEPSC frequency and $[Mg^{2+}]_o$ had a slope of 0.40 indicating that extracellular Mg^{2+}, like extracellular Ca^{2+}, stimulates spontaneous fusion with low cooperativity (Fig. 1.8B). We also tested whether extracellular Mg^{2+} enhanced spontaneous release at physiological $[Ca^{2+}]_o$. Following elevation of $[Mg^{2+}]_o$ from 1.1 to 6 mM in 1.1 mM extracellular Ca^{2+}, mEPSC frequency increased nearly two-fold (Fig. 1.8C).

We confirmed that increasing $[Mg^{2+}]_o$ over the relevant range inhibited VACC currents in these neocortical neurons. VACC currents activated by a ramp depolarization were inhibited by extracellular Mg^{2+} in a concentration-dependent manner (Fig. 1.8D). Increasing $[Mg^{2+}]_o$ shifted the activation of VACC currents in

the depolarizing direction and reduced the maximum conductance, as expected (Carbone et al., 1997) (Fig. 1.8E).

These data demonstrate that extracellular Mg^{2+} enhanced spontaneous vesicle fusion, in contrast to its effect on action potential-evoked vesicle fusion (Dodge and Rahamimoff, 1967; Ikeda et al., 2008). This is also further evidence that Ca^{2+} entry via VACC does not mediate spontaneous vesicle fusion and suggests that extracellular Ca^{2+} and Mg^{2+} act at the same site to stimulate spontaneous glutamate release.

CaSR activation increases spontaneous vesicle fusion

CaSR is activated by both increases in $[Ca^{2+}]_o$ and $[Mg^{2+}]_o$ (Brown et al., 1993) and is expressed in central nerve terminals (Ruat et al., 1995; Chen et al., 2010). CaSR stimulation inhibits the activity of a nonselective cation channel in nerve terminals and impairs synaptic transmission (Smith et al., 2004; Phillips et al., 2008). To test the hypothesis that CaSR activation controls spontaneous vesicle fusion, we first examined the effect of Calindol, an allosteric CaSR agonist (Kessler et al., 2004), on mEPSC frequency. Spontaneous vesicle fusion was increased substantially by Calindol (5 μM, Fig. 1.9A). On average, an 800 second application of Calindol increased mEPSC frequency to 9.7 ± 3.8 times that of baseline (Fig. 1.9B). We also tested the effect of the FDA-approved calcimimetic cinacalcet on spontaneous glutamate release. Cinacalcet is an allosteric modulator of CaSR, increasing the sensitivity of CaSR to extracellular Ca^{2+} and decreasing the release of parathyroid hormone from the parathyroid gland

(Nemeth et al., 2004; Kawata et al., 2007). Cinacalcet (5 μM) produced a robust and reversible increase in spontaneous release rate (Fig. 1.9C). Average mEPSC frequency at the end of a 900 second application of cinacalcet was 7.9 ± 3.0 times that of baseline. Taken together, these results demonstrate that two independent specific allosteric agonists for CaSR stimulated spontaneous glutamate release.

We next tested whether gadolinium (Gd^{3+}), a high-affinity CaSR agonist also stimulated spontaneous glutamate release in these neurons (Brown et al., 1993). Gd^{3+} (20 μM) produced a large reversible increase in mEPSC frequency (Fig. 1.9D). On average, mEPSC frequency was 31 ± 11 times that of baseline after 200 second application of Gd^{3+}. These results further suggest that VACCs are not primary mediators of spontaneous glutamate release, as Gd3+ is a potent inhibitor of VACC-mediated Ca^{2+} influx (Biagi and Enyeart, 1990).

We further examined the role of CaSR signaling in spontaneous vesicle fusion using a CaSR mutant mouse ($CaSR^{-/-}$) (Ho et al., 1995). The CaSR gene in $CaSR^{-/-}$ mice contains an exon deletion and expresses mutant CaSR with reduced function (Oda et al., 1998). Expression of the CaSR mutant in human embryonic kidney cells confirmed that the exon deletion blocked plasma membrane expression of the receptor (Wang et al., 2009). mEPSCs were recorded from both $CaSR^{+/+}$ and $CaSR^{-/-}$ neurons (Fig. 1.9E). In $CaSR^{-/-}$ neurons mEPSC frequency increased as $[Ca^{2+}]_o$ was sequentially increased (see also Fig. 1.1) indicating that CaSR-independent pathways also contribute to the $[Ca^{2+}]_o$-dependence of mEPSC frequency. The slope of the log-log

concentration-effect plot was 0.83, similar to that observed for the $CaSR^{+/+}$ neurons. However, the concentration-effect curves of mEPSC frequency versus $[Ca^{2+}]_o$ for $CaSR^{+/+}$ and $CaSR^{-/-}$ neurons diverged at lower Ca^{2+} concentrations (Fig. 1.9F). We used linear regression of the logarithmically transformed data to test for overall differences between the two datasets. The lines describing log mEPSC frequency versus log $[Ca^{2+}]_o$ had different intercepts for $CaSR^{+/+}$ and $CaSR^{-/-}$ neurons confirming a difference in the $[Ca^{2+}]_o$-dependence of mEPSC frequency for the two genotypes ($p=0.04$, data not shown). The non-saturating relationship between mEPSC frequency and $[Ca^{2+}]_o$ in $CaSR^{-/-}$ neurons was fit by least squares to an empirical power function (Equation 1; Fig. 1.9F) (Reid et al., 1998; Bucurenciu et al., 2010). We proposed that the $CaSR^{+/+}$ data represented the combination of this CaSR-independent modulation and the effect of CaSR activation on mEPSC frequency. We therefore described the $CaSR^{+/+}$ data with the sum of a power function and a Hill equation (Equation 2) using the parameters obtained from the $CaSR^{-/-}$ fit, a measured affinity for CaSR-modulated currents at murine nerve terminals [0.72 mM, (Phillips et al., 2008)], a Hill coefficient of 0.55 derived from the limiting slope of the normalized $CaSR^{+/+}$ data (Fig. 1.2C), and an arbitrary maximum CaSR-dependent mEPSC frequency of 3.2 s^{-1} (Fig. 1.9F). The model predicts that the difference between the curves represents the CaSR-dependent portion of spontaneous release. The divergence of the two curves indicates that the relative contribution of the CaSR-dependent spontaneous release increases at lower $[Ca^{2+}]_o$. Our data suggest that at physiological $[Ca^{2+}]_o$ and $[Mg^{2+}]_o$ (both 1.1 mM) CaSR activation mediates ~ 30%

of the spontaneous release. Average mEPSC frequency was 3.2 ± 0.4 s^{-1} for $CaSR^{+/+}$ and 2.3 ± 0.4 s^{-1} for $CaSR^{-/-}$ neurons ($p = 0.75$, $n = 74$ and 23 for $CaSR^{+/+}$ and $CaSR^{-/-}$ neurons, respectively). Taken together, these data indicate that CaSR activation stimulates spontaneous vesicle fusion and may regulate spontaneous glutamate release over the range of $[Ca^{2+}]_o$ that occur under physiological and pathological conditions (Nicholson et al., 1978; Jones and Keep, 1988; Nilsson et al., 1996).

DISCUSSION

Calcium is a pivotal regulator of neuronal communication with numerous synaptic targets. Dissection of the contributions of the component signaling pathways is key to understanding synaptic transmission (Meinrenken et al., 2003; Chicka et al., 2008; Neher and Sakaba, 2008; Smith et al., 2008; Peters et al., 2010). Here we confirm that increasing external calcium stimulates spontaneous release of glutamate at central neurons (Yamasaki et al., 2006; Xu et al., 2009a; Groffen et al., 2010) but a number of our findings indicate surprising differences between evoked and spontaneous release pathways. First, the $[Ca^{2+}]_o$-dependence of spontaneous release is very low. Second, during spontaneous release Ca^{2+} does not enter via VACC. Third, increases in $[Ca^{2+}]_i$ are not necessary for enhancement of spontaneous release by extracellular Ca^{2+}. Fourth, extracellular magnesium and allosteric agonists for CaSR increased mEPSC frequency. Finally, CaSR null mutants have decreased spontaneous release. These discoveries indicate that calcium regulates spontaneous and evoked glutamate release differently, and that presynaptic GPCR activation by extracellular Ca^{2+} can stimulate spontaneous vesicle fusion.

External calcium modulation of spontaneous release

The steep cooperativity between transmitter release and $[Ca^{2+}]_i$ at concentrations between 2 and 20 µM has been explained by a model in which 5 calcium ions bind cooperatively to synatoptagmin (Geppert et al., 1994; Bollmann

et al., 2000; Schneggenburger and Neher, 2000). However at lower concentrations of $[Ca^{2+}]_i$, transmitter release occurs with substantially greater probability than is predicted by this model, which manifests as a reduction in the slope of the foot of the concentration-effect relationship (Lou et al., 2005; Sun et al., 2007). Modifications have been proposed to account for the increased release rate at lower $[Ca^{2+}]_i$ relative to predicted values, assuming that all vesicles share the same sensitivity to $[Ca^{2+}]_i$. An allosteric model consisting of a Ca^{2+}-independent pathway for vesicle fusion in addition to five binding sites for Ca^{2+} well describes the relationship between $[Ca^{2+}]_i$ and transmitter release (Lou et al., 2005). The data are also well fit by a model where spontaneous and evoked transmission are mediated by separate intracellular Ca^{2+} sensors with different Ca^{2+} cooperativity (Sun et al., 2007). While the exact $[Ca^{2+}]_i$ was not known, our data clearly show that the presence of CaSR increased the mEPSC frequency at lower $[Ca^{2+}]_o$ (≤ 0.6 mM; Fig. 1.9F) and therefore provides an additional mechanism to contribute to the apparent reduction in cooperativity. Interestingly, the limiting slope for the concentration-effect relationship we observed (0.63) in $CaSR^{+/+}$ neurons was close to the 0.66 measured over the low part of the range at the calyx of Held (Lou et al., 2005). A similar dependence of mEPSC frequency on $[Ca^{2+}]_o$ was previously reported at the neuromuscular junction (Hubbard, 1961) and in hippocampal neurons (Groffen et al., 2010).

It has recently been reported that the intracellular Ca^{2+}-sensor for spontaneous release is distinct from the sensor for action potential evoked release (Groffen et al., 2010). This result, combined with the finding that evoked

and spontaneous vesicles use different pools (Sara et al., 2005; Fredj and Burrone, 2009) suggests another level of complexity in the link between calcium and exocytosis. One study recently reported a higher order of dependence on $[Ca^{2+}]_o$ for spontaneous inhibitory and excitatory release in central neurons (Xu et al., 2009a). Even so, the Hill coefficient of 1.5-2.0 was lower than values reported for evoked release (3-5) at other central synapses (Dodge and Rahamimoff, 1967; Augustine and Charlton, 1986; Borst and Sakmann, 1996; Reid et al., 1998; Rozov et al., 2001; Ikeda et al., 2008) indicating that intracellular calcium microdomains, which are tightly defined by $[Ca^{2+}]_o$ and VACC activation, are not the likely mechanism linking $[Ca^{2+}]_o$ and spontaneous release. This was directly supported by our findings that neither external Cd^{2+}, Mg^{2+}, Gd^{3+}, nor intracellular BAPTA inhibited spontaneous release (Fig.s 1.4,1.8,1.9).

Miniature EPSCs and mIPSCs have previously been reported to be resistant to VACC blockers (Abenavoli et al., 2002; Yamasaki et al., 2006) and most attention had focused on the role of intracellular calcium stores as triggers of spontaneous release (Llano et al., 2000). In parathyroid cells CaSR activates phospholipase C (PLC) through G_q (Brown and MacLeod, 2001) which increases inositol triphosphate (Wang et al., 2003; Awumey et al., 2007). In HEK cells transfected with exogenous CaSR, activation of the receptor produces increases in $[Ca^{2+}]_i$ (Breitwieser and Gama, 2001). If CaSR also couples to G_q and PLC in nerve terminals, at least three possible mechanisms by which activation of CaSR promotes vesicle fusion could be envisioned. First, CaSR activation could increase IP_3 and promote Ca^{2+} release from neuronal intracellular stores

(Khodakhah and Ogden, 1993), elevating $[Ca^{2+}]_i$ and promoting exocytosis. Ca^{2+} release from intracellular stores has been shown to promote spontaneous neurotransmitter release in hippocampal and neocortical neurons (Emptage et al., 2001; Sharma and Vijayaraghavan, 2003; Vyleta and Smith, 2008). However, our demonstration that intracellular BAPTA does not decrease the enhancement of spontaneous release by extracellular Ca^{2+} argues against a primary role for intracellular calcium release. However, our data does not rule out completely the possibility that increases in $[Ca^{2+}]_o$ produce small increases in $[Ca^{2+}]_i$ that enhance the fusion activity of a high-affinity sensor, and that these small increases in $[Ca^{2+}]_i$ are relatively insensitive to chelation by BAPTA. On average an increase in $[Ca^{2+}]_o$ produced a small increase in $[Ca^{2+}]_i$ measured as a submaximal increase in fluorescence of the relatively high-affinity intracellular Ca^{2+} indicator, Oregon Green BAPTA-1 (Kd ~ 170 nM). However, even the Ca^{2+} sensor Doc2b, proposed to specifically catalyze spontaneous vesicle fusion (Groffen et al., 2010), has a lower affinity for Ca^{2+} than BAPTA (Doc2b ~ 1μM half-maximal activation by Ca^{2+} versus Kd ~ 220 nM for BAPTA (Pethig et al., 1989; Naraghi and Neher, 1997; Groffen et al., 2010)). We are unable to measure the concentration of intracellular BAPTA in experiments using the cell-permeable form of the chelator, and the relative concentrations of BAPTA and Ca^{2+} sensor will be important for determining the sensitivity of the sensor to Ca^{2+} in the presence of exogenous chelator. However, control experiments indicated that BAPTA was present in the nerve terminals at high enough concentrations to almost completely inhibit stimulus-evoked neurotransmission (Fig. 1.7C,D).

Taken together, our results indicate that increases in intracellular [Ca^{2+}] that are sensitive to BAPTA chelation are not required for the enhancement of spontaneous release by extracellular Ca^{2+}, and argue against calcium influx or release from intracellular stores being primary mediators of spontaneous exocytosis in glutamatergic neurons.

A second potential mechanism by which G_q and PLC activation could promote exocytosis is by controlling diacylglycerol (DAG) levels in the nerve terminal plasma membrane. DAG analogues potentiate both spontaneous and AP-evoked neurotransmitter release, with sites of action including presynaptic protein kinase C (PKC) and the munc13 family of vesicle priming proteins (Weirda et al., 2007; Lou et al., 2008). Thus, PLC-mediated hydrolysis of PIP_2 could promote spontaneous fusion by increasing DAG levels in the presynaptic membrane and activating PKC/munc13-dependent pathways.

Third, PIP_2 has recently been identified as a key molecule involved in the endocytosis of synaptic membrane after vesicle exocytosis, with PIP_2 hydrolysis being necessary for vesicle scission from the plasma membrane (Liu et al., 2009). Because endocytosis and exocytosis are functionally coupled and successful endocytosis is necessary for exocytosis (Hosoi et al., 2009), activation of CaSR and PLC-mediated PIP_2 hydrolysis may help maintain available release sites or a pool of recycling synaptic vesicles. PIP_2 also helps localize synaptotagmin, the Ca^{2+} sensor for action potential-evoked exocytosis, to presynaptic release sites and increases the rate of Ca^{2+}/synaptotagmin-catalyzed synaptic vesicle fusion (Bai et al., 2004). PIP_2 also enhanced the fusion

capabilities of Doc2b, and synaptotagmin and Doc2b compete for binding to the SNARE complex (Groffen et al., 2010). If synaptotagmin and Doc2b primarily catalyze evoked and spontaneous release, respectively, and have different sensitivities to PIP_2, then a PLC-catalyzed reduction of PIP_2 levels at the release site could change the percentage of vesicles that fuse spontaneously.

Consequences of presynaptic CaSR signaling in central neurons

Previously CaSR activation was shown to modulate non-selective cation channels (NSCCs) in central nerve terminals - NSCC current activation being inversely related to $[Ca^{2+}]_o$ (Smith et al., 2004; Chen et al., 2010). NSCC currents were proposed to broaden the presynaptic action potential, prolong calcium entry and potentiate synaptic transmission (Smith et al., 2004). Consistent with this, evoked release was decreased by CaSR agonists (other than calcium) and enhanced in $CaSR^{-/-}$ neuronal pairs (Phillips et al., 2008). The CaSR-NSCC signaling pathway was proposed to attenuate the impact of the physiological and pathological decreases in brain $[Ca^{2+}]_o$ (Nicholson et al., 1978; Nilsson et al., 1996) which are expected to substantially reduce release probability (Rusakov and Fine, 2003). However, the change in mEPSC frequency (Fig. 2B) is more than an order of magnitude slower than the change in NSCC currents following alteration of $[Ca^{2+}]_o$ indicating that changes in spontaneous release will only occur after sustained decreases in $[Ca^{2+}]_o$ such as those observed during prolonged neuronal activity or pathological stimuli (Nilsson et al., 1996).

The CaSR-mEPSC pathway may serve additional roles if CaSR is modulated by other agonists besides Ca^{2+} and Mg^{2+} under physiological conditions. The polyamines spermine and spermidine are released by brain tissue and may function as neuromodulators via the CaSR (Masuko et al., 2003; Chen et al., 2007). As well as decreasing evoked release (Phillips et al., 2008) our data predict that polyamines will increase spontaneous release of glutamate. This could be important to sustain or grow new synaptic connections (McKinney et al., 1999; Vizard et al., 2008). The recent description of the link between CaSR mutations and juvenile myoclonic epilepsy (Kapoor et al., 2008) also points to the importance of the pathway in regulating neuronal excitability. Gain of function mutations of CaSR have previously been associated with seizures and low serum Ca^{2+} (Pearce et al., 1996) although the mechanism by which this occurs remains unclear.

Other modulators of mEPSC frequency

By our estimation only ~ 30% of the basal mEPSCs are triggered because of CaSR activation, however our model predicts that the contribution of CaSR activation to spontaneous release rate will be larger during periods of decreased $[Ca^{2+}]_o$. Since block of NCX increased mEPSC frequency this suggests that under basal conditions NCX has an important role countering increases in $[Ca^{2+}]_i$. It is unclear how CaSR-independent but extracellular Ca^{2+}-dependent spontaneous release is activated (Fig. 1.9F). In addition to membrane flux through unidentified channels and release from intracellular stores (Friel and

Chiel, 2008), activation of other extracellular Ca^{2+}-sensitive GPCRs is possible. These receptors include the extracellular Ca^{2+}-sensor, GPRC6A (Wellendorph and Brauner-Osborne, 2004), which has a lower affinity than CaSR, and members of the metabotropic glutamate receptor family (Tabata and Kano, 2004).

In conclusion, we have shown that the extracellular Ca^{2+} dependence of spontaneous glutamate release in neocortical neurons is of low-order, does not require increases in $[Ca^{2+}]_i$ that are sensitive to BAPTA chelation, and involves activation of CaSR. These results demonstrate that calcium regulates action potential-evoked and spontaneous neurotransmitter release differently, and provide evidence that Ca^{2+} in the synaptic cleft can promote spontaneous vesicle fusion by activation of a presynaptic GPCR.

METHODS

Neuronal preparation. Neocortical neurons were isolated from P1-2 $CaSR^{+/+}$ or $CaSR^{-/-}$ (Ho et al., 1995) mouse pups. All animal procedures were approved by OHSU I.A.C.U.C. in accordance with the U.S. Public Health Service Policy on Humane Care and Use of Laboratory Animals and the N.I.H. Guide for the Care and Use of Laboratory Animals. Animals were deeply anesthetized with isoflurane before decapitation and removal of cortices. Cortices were then incubated in trypsin and DNAse and then dissociated with a heat polished pipette. Dispersed cells were cultured in MEM plus 5% FBS on glass coverslips.

ARAC (4 μM final concentration) was added 48 hours after plating to limit glial division. Cells were used after at least 14 days in culture.

Genotyping CaSR mutant mice. Heterozygotes for the CaSR mutation were mated to produce $CaSR^{-/-}$ as this mutation is lethal at P3-P30. DNA from mouse tail was released by treatment with 50 mM NaOH at 95°C for 15 min, followed by the addition of 1M Tris, pH 8.0, and 10 mM EDTA. PCR was then performed using DNA solution and three primers: CaSR 5': TCTCTTCTCTTTAGGTCCTGAAAGA, CaSR 3': TCATTGATGAACAGTCTTTCTCCCT, and r-neo2: TCTTGATTCCCACTTTGTCCTTGTA. The samples were run on a 1% agarose gel and identified as $CaSR^{+/+}$, $CaSR^{+/-}$, or $CaSR^{-/-}$.

Electrophysiological recordings. Cells were visualized with an Olympus IX70 inverted microscope. Recordings were made in whole-cell voltage clamp mode. Holding potential was -70 mV corrected for liquid-junction potentials. Extracellular solutions contained (in mM) 150 NaCl, 4 KCl, 10 HEPES, 10 glucose, pH 7.35. For high $[Ca^{2+}]_o$ and $[Mg^{2+}]_o$ experiments, substitution of NaCl with $CaCl_2$ or $MgCl_2$ was made to maintain osmolarity. Recordings of mEPSCs were made in the presence of tetrodotoxin (TTX, 1 μM) and bicuculline (Bic, 10 μM) to block Na^+ channels and GABA-activated currents, respectively. For VACC recordings, 2 μM TTX was used. For recordings of evoked EPSCs, bicuculline (10 μM) was included to isolate excitatory transmission. Both potassium gluconate and cesium

methane-sulfonate intracellular solutions were used. Potassium gluconate solution consisted of (in mM) 113 K^+ gluconate, 9 EGTA, 10 HEPES, 4 MgCl2, 1 CaCl2, 4 NaATP, 0.3 NaGTP, 14 creatine phosphate, pH 7.2. Cesium methane-sulfonate solution consisted of 108 Cs^+ MeSO3, 9 EGTA, 10 HEPES, 4 MgCl2, 1 CaCl2, 4 NaATP, 0.3 NaGTP, 14 creatine phosphate, pH 7.2. Electrode tips had final resistances of 3-7 MΩ. Currents were recorded with a HEKA EPC9/2 amplifier. For mEPSC recordings, currents were filtered at 1 kHz using a Bessel filter and sampled at 10 kHz. Series resistance (Rs) was monitored, and recordings were discarded if Rs changed significantly during the course of a recording. Often Rs was compensated 60-70%. For recording of VACC currents and extracellular stimulus-evoked EPSCs, currents were filtered at 3 kHz and sampled at 20 kHz. Rs was compensated by at least 70%.

For extracellular stimulation of synaptic currents, a double-barrel theta electrode was used containing two Ag/AgCl wires connected to a high-voltage stimulus isolator (World Precision Instruments, Sarasota, Florida, product # A365D). Theta glass was pulled to a tip of ~ 5 μm outside diameter and barrels contained extracellular solution containing bicuculline. Briefly, the stimulus electrode was positioned nearby visually identified small neuronal processes nearby the postsynaptic cell. Electrode was carefully moved via micromanipulator and stimulus current amplitude adjusted until small EPSCs were recorded in the postsynaptic cell held in voltage-clamp. Stimulus intensity was normally between 300 and 500 μA (100 μs duration). The intent was to evoke EPSCs containing

only a few quanta to minimize the number of activated release sites and to avoid recurrent network activity.

Imaging. For single-neuron imaging experiments examining nerve terminal $[Ca^{2+}]_i$, cells were loaded with an EGTA/Ca^{2+} free KGlu pipette solution containing either Fluo4 (100 μM) or OGB1 (200 μM) for detection of changes in $[Ca^{2+}]_i$ (Schipke et al., 2001) and Alexa Red 594 (40 μM) for visualization of cell morphology (Yu et al., 2010). All dyes were purchased from Invitrogen. Osmolarity was compensated by increasing [KGlu] to 118 mM. Images were acquired and analyzed using a 1.2 N.A. 60x water immersion objective (Olympus America, Melville, NY) and an inverted microscope (Olympus) and cooled CCD camera (Orca, Hamamatsu) with computer controlled shutter. Fluo4 and OGB1 were excited at 470-490 nm and the fluorescence collected at 505-545 nm. Alexa Red excited at 542-582 nm and the fluorescence collected at 604-644 nm. Images were collected at either 5 or 10 second intervals with a 500 ms shutter opening and data acquisition time.

After achieving the whole-cell configuration, neurons were held in voltage-clamp for 10-20 minutes to allow loading of the dyes into distal processes. The patch pipette was then carefully retracted and optical recordings were then performed. Axons were identified using established criteria (Yu et al., 2010) as long, thin, smooth processes and clearly distinguished from the thicker, spiny dendrites. Putative presynaptic boutons were identified as punctate swellings

(~ 1 μM diameter) along thin axonal fibers, hundreds of microns from the cell soma (Fig. 1.6A).

Solution and drug application. Solutions were bath applied through a perfusion pipette placed ~1 mm from the patch pipette tip. Perfusion pipette was attached to a manifold (Warner Instruments) through which multiple solutions could flow. Local solution equilibration occurred in <10 seconds as measured by open-tip conductance changes. KB-R7943 (Tocris Biosciences) was dissolved in DMSO at 50 mM stock concentration and used at 1/10000 dilution. Calindol and cinacalcet (Toronto Research Chemicals, Inc.) were dissolved in ethanol at 10 mM stock concentration and used at 1/2000 dilution. BAPTA-AM (Invitrogen) was dissolved in DMSO at 50 or 100 mM stock concentration and diluted 1/1000. Extracellular solutions containing 100 μM BAPTA were incubated in a water bath at 30°C with ultrasonic frequency agitation for ~ 30 minutes to ensure solubility. Control experiments demonstrated that these final solvent concentrations had no effect on mEPSC frequency or on stimulus-evoked EPSCs.

Analysis. Data were acquired on a PIII computer and analyzed with IgorPro (Wavemetrics, Lake Oswego, OR) and Minianalysis (Synaptosoft, Decatur, GA) software. mEPSC data were normalized to the average mEPSC frequency during at least 100 seconds of recording in baseline $[Ca^{2+}]_o$ and $[Mg^{2+}]_o$ (both 1.1 mM) unless otherwise noted. For individual recordings in which mEPSC frequency desensitization was visible the peak 30 seconds of data was averaged (10

second bins). Otherwise, steady-state mEPSC frequency changes were measured. Statistical significance was determined using Student's t-test or Mann-Whitney test as appropriate (Microsoft EXCEL, Richmond, WA; Graphpad Prism). p-values < 0.05 were considered significant. Averaged data values are reported as means ± SEM.

Fluorescence data were analyzed using Wasabi software (Hammamatsu Photonics, Herrsching, Germany). Fluorescent regions of interest were defined manually. For analysis of nerve terminal Ca^{2+} indicator fluorescence signals, small elliptical regions of interest were drawn around the outside of putative synaptic boutons and maximum intensity analyzed over time. These signals were averaged over all boutons for an individual neuron and those single neuron averages combined to produce average diary plots (Fig. 1.6). In all imaging experiments, background fluorescence (signal emanating from dark regions of the coverslip) was averaged and subtracted in time.

Extracellular stimulus-evoked charge transfer (Fig. 1.7D) was calculated as the integral of the stimulus-evoked currents (Fig. 1.7C). Currents were baseline subtracted and only sweeps with stable baselines before stimulus were included in analysis. EPSC duration was determined by visual inspection, and currents were integrated for an average of 13 ms following stimulus artifact. For the representative recording shown in Fig. 4D, currents were integrated for 10 ms.

Curve fitting was performed using IgorPro. VACC conductance was calculated by transforming VACC currents (elicited with ramp depolarization)

using the equation $G = I/(V - V_{rev})$. Current reversal potentials (V_{rev}) were estimated by extrapolating the linear portion of the current traces to zero. Plots of conductance versus V_m were fit with the Boltzmann function $G = G_{max}/(1 + e^{((V_{1/2} - V)/k)})$, where G_{max} is maximal conductance, $V_{1/2}$ is half-maximal activation voltage, and k is the slope factor.

Miniature EPSC frequency versus $[Ca^{2+}]_o$ for $CaSR^{-/-}$ data were fit with a power function of the form:

$$y = y_o + Ax^z \quad (1)$$

where y equals the mEPSC frequency at $[Ca^{2+}]_o$ of x, y_o is the base of the curve, z is the exponent, and A is the coefficient.

$CaSR^{+/+}$ data were fit using the sum of a power function and Hill equation of the form:

$$y = y_o + Ax^z + y_{max} / [1 + (EC_{50}/x)^n] \quad (2)$$

where y_{max} is the maximum mEPSC frequency attributed to activation by CaSR and n is the Hill coefficient.

FIGURES/FIGURE LEGENDS

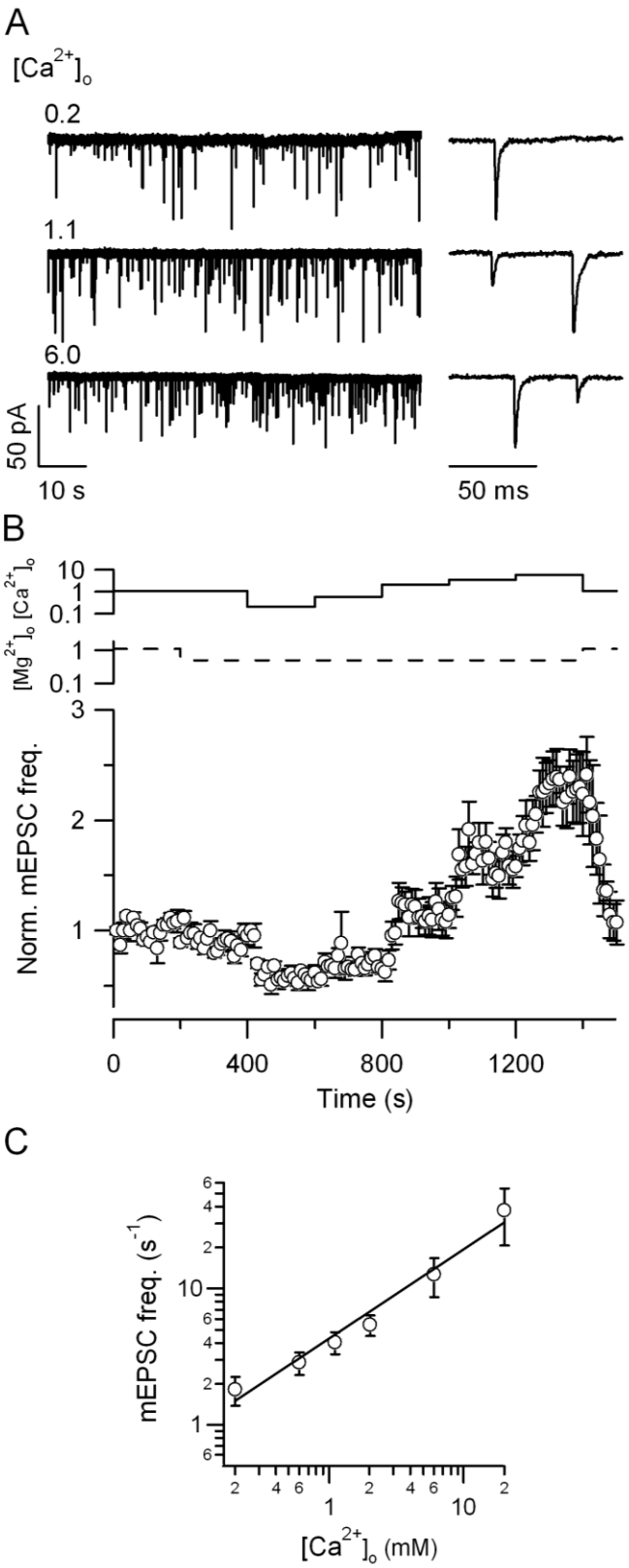
A
[Ca2+]o
0.2
1.1
6.0
50 pA
10 s
50 ms
B
[Ca2+]o
10
1
0.1
[Mg2+]o
1
0.1
Norm. mEPSC freq.
3
2
1
0
400
800
1200
Time (s)
C
mEPSC freq. (s-1)
6
4
2
10
6
4
2
1
6
2 4 6 1 2 4 6 10 2
[Ca2+]o (mM)

Figure 1.1. Spontaneous vesicle fusion is enhanced by extracellular Ca^{2+}.

(A) Recording of mEPSCs in whole-cell voltage clamp in the presence of TTX (1 μM) and bicuculline (10 μM). mEPSC frequency increased with $[Ca^{2+}]_o$ (indicated on left in mM). $[Mg^{2+}]_o$ was 0.5 mM for these recordings. (B) Average normalized diary plot showing that stair-step changes in $[Ca^{2+}]_o$ dose-dependently and reversibly modulated mEPSC (n = 5). $[Ca^{2+}]_o$ was increased stepwise from 0.2 to 6 mM. (C) Concentration-effect curve for mEPSC frequency versus $[Ca^{2+}]_o$. mEPSC frequency was 1.8 ± 0.43, 2.9 ± 0.55, 4.0 ± 0.75, 5.4 ± 0.92, 13 ± 4.1, and 38 ± 17 s^{-1} for $[Ca^{2+}]_o$ = 0.2, 0.6, 1.1, 2, 6, and 20 mM (n = 8, 11, 10, 11, 11, and 3, respectively).

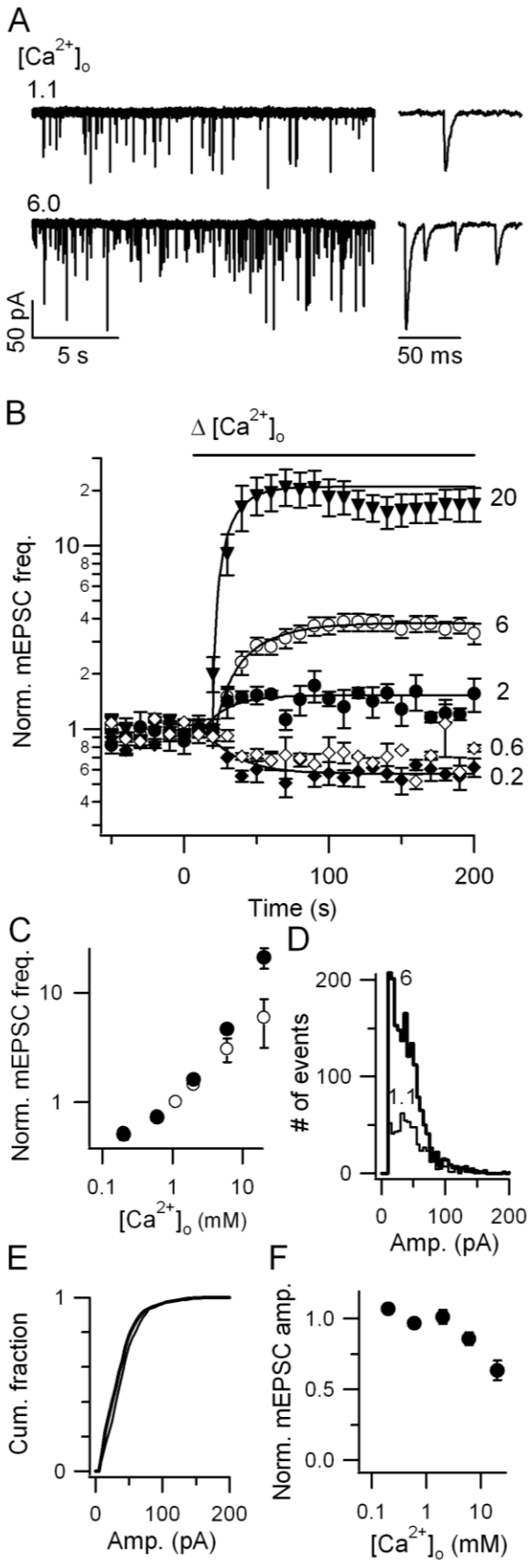
A
[Ca2+]o
1.1
6.0
50 pA
5 s
50 ms
B
Δ [Ca2+]o
Norm. mEPSC freq.
20
6
2
0.6
0.2
Time (s)
C
Norm. mEPSC freq.
[Ca2+]o (mM)
D
# of events
6
1.1
Amp. (pA)
E
Cum. fraction
Amp. (pA)
F
Norm. mEPSC amp.
[Ca2+]o (mM)

Figure 1.2. mEPSC frequency and amplitude dependence on $[Ca^{2+}]_o$. (A) Representative traces show that a single-step change in $[Ca^{2+}]_o$ from 1.1 (top) to 6 mM (bottom) increased mEPSC frequency. $[Mg^{2+}]_o$ = 0.5 mM for these recordings. (B) Diary plots of mEPSC frequency versus time show changes in mEPSC frequency in response to changing $[Ca^{2+}]_o$ from 1.1 to concentrations indicated on the right (in mM). Data points were normalized to average mEPSC frequency in 1.1 mM $[Ca^{2+}]_o$ during 100 seconds preceding $[Ca^{2+}]_o$ change. n = 5, 2, 4, 14, and 5 for steps to 0.2, 0.6, 2.0, 6.0 and 20 mM, respectively. Diary plots were well-described by single exponential functions with average time constants of 20.4 ± 6.4, 19.0 ± 7.4, 27.9 ± 4.9, and 13.9 ± 2.6 seconds for $[Ca^{2+}]_o$ changes to 0.2, 2, 6, and 20 mM, respectively. (C) Normalized concentration-effect curves for mEPSC frequency versus $[Ca^{2+}]_o$ from experiment in (B) (closed circles) and from data shown in Fig. 1.1C (open circles). Curve generated from single-step $[Ca^{2+}]_o$ change experiment is steeper for higher Ca^{2+} concentrations than curve generated by experiments in Fig. 1.1. Note that curves do not saturate. (D, E) Amplitude histograms of mEPSCs from recording in (A). Events from 200 seconds of recording in either $[Ca^{2+}]_o$ are shown. Elevation of $[Ca^{2+}]_o$ produced a small decrease in mEPSC amplitude. (F) Concentration-effect curve for average steady-state mEPSC amplitude versus $[Ca^{2+}]_o$. All points normalized to average mEPSC amplitude during 100 seconds of recording before $[Ca^{2+}]_o$ was changed. Normalized mEPSC amplitude was 1.1 ± .03, 0.97 ± 0.03, 1.0 ± 0.05, 0.86 ± 0.03, and 0.64 ± .07 that of control for 0.2, 0.6, 2, 6, and 20 mM $[Ca^{2+}]_o$ (n = 6, 2, 4, 4, and 5, respectively).

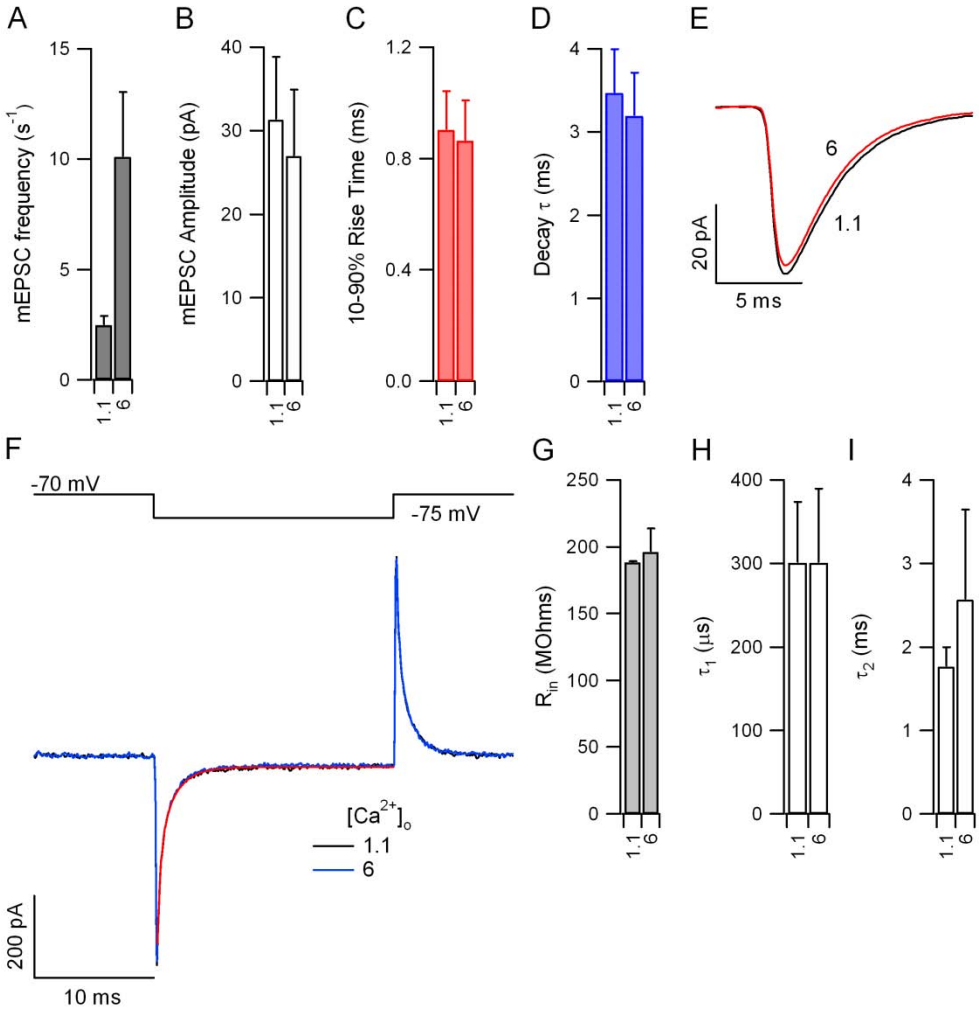

Figure 1.3. Extracellular Ca^{2+} -induced mEPSC frequency increases are associated with relatively small biophysical changes. (A) mEPSC frequency increases upon elevation of $[Ca^{2+}]_o$ were analyzed for three representative recordings. mEPSC frequency increased from 2.5 ± 0.42 to 10 ± 3.0 (s^{-1}) upon elevation of $[Ca^{2+}]_o$ from 1.1 to 6 mM (p = 0.09). (B) mEPSC frequency increase in (A) was associated with a small decrease in mEPSC amplitude (see Fig. 1.2 D-F). Average event amplitude was 31 ± 7.5 and 27 ± 8.0 pA in 1.1 and 6 mM

extracellular Ca^{2+}, respectively (p = 0.07). (C, D) Average 10-90% rise time decreased from 0.90 ± 0.14 to 0.86 ± 0.15 ms (p = 0.02) and the average decay time constant decreased from 3.5 ± 0.53 to 3.2 ± 0.52 (p = 0.005) upon elevation of $[Ca^{2+}]_o$. (E) Average mEPSCs in control (1.1 mM, black) and elevated $[Ca^{2+}]_o$ (6 mM, red) for representative recording in Fig. 1.2A. Traces are averages of 302 and 917 events for control and high $[Ca^{2+}]_o$, respectively. (F) A 5 mV hyperpolarizing voltage pulse (top) elicited transient capacitive followed by steady-state currents (bottom). Traces are individual sweeps from a representative recording. Currents were similar in either 1.1 (black) or 6 mM (blue) extracellular Ca^{2+}. Capacitive transient currents were best fit with a double-exponential function (red) of the form $A(t) = A_1(e^{-t/\tau 1}) + A_2(e^{-t/\tau 2}) + A_\infty$, where A is the current amplitude at time t, and A_∞ is the steady-state current amplitude. (G) Average R_{in} was calculated with Ohm's law using the steady-state current and was 188 ± 0.90 and 196 ± 17 MΩ in 1.1 and 6 mM extracellular Ca^{2+}, respectively (p = 0.72). (H, I) $\tau 1$ and $\tau 2$ did not change when $[Ca^{2+}]_o$ was elevated from 1.1 to 6 mM. $\tau 1$ was 301 ± 73 ms and 301 ± 89 ms and $\tau 2$ was 1.77 ± 0.23 ms and 2.57 ± 1.1 ms in 1.1 and 6 mM extracellular Ca^{2+} (p = 1.0 and 0.48, respectively). All statistical comparisons were performed using paired t-tests.

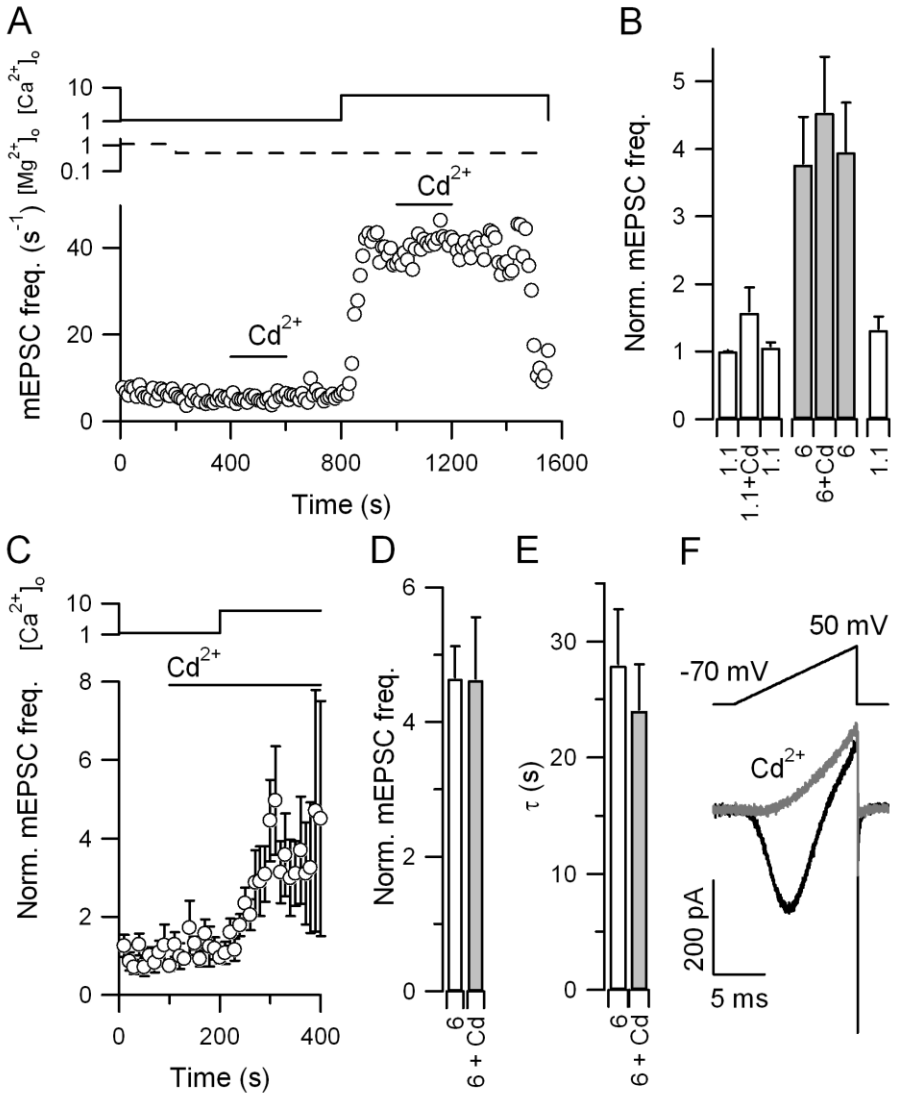

Figure 1.4. Spontaneous release is independent of VACC-mediated Ca^{2+} influx. (A) Representative diary plot of mEPSC frequency versus time. Cd^{2+} did not decrease mEPSC frequency at baseline or at elevated $[Ca^{2+}]_o$. (B) Cumulative data for experiment in (A) for six recordings. (C) Average normalized diary plot of mEPSC frequency versus time demonstrates that Cd^{2+} pretreatment did not prevent the enhancement of mEPSC frequency by elevation of $[Ca^{2+}]_o$ (n

= 6). (D,E) Average magnitude and rise times of mEPSC frequency increases induced by $[Ca^{2+}]_o$ = 6 mM (n = 7). Neither the magnitude nor kinetics of extracellular Ca^{2+}-enhancement of mEPSC frequency were different for Cd^{2+}-pretreated cells (grey bars) than for control (open bars). (F) VACC currents (bottom) elicited by ramp depolarization (1 mV/ms) protocol (top) confirm inhibition of Ca^{2+} currents by Cd^{2+} (average of 5 and 3 sweeps for control and Cd^{2+} traces, respectively).

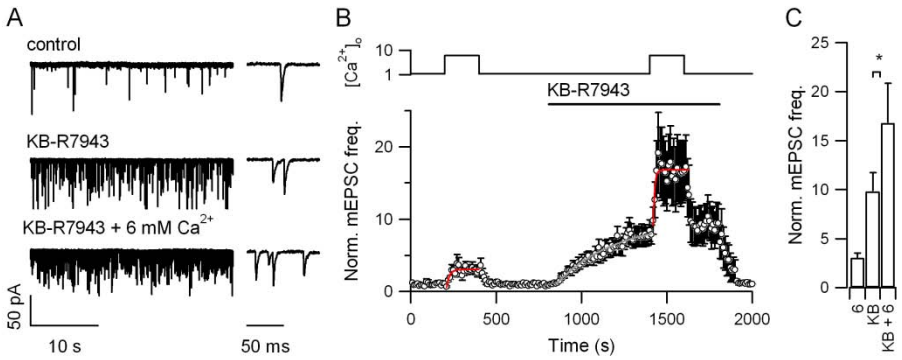

Figure 1.5. NCX controls baseline spontaneous vesicle fusion but not $[Ca^{2+}]_o$ dependence. (A) Representative mEPSCs at baseline (top), after KB-R7943 treatment (middle), and after elevation of $[Ca^{2+}]_o$ from 1.1 to 6 mM in presence of KB-R7943 (bottom). KB-R7943 increased mEPSC frequency, which was further enhanced by elevated $[Ca^{2+}]_o$. (B) Average normalized diary plot of mEPSC frequency versus time confirms these observations for 5 recordings. Enhancement of mEPSC frequency by KB-R7943 was fit with a single exponential function with time constant of 350 seconds. Rising phases of extracellular Ca^{2+}-enhancement of mEPSC frequency were fit with single exponential functions with time constants of 17 and 9 seconds for before and after KBR7943 application, respectively. (C) Summary data for experiment in (A,B) shows normalized increases in mEPSC frequency compared to baseline for 6 mM extracellular Ca^{2+} alone, KBR7943 alone, and 6 mM Ca^{2+} in the presence of KBR7943.

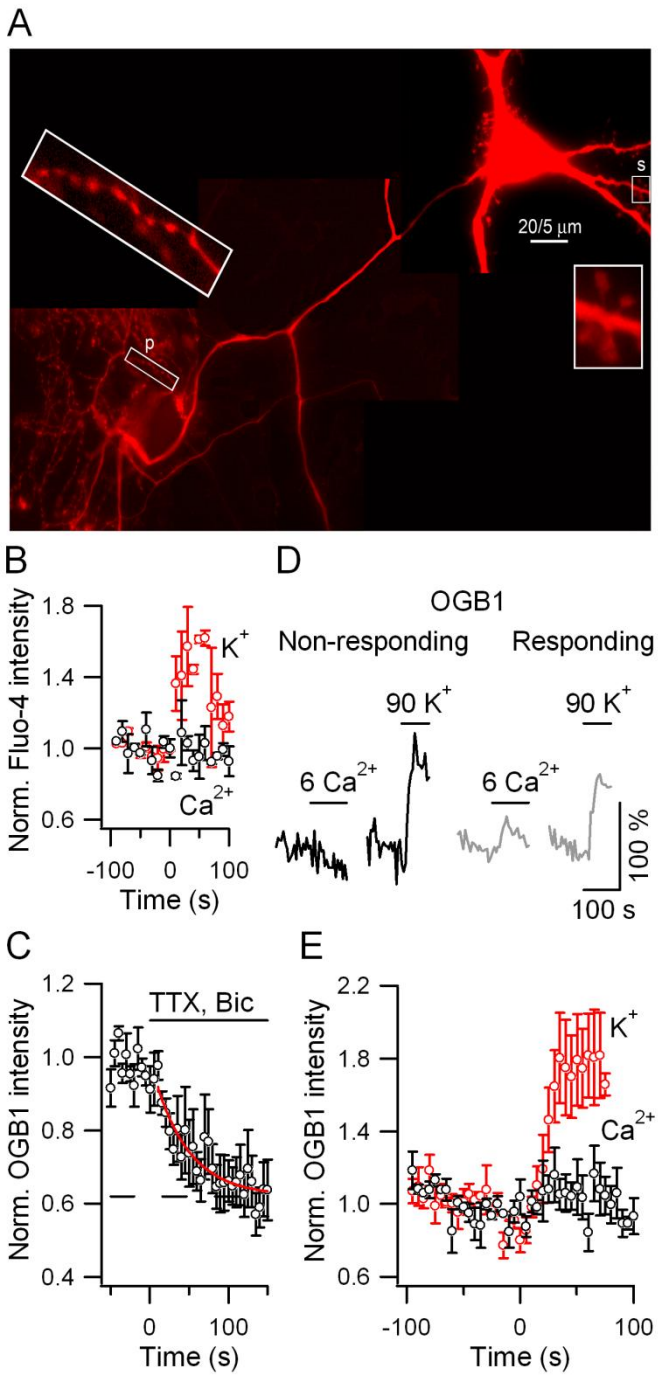

Figure 1.6. Nerve terminal $[Ca^{2+}]_i$ response to change of $[Ca^{2+}]_o$. (A) Reconstructed image of pyramidal neuron showing putative presynaptic boutons on distal axonal collaterals. Insets show blow-up images of boutons (left) and dendritic spines (right). Scale bar is 20 μM (5 μM for insets). (B) Average

normalized diary plot of Fluo-4 intensity versus time for responses to extracellular Ca^{2+} elevation (to 6 mM) or 90 mM extracellular K+ in the same boutons (n = 2 neurons, average of 35 boutons/neuron). (C) Average normalized diary plot of nerve terminal OGB1 intensity decrease in response to tetrodotoxin and bicuculline perfusion (n = 5 neurons). The decay was well described with a single exponential function with time constant of 44 seconds. (D) Average nerve terminal OGB1 fluorescence changes in response to Ca^{2+} elevation or 90 mM K+ for two different neurons. Nerve terminals from neuron on left were insensitive to enhancement of $[Ca^{2+}]_o$ (average signal from 13 putative boutons), while those from neuron on right displayed fluorescence increase (average signal from 35 putative boutons). Both sets of boutons showed robust response to depolarization with K+. (E) Average normalized bouton OGB1 fluorescence plotted as a function of time for all recordings (n = 5, 13-53 boutons/recording).

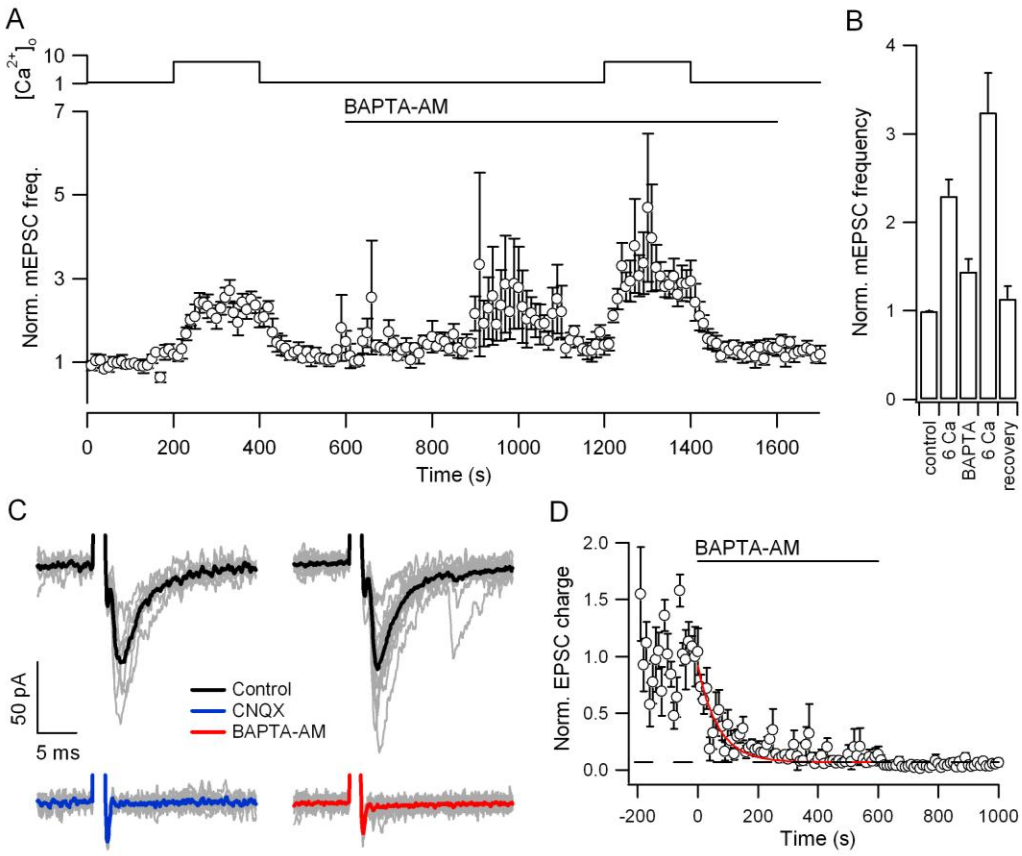

Figure 1.7. Enhancement of spontaneous release by extracellular Ca^{2+} is insensitive to intracellular BAPTA. (A) Average normalized diary plot of mEPSC frequency versus time showing effect of elevation of $[Ca^{2+}]_o$ from 1.1 to 6 mM both before and after 10 minute application of BAPTA-AM (100 μM, n = 6). Intracellular BAPTA did not prevent enhancement of mEPSC frequency by elevation of $[Ca^{2+}]_o$. (B) Histogram of normalized steady-state mEPSC frequencies. (C) Stimulus evoked EPSCs before (left, top, 7 individual traces) or after (left, bottom) treatment with CNQX (20 μM, 9 individual traces) or control EPSCS before (right, top, 15 individual traces) or after (right, bottom) 400 seconds BAPTA-AM (100 μM, 20 individual traces) from the same recording.

Control EPSCs before BAPTA-AM perfusion were recorded after washout of CNQX. Average traces are black, blue, or red for control, CNQX, and BAPTA-AM, respectively. Stimulus artifact subtracted from traces for clarity. (D) Average normalized diary plot of EPSC charge transferred versus time confirms inhibition of evoked synaptic transmission by BAPTA-AM (n = 5). Plot fitted with single exponential function with average time constant (68 s) and base (0.07) from individual recordings.

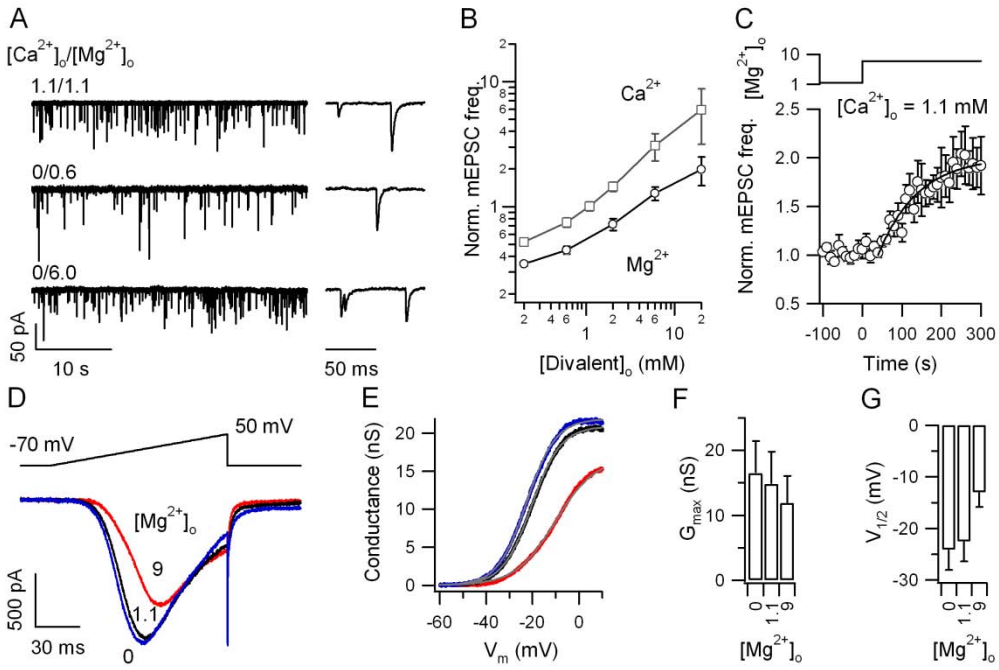

Figure 1.8. Extracellular Mg^{2+} increases spontaneous glutamate release but inhibits VACC currents. (A) mEPSCs were recorded in control $[Ca^{2+}]_o$ and $[Mg^{2+}]_o$ (both 1.1 mM, top). Removal of extracellular Ca^{2+} and decreasing $[Mg^{2+}]_o$ markedly reduced mEPSC frequency (middle). Elevation of $[Mg^{2+}]_o$ in the absence of extracellular Ca^{2+} increased mEPSC frequency (bottom). (B) Concentration-effect curves for mEPSC frequency versus $[Mg^{2+}]_o$ (circles) and $[Ca^{2+}]_o$ (squares, re-plotted from Fig. 1.2). Lines are drawn between points for clarity. All points normalized to mEPSC frequency in control $[Ca^{2+}]_o$ and $[Mg^{2+}]_o$ (both 1.1 mM). (C) Average normalized diary plot of mEPSC frequency versus time demonstrates that elevation of $[Mg^{2+}]_o$ from 1.1 to 6 mM increased mEPSC frequency in the presence of control $[Ca^{2+}]_o$ (1.1 mM; n = 6). Average mEPSC frequency increase was fit with a single exponential function with time constant of

100 seconds. (D) Representative recording of VACC currents elicited by ramp depolarization (-70 to 50 mV at 1 mV/ms, top) in zero, 1.1, or 9 mM extracellular Mg^{2+}. Traces are averages of three consecutive sweeps. Currents remaining in Cd^{2+} (100 μM) are subtracted from the average traces. $[Ca^{2+}]_o$ = 2 mM for these recordings. (E) Plots of conductance versus membrane voltage for VGCC currents in (D) (see Methods). Extracellular Mg^{2+} both decreased G_{max} and shifted $V_{1/2}$ to less negative potentials. (F,G) Histograms show average maximal conductance and $V_{1/2}$ as a function of $[Mg^{2+}]_o$ for three recordings. G_{max} was 22, 21, and 17 nS and $V_{1/2}$ was -23, -20, and -11 mV for $[Mg^{2+}]_o$ = 0, 1.1, and 9 mM, respectively (n = 3).

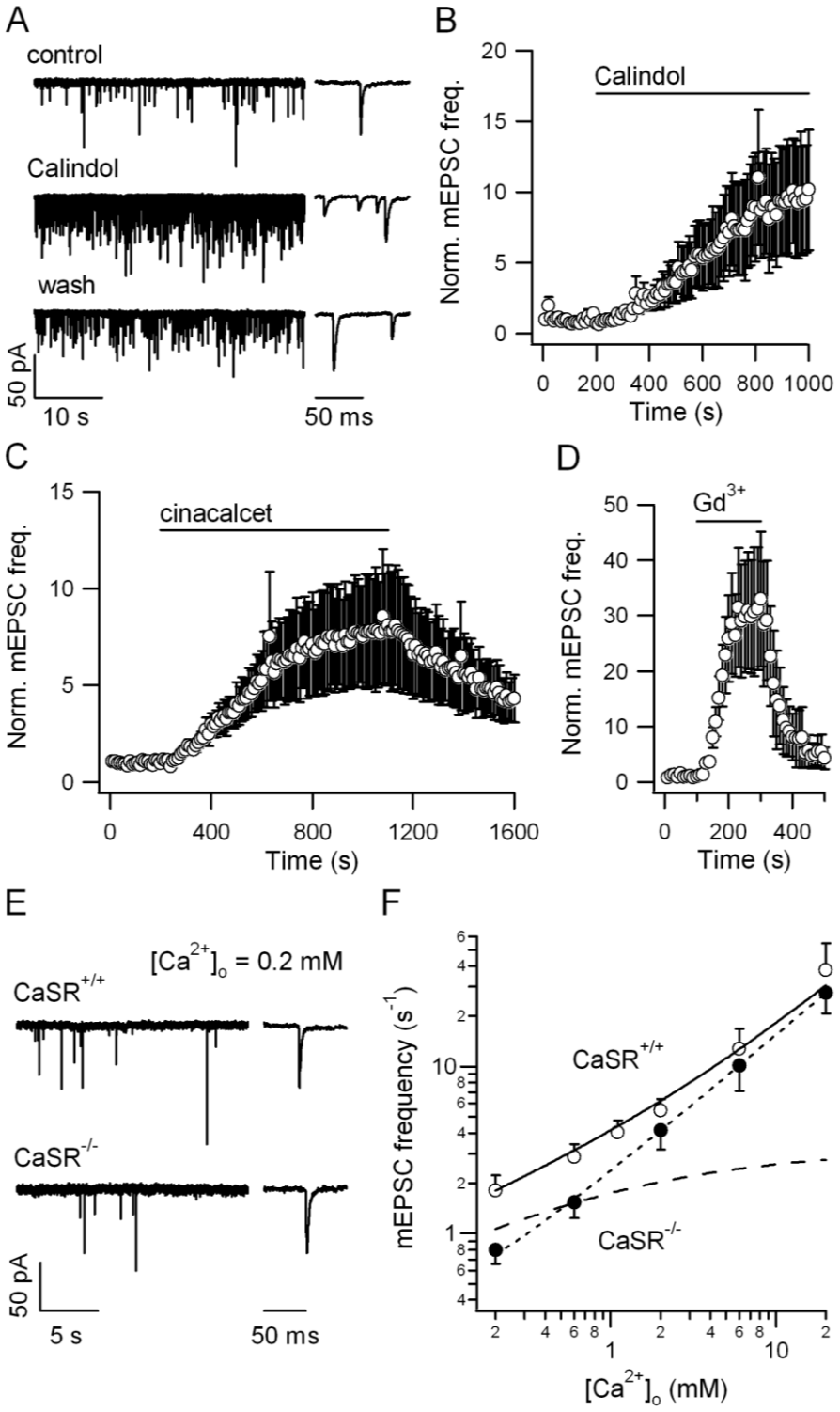

Figure 1.9. CaSR activation enhances spontaneous glutamate release. (A) mEPSCs were recorded before (top), after 10 minutes of Calindol application

(5 μM; middle), and after 15 minutes of wash (bottom). Calindol produced a marked increase in mEPSC frequency. (B) Average normalized diary plot of mEPSC frequency versus time confirms that Calindol increased spontaneous glutamate release (n = 6). (C,D) Average normalized diary plots show that cinacalcet (5 μM, n = 4) and Gd3+ (20 μM, n = 4) reversibly enhance spontaneous release rate. (E) Traces show mEPSCs recorded from $CaSR^{+/+}$ (top) and $CaSR^{-/-}$ neurons (bottom) in low $[Ca^{2+}]_o$ (0.2 mM). $[Mg^{2+}]_o$ = 0.5 mM for these experiments. (F) Non-normalized concentration-effect curves of mEPSC frequency versus $[Ca^{2+}]_o$ for $CaSR^{+/+}$ (open circles) and $CaSR^{-/-}$ (closed circles) neurons. mEPSC frequency was reduced in $CaSR^{-/-}$ neurons over the low range of $[Ca^{2+}]_o$. $CaSR^{-/-}$ data were fit with a power function (Equation 1, small dashes; y_o = 0.16, A = 2.23 s^{-1}, z = 0.84) and $CaSR^{+/+}$ data were described by the sum of a power function and Hill equation (Equation 2, black curve; A=2.23 s^{-1}, z=0.84, y_{max} = 3.2 s^{-1}, EC_{50} = 0.72 mM, and n = 0.55). Hill function alone represented by big dashes.

CHAPTER 2

Phospholipase C activity maintains synaptic vesicle fusion in neocortical neurons

CHAPTER 2

Phospholipase C activity maintains synaptic vesicle fusion in neocortical neurons

Nicholas P. Vyleta and Stephen M. Smith.

Division of Pulmonary & Critical Care Medicine, Oregon Health & Science University, Portland, OR 97239.

NPV performed all experiments and analyses and wrote this thesis chapter.

INTRODUCTION

The family of phospholipase C (PLC) enzymes catalyzes the hydrolysis of phosphatidylinositol-(4,5)-bisphosphate (PIP_2) to inositol triphosphate (IP_3) and diacylglycerol (DAG) (Rhee, 2001). The β isoform, PLCβ, is activated by GPCRs that couple to the G-protein family G_q. Stimulation of the G_q-coupled M1-muscarinic receptor in reconstituted cells directly demonstrated a PLC-mediated degradation of PIP_2 and simultaneous production of DAG and IP_3 (Horowitz et al., 2005). In these cells production of DAG had a time constant of ~ 20 seconds and was blocked by pharmacological inhibition of PLC. Interestingly, agonists for some G_q-coupled GPCRs increase the rate of spontaneous exocytosis in central neurons. For instance, the type-I metabotropic glutamate receptor agonist DHPG increased the frequency of miniature excitatory postsynaptic currents (mEPSCs) in slices of rat barrel cortex (Simkus and Stricker, 2002), and we provide evidence that activation of calcium-sensing receptor (CaSR) stimulates spontaneous release (Chapter 1 of this thesis). Exogenously applied DAG analogues increase the rate of spontaneous exocytosis (Weirda et al., 2007; Lou et al., 2008) and the size of the readily releasable pool (RRP) of vesicles in central neurons (Stevens and Sullivan, 1998). Thus DAG is a potent modulator of synaptic vesicle fusion. Additionally, PIP_2 has been identified as a key molecule in vesicle endocytosis (Liu et al., 2009) and exocytosis, where it enhances the ability of Ca^{2+} sensors to catalyze vesicle fusion (Bai et al., 2004; Groffen et al., 2010). Based on these results, we predicted that PLC may be an important

regulator of presynaptic function, acting as a metabolic intermediate between nerve terminal GPCR activation and PIP_2/DAG levels.

We have investigated the role of PLC in synaptic transmission by recording mEPSCs and readily releasable pool (RRP) size in neocortical neurons while inhibiting PLC with the aminosteroid U73122 (Horowitz et al., 2005). Our data suggests that PLC activity affects spontaneous vesicle fusion in complex ways, with PLC inhibition producing a robust inhibition of spontaneous release in a subset of neurons. In addition, we show that PLC inhibition decreases the size of the RRP measured with hypertonic-sucrose stimulation.

RESULTS/DISCUSSION

Inhibition of PLC reduces spontaneous glutamate release in a subset of neurons.

We made whole-cell patch clamp recordings from neocortical neurons voltage-clamped at -70 mV. We first investigated the effect of PLC inhibition on spontaneous, action potential-independent glutamate release. All mEPSC recordings were performed in the presence of tetrodotoxin (TTX, 1 μM) and bicuculline methiodide (10 μM). We measured the effect of PLC inhibition on mEPSC frequency using the aminosteroid PLC inhibitor U73122 (Smith et al., 1990; Horowitz et al., 2005). Interestingly, we observed two distinct effects of PLC inhibition on spontaneous release: First, in some recordings, a 20 minute application of U73122 (5 μM) resulted in a profound decrease in mEPSC

frequency as shown by the representative traces (Fig. 2.1A). The representative diary plot of mEPSC frequency versus time shows an example of a simple monoexponential decay in mEPSC frequency to less than 10 % of baseline levels induced by U73122 (Fig. 2.1B). In other recordings, U73122 produced more complex effects. In some recordings, U73122 application resulted in oscillation of spontaneous release, including a strong enhancement measured late in the recording (Fig. 2.1C). When all recordings were grouped together, U73122 produced an initial enhancement of mEPSC frequency which was followed by a decrease to below baseline levels (Fig. 2.1D).

The relatively inactive analogue of U73122, U73343 (Smith et al., 1990; Horowitz et al., 2005) was used as a negative control for these experiments. Interestingly, U73343 always produced a robust monophasic enhancement of mEPSC frequency that was completely reversible, indicating an effect of this molecule on spontaneous release that was independent of PLC activity (Fig. 2.1D). We can thus interpret the effect of U73122 on mEPSC frequency to be representative of at least two simultaneous processes: 1. A relatively slow, PLC-dependent inhibition of spontaneous vesicle fusion and 2. An enhancement of spontaneous vesicle fusion that is PLC-independent. The PLC-independent process is represented by the enhancement of spontaneous release in the presence of the PLC-inactive analogue U73343 (Fig. 2.1D). A similar molecule to U73122 and U73343 in chemical structure is the neurosteroid pregnenolone sulfate (PREGS). PREGS enhanced spontaneous glutamate release and action potential-induced release probability in hippocampal neurons (Meyer et al.,

2002). This could explain the facilitation of spontaneous release by U73343 and possibly U73122 that we measure. Alternatively, PLC inhibition itself could be producing two different effects on mEPSC frequency with two different time courses. It has been demonstrated that PIP_2 interacts directly with some ion channels in the plasma membrane and that PLC can modulate ion channel open probability by PIP_2 hydrolysis (Suh et al., 2006), including the Ca^{2+} permeable channel TRPV1 (Lukacs et al., 2007). Ca^{2+} influx through such a channel may produce an increase in mEPSC frequency through an elevation of $[Ca^{2+}]_i$.

Extracellular $[Ca^{2+}]$ dependence of spontaneous release requires PLC activity.

We have shown that extracellular Ca^{2+} enhances spontaneous glutamate release from neocortical neurons (Chapter 1 of this thesis). We demonstrated that activation of CaSR increases mEPSC frequency (Fig. 1.7) and hypothesized that CaSR in the nerve terminal may activate PLC through G_q. We therefore tested if PLC activity was required for the enhancement of mEPSC frequency by elevation of $[Ca^{2+}]_o$. Preliminary data demonstrate a marked reduction in the response of mEPSC frequency to a step change in $[Ca^{2+}]_o$ from 1.1 to 6 mM after a 20 minute incubation in U73122 (Fig. 2.2A), consistent with the hypothesis that CaSR activation promotes spontaneous release through activation of PLC. We next hypothesized that PLC activation by CaSR or other presynaptic GPCRs might enhance spontaneous release rate by increasing levels of DAG in the presynaptic membrane. Phorbol esters are synthetic DAG analogues and

enhance spontaneous release in central neurons (Lou et al., 2008). We proposed that if elevation of $[Ca^{2+}]_o$ ultimately enhanced spontaneous release rate by producing DAG, then exogenously applied DAG analogues might occlude the effect of elevation of $[Ca^{2+}]_o$ on spontaneous release. The average normalized diary plot of mEPSC frequency versus time shows the effect of increasing $[Ca^{2+}]_o$ from 1.1 to 6 mM both before and after application of phorbol 12,13-dibutyrate (PDBu, 1 μM) on mEPSC frequency. PDBu produced a robust enhancement of spontaneous release rate, as expected. However, elevation of $[Ca^{2+}]_o$ still enhanced mEPSC frequency to a similar extent after PDBu, suggesting that extracellular Ca^{2+} and PDBu may act through separate pathways to enhance spontaneous release. Future experiments are required to confirm that 1 μM PDBu is a saturating dose of phorbol ester with regards to spontaneous release, which is essential for the interpretation of an occlusion experiment.

PLC activity maintains the size of the readily releasable pool of synaptic vesicles.

We next wished to test whether the effects of PLC inhibition were specific to spontaneous neurotransmitter release or if PLC activity had a more general role in maintaining synaptic transmission. We induced RRP exocytosis by applying hypertonic sucrose solution and recorded excitatory postsynaptic currents (EPSCs) in voltage-clamp (Rosenmund and Stevens, 1996). 500 mM sucrose evoked large inward currents that were inhibited by a 20 minute application of U73122 (Fig. 2.3A). On average, the total sucrose-induced charge transfer was

772 ± 299 pC before and 225 ± 93 pC after U73122 (Fig. 2.3B, n = 7, p = 0.048, paired t-test). This inhibition was not reversible over the time course of our experiment (data not shown). We next confirmed that this inhibition of synaptic vesicle fusion was specific to PLC blockade by measuring the effect of U73343 on sucrose-induced currents. A 20 minute application of U73343 produced an apparent increase in sucrose-induced currents that was reversible (Fig. 2.3C). However, summary data show that this trend failed to reach statistical significance. On average, total sucrose induced charge transfer was 645 ± 165 pC before and 769 ± 198 pC after U73343 (Fig. 2.3D, n = 7, p = 0.061; paired t-test). Taken together, these results demonstrate that inhibition of PLC decreases the size of the synaptic vesicle pool available to fuse in response to hypertonic solution, and suggest that at baseline PLC has a role in maintaining the size of the readily releasable pool of synaptic vesicles in excitatory neocortical neurons.

Increasing vesicle exocytosis accelerates the inhibition of RRP size by PLC blockade.

Experiments in Fig. 2.3 measured the effect of U73122 on sucrose-induced synaptic currents after 20 minute drug treatment. We wished to better resolve the rate at which PLC blockade inhibits RRP size. Sucrose-induced currents were evoked every 300 seconds beginning directly before application of U73122 (time = 0). Sucrose-induced EPSCs were decreased with sequential application of hypertonic solution (Fig. 2.4A, top traces). A 300 second interstimulus interval resulted in a decrease which was well fit with a single exponential function with

time constant of 545 seconds (Fig. 2.4B, open triangles). We next evoked sucrose-induced currents every 100 seconds. Inhibition of sucrose-induced charge transfer was faster if currents were evoked every 100 seconds than if they were evoked every 300 seconds (Fig. 2.4A). The average data were fit with a single exponential function with time constant of 169 seconds (Fig. 2.4B). We compared inhibition of sucrose-induced charge transfer at 300 seconds of U73122 application for either a 300 second or 100 second interstimulus interval. Normalized charge transfer was 0.62 ± 0.13 and 0.32 ± 0.07 of control with a 300 or 100 second interstimulus interval ($p = 0.04$, $n = 5$ and 8, respectively). Taken together, these data indicate that inhibition of the readily releasable pool of synaptic vesicles by PLC blockade is significantly faster if vesicles are forced to fuse more frequently. This suggests a role for PLC activity in recovery from synaptic vesicle exocytosis. One possible explanation for our results may be provided by the recent demonstration that PIP_2 hydrolysis by phospholipases is a key step in scission of synaptic vesicle membrane during endocytosis following exocytosis (Liu et al., 2009). Because endocytosis and exocytosis are functionally coupled and successful endocytosis is necessary for exocytosis (Hosoi et al., 2009), PLC-mediated PIP_2 hydrolysis may help maintain available release sites or a pool of recycling synaptic vesicles. Blockade of PLC and therefore PIP_2 hydrolysis in our experiments may result in a depletion of available presynaptic release sites due to incomplete endocytosis of vesicles fused in response to hypertonic solution.

DAG analogues only partially rescue inhibition of RRP by PLC blockade.

We hypothesized that PLC blockade may mediate its inhibition of RRP size by decreasing DAG levels in the presynaptic membrane. Phorbol esters increase both the size and recovery rate of the RRP of synaptic vesicles evoked with hypertonic sucrose solution (Stevens and Sullivan, 1998). We predicted that if the inhibition of sucrose-induced currents by PLC blockade resulted from a depletion of DAG, then application of exogenous phorbol ester should rescue sucrose-induced EPSCs. We evoked hypertonic sucrose-induced currents every 100 seconds while simultaneously applying U73122 and PDBu. Representative traces from one recording of sucrose-induced EPSCs sampled both 300 and 600 seconds after application of U73122 show that U73122 still inhibited neurotransmitter release in the presence of PDBu (Fig. 2.5A). The average normalized diary plots of total sucrose-induced charge transfer versus time suggest that phorbol ester application may slow the inhibition of RRP currents by PLC blockade (Fig 2.5B). A comparison of total sucrose-induced charge transfer between 500 and 600 seconds after onset of U73122 application reveals that inhibition of RRP is less complete in the presence of PDBu. Average total charge transfer was 0.14 ± 0.03 and 0.28 ± 0.02 of control for U73122 alone and U73122 + PDBu ($p = 0.02$, $n = 14$ and 6 data points, respectively). However, the two curves intersect and inhibition is equal by 700 seconds of U73122 application (Fig. 2.5B). Average time constants for inhibition of sucrose-induced currents by U73122 were 220 ± 44 and 349 ± 86 seconds for U73122 alone and U73122 + PDBu, suggesting that PDBu slows RRP inhibition, however this difference was

not statistically significant ($p = 0.18$, $n = 8$ and 3, respectively). Additional recordings should be made in the presence of PDBu to more clearly elucidate whether or not inhibition of RRP by U73122 is slowed by PDBu. Taken together, these results suggest that inhibition of neurotransmitter release by PLC blockade may be mediated partially by a decrease in DAG levels in the presynaptic membrane, however the role of DAG appears to be minor.

CONCLUSIONS

We have demonstrated multiple effects of the PLC inhibitor, U73122 on synaptic transmission. PLC inhibition regulated spontaneous glutamate release in complex ways, producing a simple and robust decrease in mEPSC frequency in a subset of neurons and multiphasic responses including enhancement of release in others. The relatively inactive analogue of U73122, U73343 enhanced spontaneous release indicating an effect of the aminosteroid compounds on spontaneous glutamate release that is independent of PLC activity. Relative to the negative control compound, U73122 on average produced a marked reduction in spontaneous release rates.

We further investigated the role of PLC activity in synaptic transmission by eliciting exocytosis of the readily releasable pool of synaptic vesicles with hypertonic sucrose solution during PLC inhibition. PLC inhibition with U73122 produced a substantial decrease in sucrose-induced currents that was accelerated with increased stimulation frequencies and was prevented to only a minor extent by application of phorbol ester. These results suggest that PLC activity maintains synaptic transmission by mechanisms in addition to controlling presynaptic DAG levels, and indicate that PLC has a general role in synaptic recovery from exocytosis, possibly by facilitating endocytosis of fused vesicles. Future experiments in which PIP_2 levels are manipulated by additional means should be performed to test this hypothesis.

We also asked whether the enhancement of spontaneous release by extracellular Ca^{2+} required PLC activity. The enhancement of mEPSC frequency in response to elevation of $[Ca^{2+}]_o$ was markedly reduced after 20 minutes of U73122 application. These data suggest that extracellular Ca^{2+} may act through activation of PLC to promote spontaneous vesicle fusion. However, the effect of U73122 on RRP currents suggests a more general role for PLC activity in maintaining synaptic vesicle fusion. Thus, it may not be safe to conclude that extracellular Ca^{2+} stimulates spontaneous release by activation of PLC, since PLC may mediate its effects at a downstream step common to the fusion of vesicles in response to any stimuli. We then measured the Ca^{2+}-enhancement of spontaneous release after application of phorbol ester to stimulate DAG dependent pathways and increase spontaneous release. Elevation of $[Ca^{2+}]_o$ enhanced mEPSC frequency to a similar extent both before and after PDBu application, arguing against DAG being a downstream signaling molecule activated by extracellular Ca^{2+} and promoting spontaneous release. More experiments will be required to better understand signaling pathways downstream of extracellular Ca^{2+} coupling to spontaneous vesicle fusion.

It is also worth noting that although the effects of U73122 on spontaneous glutamate release were variable between recordings and sometimes an enhancement of release was measured, U73122 always inhibited RRP currents evoked with hypertonic sucrose. This inhibition was clear even when currents were elicited at 100 second intervals.

METHODS

Neuronal preparation. Neocortical neurons were isolated from P1-2 mouse pups. All animal procedures were approved by OHSU I.A.C.U.C. in accordance with the U.S. Public Health Service Policy on Humane Care and Use of Laboratory Animals and the N.I.H. Guide for the Care and Use of Laboratory Animals. Animals were deeply anesthetized with isoflurane before decapitation and removal of cortices. Cortices were then incubated in trypsin and DNAse and then dissociated with a heat polished pipette. Dispersed cells were cultured in MEM plus 5% FBS on glass coverslips. ARAC (4 μM final concentration) was added 48 hours after plating to limit glial division. Cells were used after at least 14 days in culture.

Electrophysiological recordings. Cells were visualized with an Olympus IX70 inverted microscope. Recordings were made in whole-cell voltage clamp mode. Holding potential was -70 mV corrected for liquid-junction potentials. Extracellular solutions contained (in mM; unless otherwise noted) 150 NaCl, 4 KCl, 10 HEPES, 10 glucose, 1.1 $CaCl_2$, 1.1 $MgCl_2$, pH 7.35. For high $[Ca^{2+}]_o$ experiments, substitution of NaCl with $CaCl_2$ was made to maintain osmolarity. Recordings of mEPSCs and hypertonic sucrose-induced currents were made in the presence of tetrodotoxin (TTX, 1 μM) and bicuculline (Bic, 10 μM) to block Na^+ channels and GABA-activated currents, respectively. Both potassium gluconate and cesium methane-sulfonate intracellular solutions were used.

Potassium gluconate solution consisted of (in mM) 113 K^+ gluconate, 9 EGTA, 10 HEPES, 4 MgCl2, 1 CaCl2, 4 NaATP, 0.3 NaGTP, 14 creatine phosphate, pH 7.2. Cesium methane-sulfonate solution consisted of 108 Cs^+ MeSO3, 9 EGTA, 10 HEPES, 4 MgCl2, 1 CaCl2, 4 NaATP, 0.3 NaGTP, 14 creatine phosphate, pH 7.2. Electrode tips had final resistances of 3-7 MΩ. Currents were recorded with a HEKA EPC9/2 amplifier. For mEPSC recordings, currents were filtered at 1 kHz using a Bessel filter and sampled at 10 kHz. Series resistance (Rs) was monitored, and recordings were discarded if Rs changed significantly during the course of a recording. Often Rs was compensated 60-70%. For recording of hypertonic sucrose-induced currents, currents were filtered at 3 kHz and sampled at 20 kHz. Rs was compensated by at least 70%.

Solution and drug application. For recordings of mEPSCs, solutions were bath applied through a perfusion pipette placed ~1 mm from the patch pipette tip. Perfusion pipette was attached to a manifold (Warner Instruments) through which multiple solutions could flow. Local solution equilibration occurred in <10 seconds as measured by open-tip conductance changes. U73122 and U73433 exhibit minimal solubility in aqueous buffers, and only low solubility (1-5 mM) in DMSO. In order to optimize final concentration of U73122 and dilution of solvent, U73122 and U73343 stocks were prepared in DMSO at 5 mM and diluted 1/1000 for experiments. This provided a final DMSO concentration of 0.1% in our recording solution, which had no effect in control experiments. Preparation of stocks

required heating to 30°C in water bath with agitation from ultrasonic frequency waves.

For evoking of RRP currents, extracellular Tyrode's solution containing sucrose (500 mM added) was applied to neurons for 5 seconds with a custom-built Piezo-driven perfusion system described previously (Vyleta and Smith, 2008). Briefly, a piece of double-barreled theta glass was used to perfuse both control and hypertonic sucrose solutions simultaneously. A whole-cell recording was made from a neuron being bathed only by the control solution. Upon stimulation by a high-voltage stimulus isolator (World Precision Instruments, Sarasota, Florida, product # A365D), a Piezo bimorph (Piezo Systems, Inc., product # T234-A4CL-203X) moved the tip of the theta glass horizontally so that the recording was then bathed by extracellular solution containing hypertonic sucrose. Each barrel of the theta glass contained two small perfusion capillaries allowing sucrose-induced currents to be measured between either a pair of control or drug-containing solutions.

Analysis. Data were acquired on a PIII computer and analyzed with IgorPro (Wavemetrics, Lake Oswego, OR) and Minianalysis (Synaptosoft, Decatur, GA) software. mEPSC data were normalized to the average mEPSC frequency during at least 100 seconds of recording in baseline $[Ca^{2+}]_o$ and $[Mg^{2+}]_o$ (both 1.1 mM). mEPSC frequency was averaged into 10 second bins. Curve fitting was performed using IgorPro. Statistical significance was determined using Student's t-test or Mann-Whitney test as appropriate (Microsoft EXCEL, Richmond, WA;

Graphpad Prism). p-values < 0.05 were considered significant. Averaged data values are reported as means ± SEM.

Hypertonic sucrose-induced charge transfer was calculated as the integral of the total currents induced over 5 seconds of sucrose application. Duration of sucrose application was clearly identified by stimulus artifacts in the recordings (Figs. 2.3-5). As some of the currents did not show a clear transient and steady-state phase, total current was integrated in all experiments without subtracting off a steady-state component representing RRP refilling (Stevens and Sullivan, 1998).

FIGURES/FIGURE LEGENDS

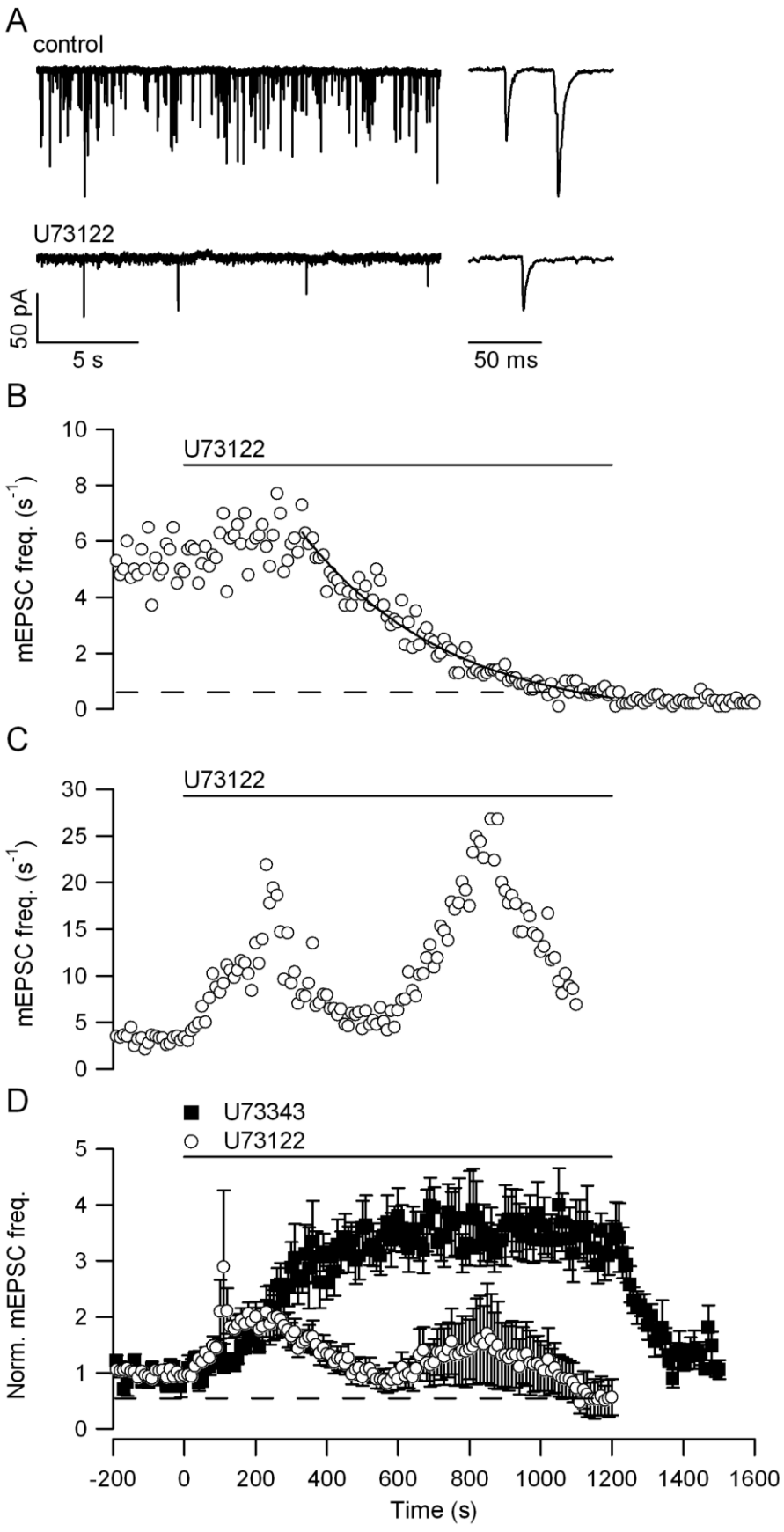
A
control
U73122
50 pA
5 s
50 ms
B
U73122
mEPSC freq. (s-1)
C
U73122
mEPSC freq. (s-1)
D
U73343
U73122
Norm. mEPSC freq.
Time (s)

Figure 2.1. PLC inhibition by U73122 reduces mEPSC frequency in a subset of neurons. (A) Representative mEPSC traces before (top) or after (bottom) 20 minute U73122 (5 μM) application. Traces shown on expanded time scale on right. (B) Representative diary plot of mEPSC frequency versus time for one recording. U73122 slightly elevated and then reduced mEPSC frequency to ~ 12 % of baseline (dashed line). Decay fit with single exponential function with τ = 405 seconds. Note that spontaneous release continues to decrease even after washout of drug. (C) Representative diary plot for another recording showing a different response to U73122. U73122 induced oscillating behavior in mEPSC frequency, including a strong late-phase enhancement. (D) Average normalized diary plots of mEPSC frequency versus time for application of either U73122 (n = 7-12, decreasing with time) or inactive analogue U73343 (5 μM, n = 5). U73343 produced a robust potentiation of spontaneous release that was completely reversible. U73122 on average produced complex effects including early increase and late oscillation to below baseline levels (dashed line at 0.54).

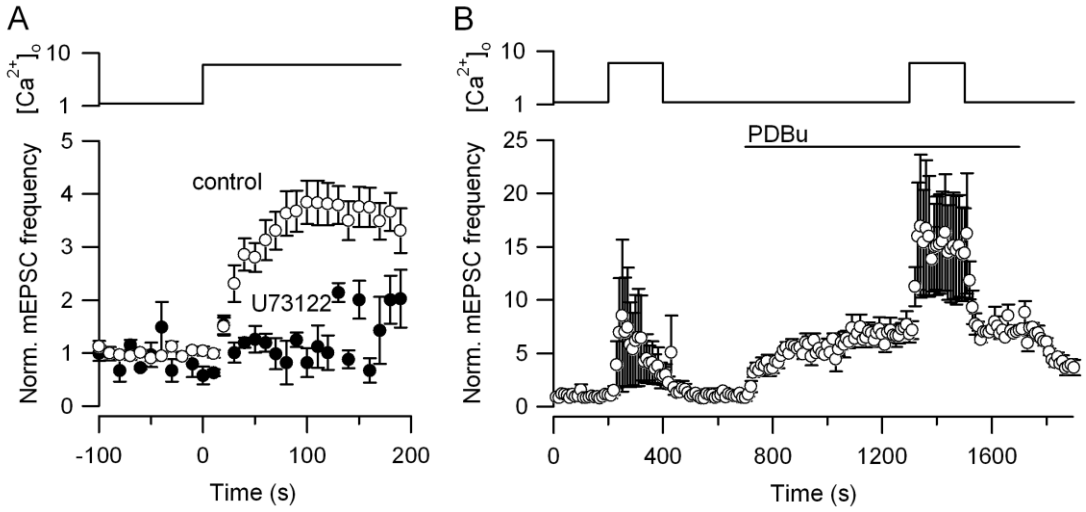

Figure 2.2. PLC activity is required for enhancement of spontaneous glutamate release by extracellular Ca^{2+}. (A) Average normalized diary plots of mEPSC frequency versus time showing changes in spontaneous release when $[Ca^{2+}]_o$ was elevated from 1.1 to 6 mM in control conditions (open circles, n = 14) or after 20 minutes incubation in U73122 (5 μM, closed circles, n = 3). $[Mg^{2+}]_o$ = 0.5 mM for experiments in (A). (B) Average diary plot shows effect of elevating $[Ca^{2+}]_o$ from 1.1 to 6 mM on mEPSC frequency either before or after phorbol ester application (PDBu, 1 μM, n = 3). PDBu does not occlude the enhancement of spontaneous release by extracellular Ca^{2+}.

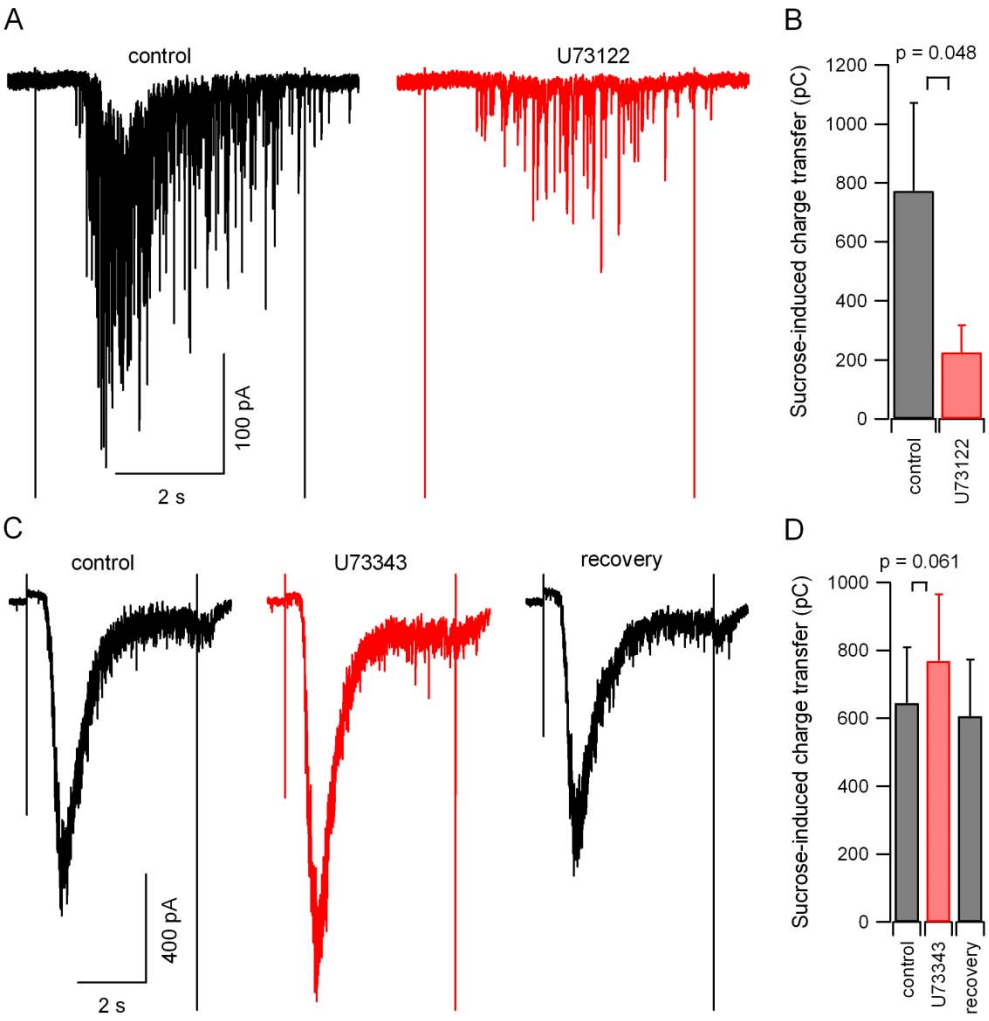

Figure 2.3. PLC blockade reduces the size of the readily releasable pool of synaptic vesicles. (A) Representative traces from one neuron of hypertonic sucrose (500 mM) directly before (control, black) and at the end of a 20 minute application of U73122 (5 μM, red). (B) Histograms show summary data from experiments represented in (A). On average, U73122 inhibited total sucrose-induced charge transfer by 73 % (n = 7). (C) Representative traces from one neuron of H.S.-induced currents before (control, black), after 20 minute

application of U73343 (5 μM, red), or after 5 minutes washout (recovery, black). U73343 reversibly increased sucrose-induced currents. (D) Summary data of U73343 effect on total sucrose-induced charge transfer (n = 7 for control and U73343 comparison, 4 for recovery).

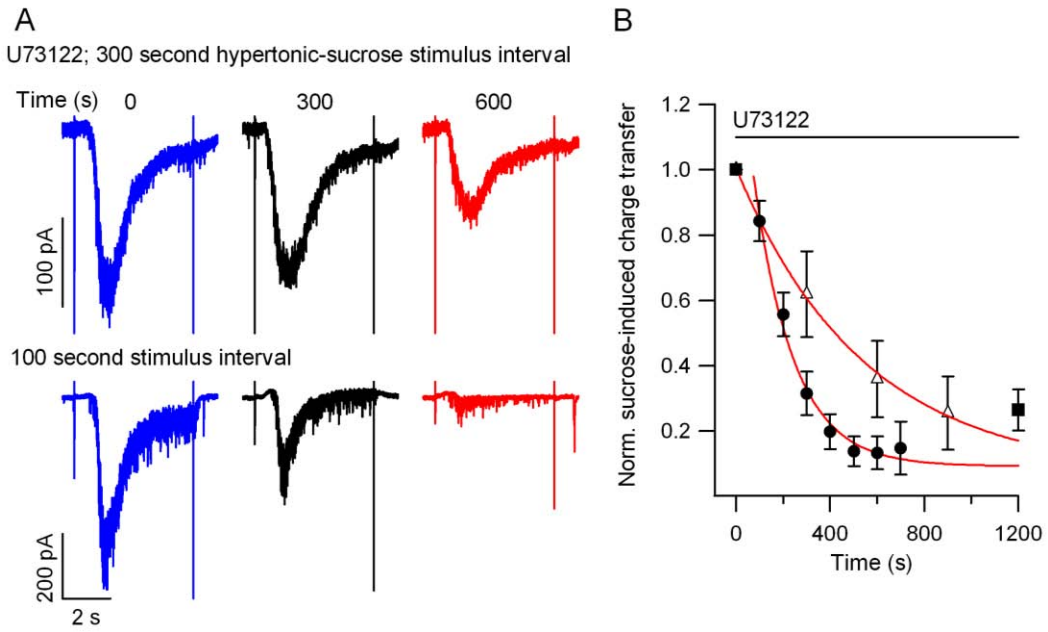

Figure 2.4. Inhibition of exocytosis by PLC blockade is accelerated by enhanced vesicle turnover. (A) Hypertonic sucrose-induced currents evoked every 300 seconds for one recording (top), or evoked every 100 seconds for another recording (bottom). Traces represent currents elicited just before (blue), 300 seconds after (black), or 600 seconds after (red) onset of U73122 application (5 μM). Note that inhibition of readily releasable pool is more complete at higher stimulation frequency. (B) Average normalized diary plots of sucrose-induced charge transfer versus time for different interstimulus intervals. For all datasets, U73122 was applied at time = 0. Inhibition of readily releasable pool was faster if currents were evoked every 5 minutes (300 s) than for every 20 minutes (open triangles compared to closed square, n = 3-5 and 7, respectively), and faster yet if evoked every 100 seconds (closed circles, n = 4-9). Average data were best fit

with single exponential functions with time constants of 545 and 169 seconds for 300 and 100 second interstimulus intervals, respectively.

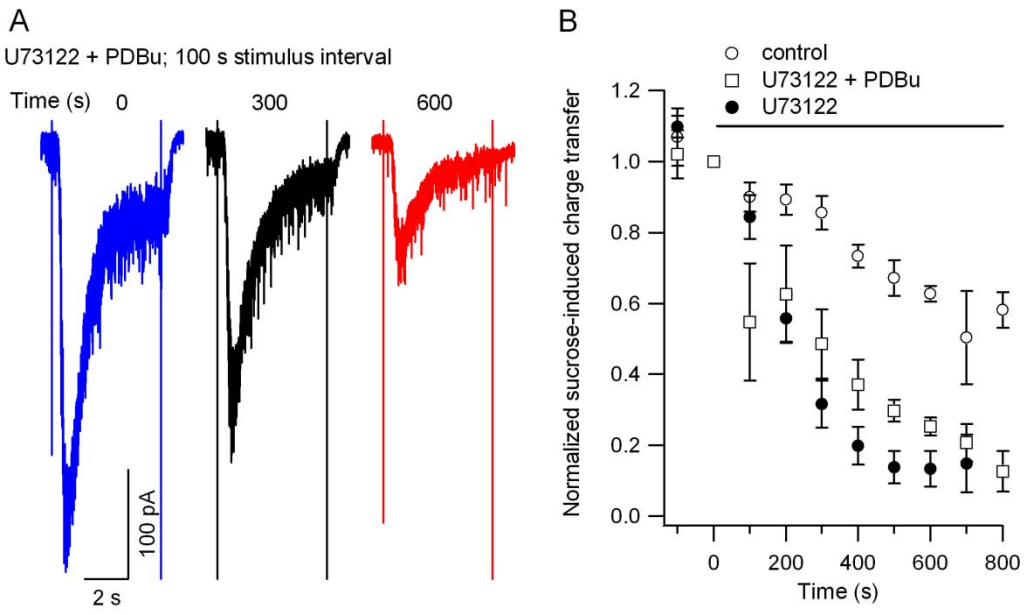

Figure 2.5. Phorbol esters only partially prevent inhibition of readily releasable pool by PLC blockade. (A) Hypertonic sucrose-induced currents evoked at 100 second interval from representative recording. Traces show currents recorded just before (blue), 300 seconds after (black), or 600 seconds after (red) simultaneous application of U73122 (5 μM) and PDBu (1 μM). (B) Average normalized diary plots of total sucrose-induced charge transfer versus time for currents evoked with 100 second interstimulus interval in control conditions (open circles, n = 4-6), during application of U73122 alone (closed circles, n = 4-9,), or during simultaneous application of U73122 and PDBu (open squares, n = 3-5). Data normalized to values at time = 0.

CHAPTER 3

Fast Inhibition of Glutamate-activated Currents by Caffeine

CHAPTER 3

Fast Inhibition of Glutamate-activated Currents by Caffeine

Nicholas P. Vyleta & Stephen M. Smith.

Division of Pulmonary & Critical Care Medicine, Oregon Health & Science University, Portland, OR 97239.

PLoS ONE 3(9): e3155.

NPV performed all experiments within the study and designed and built a custom Piezo-driven perfusion system making glutamate and NMDA application experiments possible. NPV wrote the manuscript with revisions by SMS.

ABSTRACT

Background Caffeine stimulates calcium-induced calcium release (CICR) in many cell types. In neurons, caffeine stimulates CICR presynaptically and thus modulates neurotransmitter release.

Methodology/Principal Findings Using the whole-cell patch-clamp technique we found that caffeine (20 mM) reversibly increased the frequency and decreased the amplitude of miniature excitatory postsynaptic currents (mEPSCs) in neocortical neurons. The increase in mEPSC frequency is consistent with a presynaptic mechanism. Caffeine also reduced exogenously applied glutamate-activated currents, confirming a separate postsynaptic action. This inhibition developed in tens of milliseconds, consistent with block of channel currents. Caffeine (20 mM) did not reduce currents activated by exogenous NMDA, indicating that caffeine block is specific to non-NMDA type glutamate receptors.

Conclusions/Significance Caffeine-induced inhibition of mEPSC amplitude occurs through postsynaptic block of non-NMDA type-Ionotropic glutamate receptors. Caffeine thus has both pre and postsynaptic sites of action at excitatory synapses.

INTRODUCTION

The popular stimulant, caffeine, modulates intracellular calcium signaling in many cell types (Ehrlich et al., 1994). The ryanodine receptor (RyR) is one target for caffeine. Millimolar concentrations (5-20 mM) of caffeine stimulate calcium-induced calcium release (CICR) from intracellular stores. Caffeine sensitizes RyR so that low nanomolar concentrations of cytosolic calcium activate RyR leading to calcium efflux into the cytoplasm (Rousseau et al., 1988). In addition, caffeine also acts on the other primary endoplasmic reticulum calcium release channel, the inositol triphosphate receptor (IP_3R), over the same concentration range. Caffeine inhibited IP_3R single-channel openings with a half-maximal inhibition of 1.6 mM (Bezprozvanny et al., 1994). Therefore, depending on the relative densities of RyR and IP_3R in a particular cell, caffeine can either stimulate or block calcium release from intracellular stores.

Caffeine has been used extensively to study calcium signaling in neurons. Caffeine increases spontaneous glutamate release from nerve terminals (Sharma and Vijayaraghavan, 2003) and can induce presynaptic long-term potentiation (Martin and Buno, 2003). Synaptically activated AMPA receptor-mediated CICR has also been described using caffeine (Morton-Jones et al., 2007).

Here, we demonstrate that caffeine decreases the size of miniature excitatory postsynaptic currents (mEPSCs) recorded from neocortical neurons by directly inhibiting postsynaptic glutamate receptor currents. Consistent with other

reports, we also demonstrate an increase in mEPSC frequency indicating a caffeine-induced presynaptic increase in glutamate release. Thus, caffeine modulation of glutamatergic transmission involves both pre and postsynaptic targets.

RESULTS

Caffeine decreases mEPSC size in neocortical neurons. We examined the effects of caffeine (20 mM) on mEPSCs recorded from neocortical neurons. Sodium channels were blocked by tetrodotoxin (TTX) and spontaneous synaptic events recorded at -70 mV. Caffeine was applied for 300 seconds. The amplitude of mEPSCs decreased during the first 100 seconds of caffeine application (Fig. 3.1A). The insets show representative mEPSCs from the beginning and end of their respective traces on an expanded time scale. The inhibition of mEPSC amplitude was reversible (Fig. 3.1A). Amplitude histograms of all events during 200 seconds of recording directly before caffeine application and all events recorded during the last 200 seconds of caffeine application confirmed this inhibition (Fig. 3.1B). Average mEPSC amplitude is shown for seven cells before, during, and after caffeine application (Fig 3.1C). Average mEPSC amplitude was 27.6 ± 2.3 pA before and 15.7 ± 1.0 pA during caffeine application ($P < 0.001$; $n = 7$), demonstrating a 43 ± 4 % inhibition by caffeine. Miniature EPSC amplitude was reversibly decreased by caffeine in all seven cells. Fig. 3.1D shows average normalized diary plots of mEPSC frequency (top) and amplitude (bottom) for

seven cells. Caffeine increased mEPSC frequency in all seven cells, consistent with previous work (Sharma and Vijayaraghavan, 2003). The increase in mEPSC frequency was slower than the decrease in amplitude, suggesting different sites of action. These data confirm that caffeine increases mEPSC frequency in neocortical neurons, and demonstrate a reduction in mEPSC amplitude not previously described.

Caffeine blocks currents activated by exogenous glutamate. We next asked whether caffeine exerted its effects on mEPSC amplitude by a presynaptic or postsynaptic mechanism. We applied glutamate (1 mM) to test for a direct postsynaptic effect of caffeine on glutamate-activated currents (I_{glu}). Glutamate was applied with a piezoelectric-controlled perfusion device to neurons voltage-clamped at -70 mV. Glutamate was applied for 100 milliseconds and co-application with caffeine reversibly decreased peak I_{glu} amplitude (Fig. 3.2A). In these experiments glutamate applications were made after perfusion with caffeine containing solutions for >30 seconds (top 20 mM and bottom 50 mM). Bar graphs show the average results from glutamate application in the presence of 20 mM caffeine (Fig. 3.2B). Glutamate-activated currents were 3.79 ± 0.71 nA and reduced to1.63 ± 0.35 nA in the presence of caffeine (n = 7; P = 0.002). Currents recovered after caffeine wash to 3.84 ± 0.72 nA (P = 0.10 compared to control). Thus, caffeine (20 mM) reversibly reduced the magnitude of I_{glu} by 57 ± 5 %. The action of caffeine was dose-dependent (Fig 3.2C). Inhibition of I_{glu} by caffeine increased during the application (scaled traces, Fig. 3.2A). Consequently

the steady state concentration-effect relationship was left-shifted relative to that for peak glutamate-activated currents (Fig. 3.2C). Curves represent the equation:

$$I / I_{max} = 1 / [1 + ([caffeine]/IC_{50})^{n}] \quad (1)$$

where IC_{50} was 7 mM and 10 mM for inhibition of the steady-state and peak glutamate-activated currents, respectively.

Caffeine blocks glutamate-activated currents rapidly. In previous experiments (Fig. 3.2) glutamate was applied after >30 seconds of caffeine application. We next measured the kinetics of caffeine block of glutamate-activated currents by applying caffeine (20 mM) simultaneously with glutamate (1 mM). Fig. 3.3 shows I_{glu} with and without caffeine. Each trace is the average I_{glu} elicited by 5 applications of glutamate recorded with a 0.33 Hz duty cycle. Traces did not change substantially between applications. Caffeine block of I_{glu} developed during a 500 ms co-application of glutamate and caffeine. Inhibition is absent during the initial rising phase of I_{glu}, partial during the peak, and reaches steady-state by ~200 ms. The effect was reversible. The time course of caffeine block was quantified by dividing the glutamate-activated current in the presence of caffeine (I_{caff}) by the previous current elicited by glutamate alone. This ratio (I_{caff}/I_{glu}) is plotted as a function of time for the representative recording starting 10 ms after initiation of glutamate application (black, Fig. 3.3 inset). This decay was fit with a single exponential function with a time constant of 57 ms. The average time constant for inhibition was 52 ± 12 ms (n = 3). The dashed line

represents the steady-state inhibition of I_{glu} and crosses the y-axis at 0.27 for this recording. The average steady-state value for I_{caff}/I_{glu} was 0.29 ± 0.02, which agrees well with the inhibition of steady-state I_{glu} in the presence of steady-state caffeine concentration (0.28, Fig. 3.2C). Thus, caffeine action is rapid, and I_{glu} blockade develops during glutamate application (Fig. 3.2). These data demonstrate that caffeine inhibits glutamate receptor current by a fast mechanism, consistent with simple channel block but not consistent with more complex forms of regulation such as changes in receptor expression.

Caffeine-mediated block of glutamate receptor currents is specific for non-NMDA type-Ionotropic glutamate receptors. Both AMPA and NMDA-activated currents are activated by glutamate application to neocortical neurons. The mEPSCs in neocortical neurons were blocked by CNQX and thus are mediated by non-NMDA receptors (data not shown). To test if caffeine also blocked NMDA-activated currents we applied NMDA (20 μM) in the absence and presence of caffeine. NMDA-mediated currents (I_{NMDA}) were evoked in the presence of 2.5 μM glycine and in the absence of extracellular magnesium every 2 minutes. I_{NMDA} were minimally affected by the application of 20 mM caffeine (Fig. 3.4A). Average data for NMDA application to six cells is shown in Fig. 3.4B. I_{NMDA} was 3.09 ± 0.59 nA before and 2.92 ± 0.56 nA in the presence of 20 mM caffeine (n = 6; P = 0.21). After caffeine wash, I_{NMDA} recovered to 3.18 ± 0.64 (P = 0.39 compared to control). In addition, glutamate (200 μM) was applied to neurons in the presence of CNQX (25 μM) and glycine (2.5 μM) in the absence

of magnesium. These NMDA receptor-mediated currents did not change in the presence of 20 mM caffeine (n = 2, data not shown). Our results confirm that caffeine-mediated inhibition of mEPSC amplitude and I_{glu} are not mediated by NMDA receptors.

DISCUSSION

Caffeine modulates intracellular calcium and can stimulate neurotransmitter release from nerve terminals (Sharma and Vijayaraghavan, 2003). We determined that the frequency of spontaneous transmitter release was increased in recordings from neocortical neurons. Surprisingly, caffeine also produced an accompanying decrease in the amplitude of quantal events. Caffeine inhibited currents activated by direct application of glutamate to cortical neurons, confirming a postsynaptic site of action. This unexpected form of inhibition developed over tens of milliseconds and was independent of NMDA receptors, consistent with non-NMDA receptor block.

Caffeine modulates synaptic transmission by both pre- and postsynaptic mechanisms. We found that caffeine increased the frequency of mEPSCs, consistent with a previous report (Sharma and Vijayaraghavan, 2003) (Fig. 3.1). A change in the frequency of spontaneous neurotransmitter release events is a clear indicator of a presynaptic change in the probability of vesicle fusion. A change in quantal size could result from either pre or postsynaptic mechanisms (Edwards, 2007) – variation in mEPSC size was recently shown to depend on

vesicular glutamate concentration (Wu et al., 2007). We postulated that caffeine-mediated changes in mEPSC amplitude and frequency (Fig. 3.1) both resulted from presynaptic modulation. However, the distinct time courses of both changes pointed to different mechanisms of action (Fig. 3.1D). Caffeine inhibited currents activated by exogenous glutamate and quantal events by a similar amount confirming a postsynaptic action. We postulated two mechanisms by which caffeine mediated these effects: by directly blocking the glutamate activated channels or by reducing postsynaptic glutamate receptor density. However, decreases in receptor density due to endocytosis of AMPA receptors (AMPARs) is probably too slow to explain this effect since it occurs over tens of seconds(Ashby et al., 2004). In contrast, caffeine mediated block of I_{glu} was rapid, developing in tens of milliseconds (Fig. 3.3), or ~1000 times faster than endocytosis of receptors. These data support the proposal that caffeine decreases mEPSC amplitude by direct postsynaptic block of glutamate-activated channels.

Caffeine mediated inhibition of mEPSCs was slightly smaller than inhibition of peak glutamate-activated currents (43% vs. 57%, respectively). While this observation could be due to extrasynaptic glutamate receptors being more sensitive to caffeine, we feel it more likely reflects a sampling bias caused by selecting mEPSCs based on an amplitude threshold. Our use of a threshold means that proportionately more of the smaller mEPSCs in caffeine failed to reach detection reducing the amount of caffeine-mediated inhibition. This effect is evident in the mEPSC amplitude histogram (Fig. 3.1B).

Caffeine modulation of glutamate signaling. Recently it was reported that caffeine blocks CICR triggered by calcium influx through calcium permeable AMPARs (Morton-Jones et al., 2007). Glutamate or AMPA-induced increases in intracellular calcium concentration were decreased in the presence of caffeine. This result was interpreted as a caffeine-induced depletion of ryanodine-sensitive calcium store calcium. Our results provide an additional interpretation to their data: that caffeine directly blocks AMPAR-mediated calcium currents responsible for CICR. Morton-Jones et al. provide strong additional evidence, however, that glutamate-activated intracellular calcium increases are mediated by CICR by blocking them with the RyR blocker ryanodine.

In contrast to our findings, caffeine (10 mM) has been reported to increase mEPSC amplitude in recordings from barrel cortex slices (Simkus and Stricker, 2002). The authors showed an increase in median mEPSC amplitude from ~ 2.5 to 4.5 pA in the presence of caffeine. These small mEPSCs would have been difficult to distinguish from baseline fluctuations by automated analysis. In fact, the median event size represented only 3-4 channel openings (using AMPA-activated channel conductance ~ 10 pS (Swanson et al., 1997) and 70 mV driving voltage). It is possible that these small events reflected baseline channel activity that was mischaracterized as representing mEPSCs. If caffeine application increased mEPSC frequency, and these mEPSCs were larger than the baseline events, this would have resulted in an apparent increase in mEPSC size. The mEPSCs we recorded were much larger (19 to 39 pA; Fig. 3.1C) and

clearly distinguished from baseline activity since our detection threshold was ~5 pA. Thus the increased signal-noise ratio in our experiments provides strong evidence that caffeine inhibits mEPSC amplitude.

Caffeine actions *in vivo*. The widespread use of caffeine begs the question whether glutamate receptor blockade may occur in humans. Caffeine concentration in blood reaches only 60 μM after ingestion of the equivalent of 4 cups of coffee (Cysneiros et al., 2007). The blood-brain barrier is readily permeable to caffeine, so the concentration in the brain is close to that in the blood (Liu et al., 2006). Since caffeine inhibits glutamate receptors with an apparent IC_{50} of ~10 mM (Fig. 3.2C, equation 1) we suggest that ingested caffeine is unlikely to have any effect on ionotropic glutamate receptors. Instead caffeine likely produces stimulatory effects in humans through its potent antagonism of the adenosine receptor (IC_{50} 50-100 μM) (Daly et al., 1983). Adenosine-mediated activation of A1 adenosine receptors on nerve terminals impairs synaptic transmission by inhibiting voltage-gated calcium channels (Gundlfinger et al., 2007). Thus, one mechanism by which normal physiological levels of caffeine stimulates synaptic transmission is by inhibiting the adenosine binding, relieving the inhibition of voltage-gated calcium channels and producing higher probability of release of neurotransmitter.

However, it is possible that excess use of caffeine tablets may lead to brain levels at which glutamate-activated channel modulation occurs. For instance, acute caffeine toxicity has been blamed for the death of a 22-yr old woman who

experienced serum caffeine levels of ~8 mM following overdose with diet pills (Mrvos et al., 1989).

CONCLUSIONS

We have demonstrated a novel action of caffeine on excitatory transmission in the central nervous system. We show that, in addition to increasing the probability of spontaneous release of neurotransmitter, caffeine inhibits postsynaptic AMPA-type glutamate-activated channels. This occurred at caffeine concentrations regularly used for studying intracellular calcium signaling. Furthermore, our results are consistent with the hypothesis that caffeine-mediated glutamate receptor blockade may only occur under extreme conditions of toxicity.

METHODS

Neuronal preparation. Neocortical neurons were isolated from P1-2 mouse pups. All animal procedures were approved by OHSU I.A.C.U.C. in accordance with the U.S. Public Health Service Policy on Humane Care and Use of Laboratory Animals and the N.I.H. Guide for the Care and Use of Laboratory Animals. Animals were deeply anesthetized with isoflurane before decapitation and removal of cortices. Cortices were then incubated in trypsin and DNAse and then dissociated with a heat polished pipette. Dispersed cells were cultured in

MEM plus 5% FBS on glass coverslips. ARAC (4 μM final concentration) was added 48 hours after plating to limit glial division. Cells were used after at least 14 days in culture. Eight different neuronal culture preparations from eight different mice were used for these experiments.

Electrophysiological recordings. Cells were visualized with an Olympus IX70 inverted microscope. Recordings were made in whole-cell voltage clamp. Holding potential was -75 mV. Extracellular solutions contained (in mM) 150 NaCl, 4 KCl, 10 HEPES, 10 glucose, pH 7.35. NaCl was substituted with either caffeine or sucrose to maintain osmolarity. Recordings of mEPSCs were made in the presence of TTX (1 μM) and bicuculline (10 μM) to block Na channels and GABA-activated currents, respectively. TTX was also used during glutamate application experiments. Intracellular solution consisted of (in mM) 140 K^+ gluconate, 9 EGTA, 10 HEPES, 4 $MgCl_2$, 1 $CaCl_2$, 4 NaATP, 0.3 NaGTP, 1.4 phosphocreatine, pH 7.2. Electrode tips had final resistances of 3-6 MΩ. Currents were recorded with a HEKA EPC9/2 amplifier. For mEPSC recordings, currents were filtered at 1 kHz using a Bessel filter and sampled at 10 kHz. For recordings of currents evoked by applied glutamate, currents were filtered at 3 kHz and sampled at 20 kHz. Series resistance (R_s) was monitored, and recordings were discarded if R_s changed by more than 10 % during recording. For glutamate-application experiments, R_s was usually compensated by ~70 %. We estimate that in a typical experiment our inhibition of I_{glu} by caffeine (20 mM) is underestimated by ~9% (Traynelis, 1998).

Solution application. For mEPSC recordings, solutions were bath applied through a perfusion pipette placed ~1 mm from the patch pipette tip. Local solution equilibration occurred in <10 seconds as measured by open-tip conductance changes. For fast application of glutamate, a custom-built piezoelectric-driven perfusion system was used. A piece of theta glass containing four small perfusion tubes (two in each barrel) was mounted to a piezoelectric bimorph (Piezo Systems, Inc., product # T234-A4CL-203X) which was mounted to a plastic rod controlled by a micromanipulator. A high-voltage stimulus isolator (World Precision Instruments, Sarasota, Florida, product # A360D or A365D) was used to stimulate the bimorph. A TTL pulse supplied by one of the digital-to-analog outputs on the EPC9/2 was used to drive the stimulus isolator. Theta glass was pulled and broken to a tip diameter of approximately 300 microns. A smooth break of barrels and septum was achieved to minimize solution mixing at tip. During a whole-cell voltage clamp recording, the perfusion tip was located so that zero steady-state glutamate activated current was detected. Stimulation of the bimorph moved the solution interface across the neuron. Time of perfusion change to whole neuron was estimated with open-tip conductance measurements with electrode tip at a distance from the theta tube characteristic of a cell soma. Total solution change in this configuration occurred in ~5 ms.

Analysis. Data were acquired on a PIII computer and analyzed with IgorPro (Wavemetrics, Lake Oswego, OR) and Minianalysis (Synaptosoft, Decatur, GA)

software. For all experiments, statistical significance was determined using Student's t-test as appropriate (Microsoft EXCEL, Richmond, WA). Averaged data values are reported as means ± SEM.

FIGURES/FIGURE LEGENDS

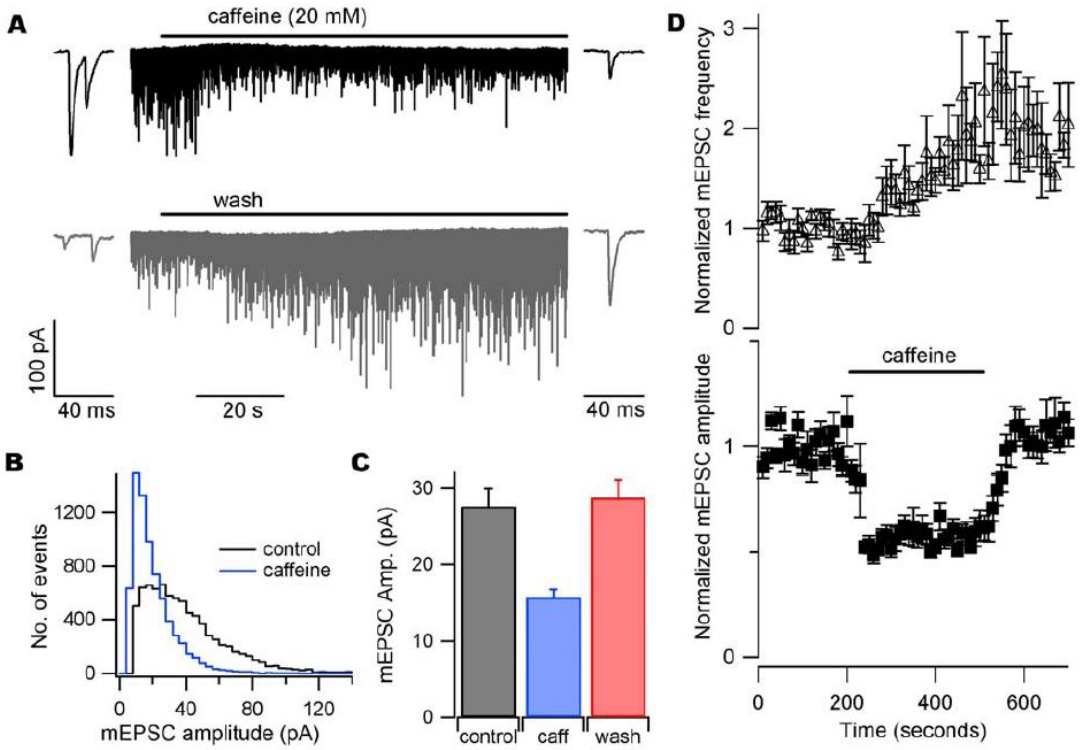

Figure 3.1. Caffeine reversibly decreases mEPSC amplitude. (A) Recording of mEPSCs in whole-cell voltage-clamp in the presence of TTX (1 μM). Caffeine (20 mM) caused a clear reversible decrease in mEPSC size. The fast rise and exponential fall of synaptic currents was clear throughout recording (insets). (B) Amplitude histograms of events in A 200 seconds immediately before caffeine (black) and during the last 200 seconds of caffeine application (blue). (C) Average mEPSC amplitudes for seven cells before (black), during (blue), and after (red) caffeine application. (D) Normalized average diary plots of mEPSC frequency (top) and amplitude (bottom), n = 7. Bin size = 10 seconds. Each point is normalized to the average of 200 seconds of data recorded before drug application.

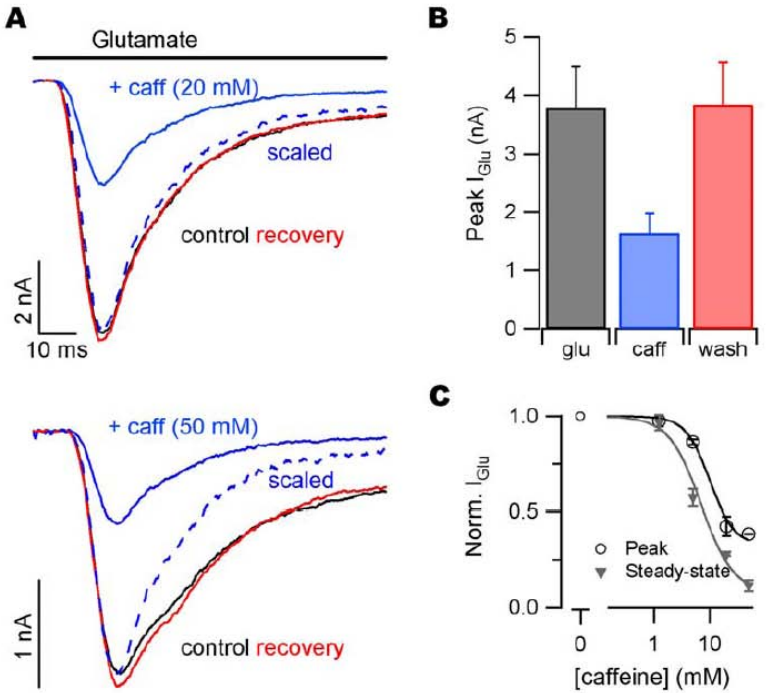

Figure 3.2. Caffeine inhibits postsynaptic glutamate-activated currents (I_{glu}). (A) Glutamate (1 mM) was applied to neurons in whole-cell voltage clamp in the presence of TTX. Individual traces from a representative recording of I_{glu} before (black), during (blue) and after (red) the addition of 20 mM (top) or 50 mM (bottom) caffeine. (B) Average peak I_{glu} for 5 consecutive applications of glutamate (3 second interval) before, during, and after 20 mM caffeine application. (C) Normalized peak (open circles) and steady-state (closed triangles) I_{glu} for 1.25, 5, 20, and 50 mM caffeine. Values normalized to average peak or steady-state I_{glu} before caffeine for each recording. Curves represent Equation 1.

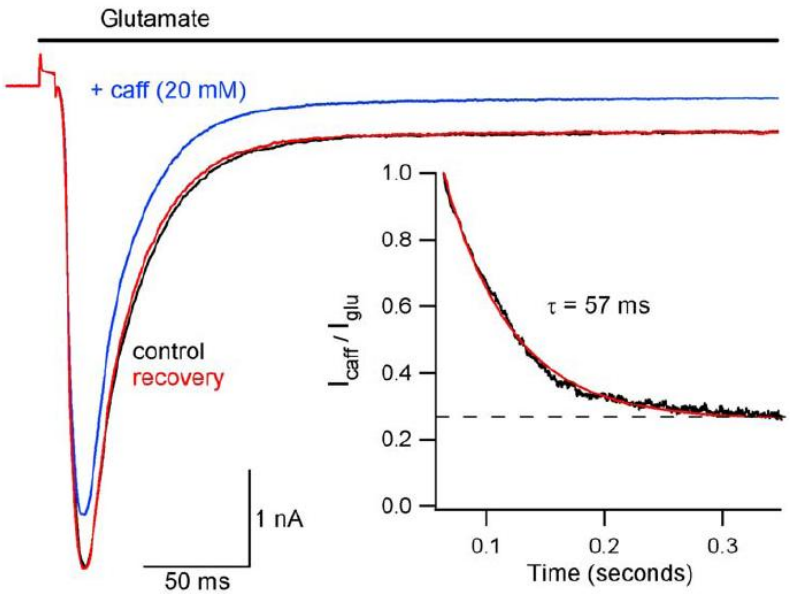

Figure 3.3. Caffeine rapidly inhibits glutamate-activated currents. After control recording of I_{glu} (black), glutamate was applied simultaneously with 20 mM caffeine (I_{caff}; blue). Recovery is shown in red. Traces are averages of 5 consecutive applications of glutamate or glutamate plus caffeine (3 second interval). Inset: I_{caff} / I_{glu} plotted versus time for representative cell (black) to show time course of inhibition of I_{glu} by caffeine. Calculation was started 10 ms after start of glutamate application, shortly before peak of I_{glu}. Decay was fit to a single exponential (red curve). Steady-state inhibition of I_{glu} (dashed line) is 0.27 for this recording.

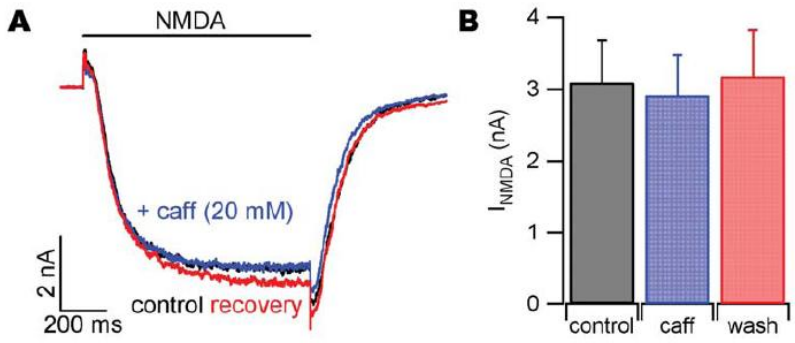

Figure 3.4. Caffeine does not inhibit postsynaptic NMDA-receptor mediated currents (I_{NMDA}). (A) NMDA (20 μM) was applied to neurons in whole-cell voltage clamp in the presence of glycine and TTX, and zero extracellular Mg^{2+}. Individual traces from a representative recording of I_{NMDA} before (black), during (blue) and after (red) the addition of 20 mM caffeine. (B) Average peak I_{NMDA} for single applications of NMDA before, during, and after 20 mM caffeine application (120 second interval).

CONCLUSIONS / FUTURE DIRECTIONS

The results of this thesis have provided insight into mechanisms regulating spontaneous release of glutamate from neocortical nerve terminals. In particular, we now have a greater understanding for how extracellular Ca^{2+} stimulates the spontaneous release process, and, importantly, how it does not. Extracellular Ca^{2+} does not promote spontaneous vesicle fusion by the same means as it does action potential evoked fusion. Notably, Ca^{2+} influx through voltage-activated calcium channels did not mediate spontaneous release. Although extracellular Ca^{2+} was previously assumed to enhance spontaneous release by increases in intracellular [Ca^{2+}], our results demonstrate that spontaneous release was insensitive to chelation of intracellular Ca^{2+} by BAPTA. Thus, our data indicate that extracellular Ca^{2+} enhances spontaneous release by a mechanism other than increasing intracellular [Ca^{2+}]. We provide evidence for a novel role of a presynaptic GPCR, the calcium-sensing receptor in regulation of spontaneous synaptic transmission. Specific CaSR agonists stimulated spontaneous release and $CaSR^{-/-}$ neurons had reduced spontaneous release over the physiological range of $[Ca^{2+}]_o$.

Previously, it was shown that activation of CaSR inhibits a nonselective cation channel conductance in neocortical nerve terminals and decreases synaptic transmission between cultured neocortical neurons (Smith et al., 2004; Phillips et al., 2008; Chen et al., 2010). Our current results add to our understanding of CaSR function in nerve terminals – CaSR activation regulates

spontaneous and action potential-evoked release in opposite directions and with distinct time courses. Our model for CaSR-dependent enhancement of spontaneous release predicts that CaSR will be activated over the physiological range of $[Ca^{2+}]_o$, and will promote spontaneous release even when $[Ca^{2+}]_o$ is reduced by synaptic activity. Importantly, at reduced $[Ca^{2+}]_o$, calcium influx-mediated exocytosis in response to presynaptic action potential is very low due to the steep dependence on $[Ca^{2+}]_o$. Thus, CaSR activation may sustain neurotransmitter release when evoked release is greatly reduced. Because spontaneous release maintains synaptic strength, CaSR stimulation of spontaneous release may play a homeostatic role during periods of reduced action potential-evoked release.

A putative signaling molecule downstream from nerve terminal GPCRs is phospholipase C. We provide evidence that PLC activity plays a crucial role in the maintenance of the readily releasable pool of synaptic vesicles. An antagonist of PLC inhibited exocytosis of the RRP in response to application of hypertonic sucrose solution. This inhibition was significantly faster if the RRP was stimulated more frequently, suggesting that PLC is involved in synaptic recovery from exocytosis. These results suggest that activation of the classical G_q-coupled GPCR signaling pathway and subsequent activation of PLC is an important regulator of nerve terminal function. Inhibition of synaptic transmission by PLC antagonist was not rescued by addition of phorbol esters, suggesting that PLC inhibition reduces neurotransmitter release by mechanisms other than reducing levels of DAG.

We also demonstrated that caffeine increased spontaneous glutamate release, consistent with Ca^{2+} release from intracellular stores being capable of activating spontaneous release. Resulting from this investigation was the demonstration of a novel inhibitory action of caffeine on postsynaptic glutamate receptors. These results add to the body of evidence that intracellular Ca^{2+} release can catalyze exocytosis, and suggest that CICR is present in neocortical nerve terminals. Additionally, our work should impact the use of caffeine as a tool for studying CICR and glutamatergic synaptic transmission – necessitating greater care in interpretation of both past and future data.

Taken together, these results add to our knowledge of how neurotransmitter release is regulated in the nerve terminal. The following questions remain underexplored and should be addressed subsequent to this thesis:

Where does the rest of the extracellular Ca^{2+}-dependence of spontaneous glutamate release come from?

If our model is correct, CaSR is activated over the range of physiological $[Ca^{2+}]_o$ (≤ 1.1 mM), but at baseline $[Ca^{2+}]_o$ and $[Mg^{2+}]_o$ (both 1.1 mM) is responsible for only ~ 30 % of spontaneous release. An appealing candidate for mediating additional extracellular Ca^{2+}-dependence is another GPCR in nerve terminals, GPRC6A (Wellendorph and Brauner-Osborne, 2004). In expression systems this receptor appears to have a lower Ca^{2+}-affinity than CaSR, and a dose-response curve that does not saturate by 60 mM extracellular Ca^{2+}. This is similar to the

dose response relationship between $[Ca^{2+}]_o$ and mEPSC frequency in our neurons, which also does not saturate (Fig. 1.1,1.2) (we have performed experiments with 60 mM extracellular Ca^{2+} and saturation was still not observed). Additional investigation into the contribution of GPRC6A activation to spontaneous release should be performed. In addition, some members of the mGluR family of GPCRs are also activated by extracellular divalent cations, and could presumably couple to spontaneous release (Tabata and Kano, 2004). A type-I mGluR agonist increased mEPSC frequency in neurons from rat barrel cortex (Simkus and Stricker, 2002).

Does PLC activity maintain synaptic vesicle fusion?

Our results indicate that baseline PLC activity has a profound impact on maintaining the ability of the readily releasable pool of vesicles to fuse with the presynaptic membrane. Additional experiments should be performed to corroborate our results of PLC inhibition by U73122 on RRP size (Figs. 2.3-5). An immediate additional experiment is to inhibit PLC with U73122 during extracellular stimulation of EPSCs (Fig. 1.4). We have demonstrated the ability to reliably evoke EPSCs in these neurons over many tens of minutes with stable responses (control experiments, data not shown). This may provide a superior method for measuring the effect of PLC inhibition on synaptic transmission, as evoking release of the RRP with hypertonic sucrose appears to be a harsher stimulus and runs down at a faster rate, even in control conditions (Fig. 2.5).

Future experiments should also use other means of interrogating this pathway in addition to pharmacological inhibition of PLC with U73122. Of particular interest to these future investigations is the PLCβ1 knockout mouse (Wang et al., 2006). PLCβ1 is the phospholipase C in the cortex of the brain activated by the G_q family of G-proteins. We predict that neurons from these mice will have a smaller RRP of synaptic vesicles and that the RRP will recover from stimulation more slowly, consistent with our results with pharmacological inhibition of PLC.

Neurons from these mice could also be used to measure the dependence of spontaneous glutamate release on $[Ca^{2+}]_o$. We predict that if extracellular Ca^{2+} activates one or more presynaptic G_q-coupled GPCRs to stimulate spontaneous vesicle fusion, then the Ca^{2+}-enhancement of spontaneous release should be reduced in these neurons.

What role does calcium release from intracellular stores play in spontaneous glutamate release?

An alternative mechanism for raising $[Ca^{2+}]_i$ involves the release of calcium from intracellular calcium stores. Two distinct calcium release channels activated by different signaling pathways can release calcium from intracellular stores. The IP_3R and the RyR are both high permeability, calcium selective ion channels present in endoplasmic reticulum and mitochondrial membranes. IP_3R is activated by IP_3, a product of PIP_2 hydrolysis PLC. Calcium is the physiological agonist for RyR, producing calcium-induced calcium release. In the cerebellum,

RyR-mediated calcium release in nerve terminals of inhibitory neurons induces large miniature inhibitory postsynaptic currents (Llano et al., 2000). CICR was also shown to produce intracellular calcium transients in hippocampal synaptic boutons, and contribute to spontaneous glutamate release in those neurons (Emptage et al., 2001). The involvement of CICR and IP_3R-mediated signaling in spontaneous release of glutamate from nerve terminals has not been thoroughly evaluated. We demonstrate that pharmacological activation of RyR with caffeine does increase spontaneous release in neocortical neurons. However, our data demonstrating that chelation of intracellular calcium by the exogenous buffer BAPTA-AM does not decrease baseline spontaneous glutamate release or the enhancement of spontaneous release rate by increases in extracellular calcium (Fig. 1.7) argue against intracellular store calcium signaling being a key regulator of spontaneous release in glutamatergic neocortical nerve terminals. Importantly, caffeine could have mediated its effect on mEPSC frequency through signaling pathways other than RyR-mediated Ca^{2+} release from intracellular stores. These include antagonism of adenosine receptors (Daly et al., 1983) inhibition of phosphodiesterases and resulting increases in levels of cyclic-AMP (David, 2001). Further investigation beyond the scope of this thesis will be required to more completely elucidate the contribution of the intracellular calcium store signaling pathways to spontaneous glutamate release.

REFERENCES

Abenavoli A, Forti L, Bossi M, Bergamaschi A, Villa A, Malgaroli A (2002) Multimodal quantal release at individual hippocampal synapses: evidence for no lateral inhibition. J Neurosci 22:6336-6346.

Adler EM, Augustine GJ, Duffy SN, Charlton MP (1991) Alien intracellular calcium chelators attenuate neurotransmitter release at the squid giant synapse. J Neurosci 11:1496-1507.

Ashby MC, De La Rue SA, Ralph GS, Uney J, Collingridge GL, Henley JM (2004) Removal of AMPA receptors (AMPARs) from synapses is preceded by transient endocytosis of extrasynaptic AMPARs. The Journal of Neuroscience 24:5172-5176.

Atasoy D, Ertunc M, Moulder KL, Blackwell J, Chung C, Su J, Kavalali ET (2008) Spontaneous and evoked glutamate release activates two populations of NMDA receptors with limited overlap. J Neurosci 28:10151-10166.

Augustine GJ, Charlton MP (1986) Calcium dependence of presynaptic calcium current and post-synaptic response at the squid giant synapse. J Physiol 381:619-640.

Augustine GJ, Adler EM, Charltonc MP (1991) The calcium signal for transmitter secretion from presynaptic nerve terminals a. Annals of the New York Academy of Sciences 635:365-381.

Awatramani GB, Price GD, Trussell LO (2005) Modulation of transmitter release by presynaptic resting potential and background calcium levels. Neuron 48:109-121.

Awumey EM, Howlett AC, Putney JWJ, Diz DI, Bukoski RD (2007) Ca2+ mobilization through dorsal root ganglion Ca2+ sensing receptor stably expressed in HEK293 cells. American J Physiology Cell Physiology 292:C1895-C1905.

Bai J, Tucker WC, Chapman ER (2004) PIP2 increases the speed of response of synaptotagmin and steers its membrane-penetration activity toward the plasma membrane. Nat Struct Mol Biol 11:36-44.

Bezprozvanny I, Bezprozvannaya S, Ehrlich BE (1994) Caffeine-induced inhibition of Inositol(1,4,5)-Trisphosphate-gated Calcium Channels from Cerebellum. Molecular Biology of the Cell 5:97-103.

Biagi BA, Enyeart JJ (1990) Gadolinium blocks low- and high-threshold calcium currents in pituitary cells. American Journal of Physiology - Cell Physiology 259.

Billups B, Graham BP, Wong AYC, Forsythe ID (2005) Unmasking group III metabotropic glutamate autoreceptor function at excitatory synapses in the rat CNS. The Journal of Physiology 565:885-896.

Bollmann JH, Sakmann B, Borst JG (2000) Calcium sensitivity of glutamate release in a calyx-type terminal. Science 289:953-957.

Borst JG, Sakmann B (1996) Calcium influx and transmitter release in a fast CNS synapse. Nature 383:431-434.

Borst JG, Sakmann B (1999) Depletion of calcium in the synaptic cleft fo a calyx-type synapse in the rat brainstem. Journal of Physiology 521 Pt 1:123-133.

Breitwieser GE, Gama L (2001) Calcium-sensing receptor activation induces intracellular calcium oscillations. Am J Physiol Cell Physiol 280:C1412-1421.

Brown EM, MacLeod RJ (2001) Extracellular calcium sensing and extracellular calcium signaling. Physiological Reviews 81:239-297.

Brown EM, Gamba G, Riccardi D, Lombardi M, Butters R, Kifor O, Sun A, Hiediger MA, Lytton J, Hebert SC (1993) Cloning and characterization of an extracellular Ca(2+)-sensing receptor from bovine parathyroid. Nature 366:575-580.

Bucurenciu I, Bischofberger J, Jonas P (2010) A small number of open Ca2+ channels trigger transmitter release at a central GABAergic synapse. Nat Neurosci 13:19-21.
Bucurenciu I, Kulik A, Schwaller B, Frotscher M, Jonas P (2008) Nanodomain Coupling between Ca2+ Channels and Ca2+ Sensors Promotes Fast and Efficient Transmitter Release at a Cortical GABAergic Synapse. Neuron 57:536-545.
Carbone E, Lux HD, Carabelli V, Aicardi G, Zucker H (1997) Ca2+ and Na+ permeability of high-threshold Ca2+ channels and their voltage-dependent block by Mg2+ ions in chick sensory neurons. Journal of Physiology 504:1-15.
Carter A, Regehr W (2002) Quantal events shape cerebellar interneuron firing. Nature Neuroscience 5:1309-1318.
Chen W, Harnett MT, Smith SM (2007) Modulation of neuronal voltage-activated calcium and sodium channels by polyamines and pH. Channels 1:281-290.
Chen W, Bergsman JB, Wang X, Gilkey G, Pierpoint CR, Daniel EA, Awumey EM, Dauban P, Dodd RH, Ruat M, Smith SM (2010) Presynaptic external calcium signaling involves the calcium-sensing receptor in neocortical nerve terminals. PLoS One 5:e8563.
Chicka MC, Hui E, Liu H, Chapman ER (2008) Synaptotagmin arrests the SNARE complex before triggering fast, efficient membrane fusion in response to Ca2+. Nature Structural and Molecular Biology 15:827-835.
Chung C, Barylko B, Leitz J, Liu X, Kavalali ET (2010) Acute dynamin inhibition dissects synaptic vesicle recycling pathways that drive spontaneous and evoked neurotransmission. J Neurosci 30:1363-1376.
Cysneiros RM, Farkas D, Harmatz JS, von Moltke LL, Greenblatt DJ (2007) Pharmacokinetic and pharmacodynamic interactions between Zolpidem and caffeine. Nature Clinical Pharmacology and Therapeutics 82:54-62.
Daly JW, Butts-Lamb P, Padgett W (1983) Subclasses of adenosine receptors in the central nervous system: Interaction with caffeine and related methylxanthines. Cellular and Molecular Neurobiology 3:69-80.
David ME (2001) Cyclic nucleotide phosphodiesterases. The Journal of allergy and clinical immunology 108:671-680.
Del Castillo J, Katz B (1954) Quantal components of the end-plate potential. J Physiol 124:560-573.
Dodge FA, Rahamimoff R (1967) Co-operative action of calcium ions in transmitter release at the neuromuscular junction. Journal of Physiology 193:419-432.
Edwards RH (2007) The neurotransmitter cycle and quantal size. Neuron 55:835-858.
Ehrlich BE, Kaftan E, Bezprozvannaya S, Bezprozvanny I (1994) The pharmacology of intracellular Ca2+-release channels. Trends Pharmacological Sci 15.
Elmqvist D, Feldman DS (1965a) Spontaneous activity at a mammalian neuromuscular junction in tetrodotoxin. Acta Physiol Scand 64:475-476.
Elmqvist D, Feldman DS (1965b) Calcium dependence of spontaneous acetylcholine release at mammalian motor nerve terminals. J Physiol 181:487-497.
Emptage NJ, Reid CA, Fine A (2001) Calcium stores in hippocampal synaptic boutons mediate short-term plasticity, store-operated Ca2+ entry, and spontaneous transmitter release. Neuron 29:197-208.
Fatt P, Katz B (1950) Some observations on biological noise. Nature (London) 166:597-598.
Fatt P, Katz B (1952) Spontaneous subthreshold activity at motor nerve endings. Journal of Physiology 117:109-128.
Fontana G, Rogowski RS, Blaustein MP (1995) Kinetic properties of the sodium-calcium exchanger in rat brain synaptosomes. Journal of Physiology 485.2:349-364.

Fredj NB, Burrone J (2009) A resting pool of vesicles is responsible for spontaneous vesicle fusion at the synapse. Nature Neuroscience 12:751-759.
Friel DD, Chiel HJ (2008) Calcium dynamics: analyzing the Ca2+ regulatory network in intact cells. Trends in Neurosciences 31:8-19.
Geppert M, Goda Y, Hammer RE, Li C, Rosahl TW, Stevens CF, Sudhof TC (1994) Synaptotagmin I: A major Ca2+ sensor for transmitter release at a central synapse. Cell 79:717-727.
Groemer TW, Klingauf J (2007) Synaptic vesicles recycling spontaneously and during activity belong to the same vesicle pool. Nature Neuroscience 10:145-147.
Groffen AJ, Martens S, Arazola RD, Cornelisse LN, Lozovaya N, de Jong APH, Goriounova NA, Habets RLP, Takai Y, Borst JG, Brose N, McMahon HT, Verhage M (2010) Doc2b is a high-affinity Ca2+ sensor for spontaneous neurotransmitter release. Science 327:1614-1618.
Gundlfinger A, Bischofberger J, Johenning FW, Torvinen M, Schmitz D, Breustedt J (2007) Adenosine modulates transmission at the hippocampal mossy fibre synapse via direct inhibition of presynaptic calcium channels. Journal of Physiology 582:263-277.
Hille B (2001) Ion Channels of Excitable Membranes. Sunderland, MA: Sinauer Associates.
Hillyard DR, Monje VD, Mintz IM, Bean BP, Nadasdi L, Ramachandran J, Miljanich G, Azimi-Zoonooz A, McIntosh JM, Cruz LJ, Imperial JS, Olivera BM (1992) A new conus peptide ligand for mammalian presynaptic Ca2+ channels. Neuron 9:69-77.
Ho C, Conner DA, Pollak MR, Ladd DJ, Kifor O, Warren HB, Brown EM, Seidman JG, Seidman CE (1995) A mouse model o fhuman familial hypocalciuric hypercalcemia and neonatal severe hyperparathyroidism. Nature Genetics 11:389-395.
Horowitz LF, Hirdes W, Suh BC, Hilgemann DW, Mackie K, Hille B (2005) Phospholipase C in living cells: Activation, inhibition, Ca2+ requirement, and regulation of M current. The Journal of General Physiology 126:243-262.
Hosoi N, Holt M, Sakaba T (2009) Calcium dependence of exo- and endocytotic coupling at a glutamatergic synapse. Neuron 63:216-229.
Hubbard JI (1961) The effect of calcium and magnesium on the spontaneous release of transmitter from mammalian motor nerve endings. J Physiology 159:507-517.
Ikeda K, Yanagawa Y, Bekkers JM (2008) Distinctive Quantal Properties of Neurotransmission at Excitatory and Inhibitory Autapses Revealed Using Variance-Mean Analysis. J Neurosci 28:13563-13573.
Jones HC, Keep RF (1988) Brain fluid calcium concentration and response to acute hypercalcaemia during development in the rat. J Physiol 402:579-593.
Jun K, Piedras-Renteria ES, Smith SM, Wheeler DB, Lee SB, Lee TG, Chin H, Adams ME, Scheller RH, Tsien RW, Shin HS (1999) Ablation of P/Q-type Ca(2+) channel currents, altered synaptic transmission, and progressive ataxia in mice lacking the alpha(1A)-subunit. Proc Natl Acad Sci U S A 96:15245-15250.
Kapoor A, Satishchandra P, Ratnapriya R, Reddy R, Kadandale J, Shankar SK, Anand A (2008) An idiopathic epilepsy syndrome linked to 3q13.3-q21 and missense mutations in the extracellular calcium sensing receptor gene. Ann Neurol 64:158-167.
Katz B, Miledi R (1965) The effect of calcium on acetylcholine release from motor nerve terminals. Proc R Soc Lond B Biol Sci 161:496-503.
Kawata T, Imanishi Y, Kobayashi K, Keno T, Wada M, Ishimura E, Miki T, Nagano N, Inaba M, Arnold A, Nishizawa Y (2007) Relationship between parathyroid

calcium-sensing receptor expression and potency of the calcimimetic, cinacalcet, in suppressing parathyroid hormone secretion in an in vivo murine model of primary hyperparathyroidism. European Journal of Endocrinology 153:587-594.
Kessler A, Faure H, Petrel C, Ruat M, Dauban P, Dodd RH (2004) N(2)-benzyl-N-(1)-(1-(1-naphthyl)ethyl)-3-phenylpropane-1,2-diamines and conformationally restrained indole analogues: development of calindol as a new calcimimetic acting at the calcium sensing receptor. BioorgMed Chem Lett 14:3345-3349.
Khodakhah K, Ogden D (1993) Functional heterogeneity of calcium release by inositol triphosphate in single Purkinje neurones, cultured cerebellar astrocytes, and peripheral tissues. Proc Natl Acad Sci 90:4976-4980.
Kimura J, Watano T, Kawahara M, Sakai E, Yatabe J (1999) Direction-independent block of bi-directional Na+/Ca2+ exchange current by KB-R7943 in guinea-pig cardiac myocytes. British Journal of Pharmacology 128:969-974.
Kullmann DM, Min MY, Asztely F, Rusakov DA (1999) Extracellular glutamate diffusion determines the occupancy of glutamate receptors at CA1 synapses in the hippocampus. Pholosphical Transactions of the Royal Society London B Biological Sciences 354:395-402.
Liu J, Sun Y, Drubin DG, Oster GF (2009) The Mechanochemistry of Endocytosis. PloS Biology 7:e1000204.
Liu X, Smith BJ, Chen C, Callegari E, Becker SL, Chen X, Cianfrogna J, Doran AC, Doran SD, Gibbs JP, Hosea N, Liu J, Nelson FR, Szewc MA, Van Deusen J (2006) Evaluation of cerebrospinal fluid concentration and plasma free concentration as a surrogate measurement for brain free concentration. Drug Metabolism and Disposition 34:1443-1447.
Llano I, Gonzalez J, Caputo C, Lai FA, Blayney LM, Tan YP, Marty A (2000) Presynaptic calcium stores underlie large-amplitude miniature IPSCs and spontaneous calcium transients. Nature Neuroscience 3:1256-1265.
Llinas R, Steinberg IZ, Walton K (1976) Presynaptic calcium currents and their relation to synaptic transmission: Voltage clamp study in squid giant synapse and theoretical model for the calcium gate. Proceedings of the National Academy of Sciences of the United States of America 73:2918-2922.
Lou X, Scheuss V, Schneggenburger R (2005) Allosteric modulation of the presynaptic Ca2+ sensor for vesicle fusion. Nature 435:497-501.
Lou X, Korogod N, Brose N, Schneggenburger R (2008) Phorbol esters modulate spontaneous and Ca2+-evoked transmitter release via acting on both Munc13 and protein kinase C. The Journal of Neuroscience 28:8257-8267.
Lukacs V, Thyagarajan B, Varnai P, Balla A, Balla T, Rohacs T (2007) Dual regulation of TRPV1 by phosphoinositides. The Journal of Neuroscience 27:7070-7080.
Martin ED, Buno W (2003) Caffeine-mediated presynaptic long-term potentiation in hippocampal CA1 pyramidal neurons. Journal of Neurophysiology 89:3029-3038.
Masuko T, Kusama-Eguchi K, Sakata K, Kusama T, Chaki S, Okuyama S, Williams K, Kashiwagi K, Igarashi K (2003) Polyamine transport, accumulation, and release in brain. Journal of Neurochemistry 84:610-617.
McKinney RA, Capogna M, Durr R, Gahwiler BH, Thompson SM (1999) Miniature synaptic events maintain dendritic spines via AMPA receptor activation. Nature Neuroscience 2:44-49.
Meinrenken CJ, Borst JG, Sakmann B (2003) Local routes revisited: the space and time dependence of the Ca2+ signal for phasic transmitter release at the rat calyx of Held. J Physiol 547:665-689.

Meyer DA, Carta M, Partridge LD, Covey DF, Valenzuela CF (2002) Neurosteroids enhance spontaneous glutamate release in hippocampal neurons. Journal of Biological Chemistry 277:28725-28732.
Morton-Jones RT, Cannell MB, Housley GD (2007) Ca2+ entry via AMPA-type glutamate receptors triggers Ca2+-induced Ca2+ release from ryanodine receptors in rat spiral ganglion neurons. Cell Calcium 43:356-366.
Mrvos RM, Reilly PE, Dean BS, Krenzelok EP (1989) Massive caffeine ingestion resulting in death. Vet Hum Toxicol 6:571-572.
Nachshen DA, Sanchez-Armass S, Weinstein AM (1986) The regulation of cytosolic calcium in rat brain synaptosomes by sodium-dependent calcium efflux. Journal of Physiology 381:17-28.
Naraghi M, Neher E (1997) Linearized Buffered Ca2+ Diffusion in Microdomains and Its Implications for Calculation of [Ca2+] at the Mouth of a Calcium Channel. J Neurosci 17:6961-6973.
Neher E, Sakaba T (2008) Multiple roles of calcium ions in the regulation of neurotransmitter release. Neuron 59:861-872.
Nemeth EF, Heaton WH, Miller M, Fox J, Balandrin MF, Van Wagenen BC, Colloton M, Karbon W, Scherrer J, Shatzen E, Rishton G, Scully S, Qi M, Harris R, Lacey D, Martin D (2004) Pharmacodynamics fo the type II calcimimetic compound cinacalcet HCl. The Journal of Pharmacology and Experimental Therapeutics 308:627-635.
Nicholson C, Bruggencate G, Stockle H, Steinberg R (1978) Calcium and potassium changes in extracellular microenvironment of cat cerebellar cortex. Journal of Neurophysiology 41:1026-1039.
Nilsson P, Laursen H, Hillered L, Hansen AJ (1996) Calcium movements in traumatic brain injury: the role of glutamate receptor-operated ion channels. Journal of Cerebral Blood Flow and Metabolism 16:262-270.
O'Brien RJ, Kamboj S, Ehlers MD, Rosen KR, Fischbach GD, Huganir RL (1998) Activity-dependent modulation of synaptic AMPA receptor accumulation. Neuron 21:1067-1078.
Oda Y, Tu CL, Pillai S, Bikle DD (1998) The calcium sensing receptor and its alternatively spliced form in keratinocyte differentiation. The Journal of Biological Chemistry 273:23344-23352.
Ouanounou A, Zhang L, Charlton MP, Carlen PL (1999) Differential modulation of synaptic transmission by calcium chelators in young and aged hippocampal CA1 neurons: evidence for altered calcium homeostasis in aging. The Journal of Neuroscience 19:906-915.
Ouanounou A, Zhang L, Tymianski M, Charlton MP, Wallace MC, Carlen PL (1996) Accumulation and extrusion of permeant Ca2+ chelators in attenuatino of synaptic transmission at hippocampal CA1 neurons. Neuroscience 75:99-109.
Pearce SH, Williamson C, Kifor O, Bai M, Coulthard MG, Davies M, Lewis-Barned N, McCredie E, Powell H, Kendall-Taylor P, Brown EM, Thakker RV (1996) A familial syndrome of hypocalcemia with hypercalciuria due to mutations in the calcium-sensing receptor. N Engl J Med 335:1115-1122.
Peters JH, McDougall SJ, Fawley JA, Smith SM, Andresen MC (2010) Primary afferent activation of thermosensitive TRPV1 triggers asynchronous glutamate release at central neurons. Neuron 65:657-669.
Pethig R, Kuhn M, Payne R, Alder E, Chen TH, Jaffe LF (1989) On the dissociation constants of BAPTA-type calcium buffers. Cell Calcium 10:491-498.
Phillips CG, Harnett MT, Chen W, Smith SM (2008) Calcium-sensing receptor activation depresses synaptic transmission. The Journal of Neuroscience 28:12062-12070.

Pi M, Faber P, Ekema G, Jackson PD, Ting A, Wang N, Fonilla-Poole M, Mays RW, Bruden KR, Harrington JJ, Quarles LD (2005) Identification of a novel extracellular cation-sensing G-protein-coupled receptor. Journal of Biological Chemistry 280:40201-40209.

Reid CA, Bekkers JM, Clements JD (1998) N- and P/Q-type Ca2+ channels mediate transmitter release with a similar cooperativity at rat hippocampal autapses. The Journal of Neuroscience 18:2849-2855.

Rhee JS, Betz A, Pyott S, Reim K, Varoqueaux F, Augustin I, Hesse D, Sudhof TC, Takahashi M, Rosenmund C, Brose N (2002) Beta phorbol ester- and diacylglycerol-induced augmentation of transmitter release is mediated by Munc13s and not by PKCs. Cell 108:121-133.

Rhee SG (2001) Regulation of phosphoinositide-specific phospholipase C. Annual Reviews Biochemistry 70:281-312.

Rosenmund C, Stevens CF (1996) Definition of the readily releasable pool of vesicles at hippocampal synapses. Neuron 16:1197-1207.

Rousseau E, LaDine J, Liu Q, Meissner G (1988) Activation of the Ca2+ release channel of skeletal muscle sarcoplasmic reticulum by caffeine and related compounds. Archives of Biochemistry and Biophysics 267:75-86.

Rozov A, Burnashev N, Sakmann B, Neher E (2001) Transmitter release modulation by intracellular Ca2+ buffers in facilitating and depressing nerve terminals of pyramidal cells in layer 2/3 of the rat neocortex indicates a target cell-specific difference in presynaptic calcium dynamics. Journal of Physiology 531.3:807-826.

Ruat M, Molliver ME, Snowman AM, Snyder SH (1995) Calcium sensing receptor: molecular cloning in rat and localization to nerve terminals. Proc Natl Acad Sci USA 92:3161-3165.

Rusakov DA, Fine A (2003) Extracellular Ca2+ depletion contributes to fast activity-dependent modulation of synaptic transmission in the brain. Neuron 37:287-297.

Sanchez-Armass S, Blaustein MP (1987) Role of sodium-calcium exchange in regulation of intracellular calcium in nerve terminals. American J Physiology Cell Physiology 252:595-603.

Sara Y, Virmani T, Deak F, Liu X, Kavalali ET (2005) An isolated pool of vesicles recycles at rest and drives spontaneous neurotransmission. Neuron 45:563-573.

Schipke CG, Ohlemeyer C, Matyash M, Nolte C, Kettenmann H, Kirchhoff F (2001) Astrocytes of the mouse neocortex express functional N-methyl-D-aspartate receptors. FASEB J:00-0439fje.

Schneggenburger R, Neher E (2000) Intracellular calcium dependence of transmitter release rates at a fast central synapse. Nature 406:889-893.

Shahrezaei V, Cao A, Delaney KR (2006) Ca2+ from one or two channels controls fusion of a single vesicle at the frog neuromuscular junction. J Neurosci 26:13240-13249.

Sharma G, Vijayaraghavan S (2003) Modulation of presynaptic store calcium induces release of glutamate and postsynaptic firing. Neuron 38:929-939.

Simkus CRL, Stricker C (2002) The contribution of intracellular calcium stores to mEPSCs recorded in layer II neurones of rat barrel cortex. Journal of Physiology 545:521-535.

Smith RJ, Sam LM, Justen JM, Bundy GL, Bala GA, Bleasdale JE (1990) Receptor-coupled signal transduction in human polymorphonuclear neutrophils: effects of a novel inhibitor of phospholipase C-dependent processes on cell responsiveness. Journal of Pharmacology Experimental Therapeautics 253:688-697.

Smith SJ (1992) Do astrocytes process neural information? Progress in Brain Research 94:119-136.
Smith SM, Renden R, von Gersdorff H (2008) Synaptic vesicle endocytosis: fast and slow modes of membrane retrieval. Trends Neurosci 31:559-568.
Smith SM, Bergsman JB, Harata NC, Scheller RH, Tsien RW (2004) Recordings from single neocortical nerve terminals reveal a nonselective cation channel activated by decreases in extracellular calcium. Neuron 41:243-256.
Stanley EF (1993) Single calcium channels and acetylcholine release at a presynaptic nerve terminal. Neuron 11:1007-1011.
Stevens CF, Wang Y (1995) Facilitation and depression at single central synapses. Neuron 14.
Stevens CF, Sullivan JM (1998) Regulation of the readily releasable vesicle pool by protein kinase C. Neuron 21:885-893.
Suh BC, Inoue T, Meyer T, Hille B (2006) Rapid chemically induced changes of PtdIns(4,5)P2 gated KCNQ ion channels. Science 314:1454-1457.
Sun J, Pang ZP, Qin D, Fahim AT, Adachi R, Sudhof TC (2007) A dual-Ca2+-sensor model for neurotransmitter release in a central synapse. Nature 450:676-682.
Sutton MA, Wall RN, Aakalu GN, Schuman EM (2004) Regulation of dendritic protein synthesis by miniature synaptic events. Science 304:1979-1983.
Swanson GT, Kamboj SK, Cull-Candy SG (1997) Single-channel properties of recombinant AMPA receptors depend on RNA editing, splice variation, and subunit composition. J Neurosci 17:58-69.
Tabata T, Kano K (2004) Calcium dependence of native metabotropic glutamate receptor signaling in central neurons. Molecular Neurobiology 29:261-270.
Takahashi A, Camacho P, Lechleiter JD, Herman B (1999) Measurement of intracellular calcium. Physiological Reviews 79:1089-1125.
Thiagarajan TC, Lindskog M, Tsien RW (2005) Adaptation to synaptic inactivity in hippocampal neurons. Neuron 47:725-737.
Traynelis SF (1998) Software-based correction of single compartment series resistance errors. Journal of Neuroscience Methods 86:25-34.
Virmani T, Ertunc M, Sara Y, Mozhayeva M, Kavalali ET (2005) Phorbol esters target the activity-dependent recycling pool and spare spontaneous vesicle recycling. J Neurosci 25:10922-10929.
Vizard TN, O'Keeffe GW, Guitierrez H, Kos CH, Riccardi D, Davies AM (2008) Regulation of axonal and dendritic growth by the extracellular calcium-sensing receptor. Nature Neuroscience 11:285-291.
Vyleta NP, Smith SM (2008) Fast inhibition of glutamate-activated currents by caffeine. PLoS ONE 3:e3155.
Wang M, Bianchi R, Chuang S-C, Zhao W, Wong RKS (2006) Group I metabotropic glutamate receptor-dependent TRPC channel trafficking in hippocampal neurons. Journal of Neurochemistry 101:411-421.
Wang X, Lundblad J, Smith SM (2009) Familial hypocalciuric hypercalcemia: reduced affinity of calcium sensing-receptor heterodimers underlies impaired receptor function. In: FEPS 2009, p P189. Ljubljana, Slovenia.
Wang Y, Awumey EK, Chatterjee PK, Somasundaram C, Bian K, Rogers KV, Dunn C, Bukoski RD (2003) Molecular cloning and characterization of a rat sensory nerve Ca2+-sensing receptor. American J Physiology Cell Physiology 285:C64-C75.
Watano T, Kimura J, Morita T, Nakanishi H (1996) A novel antagonist, No. 7943, of the Na+/Ca2+ exchange current in guinea-pig cardiac ventricular cells. British Journal of Pharmacology 119:555-563.

Weirda KDB, Toonen RFG, de Wit H, Brussaard AB, Verhage M (2007) Interdependence of PKC-dependent and PKC-independent pathways for presynaptic plasticity. Neuron 54:275-290.
Wellendorph P, Brauner-Osborne H (2004) Molecular cloning, expression, and sequence analysis of GPRC6A, a novel family C G-protein-coupled receptor. Gene 335:37-46.
Wheeler DB, Randall A, Tsien RW (1994) Roles of N-type and Q-type Ca2+ channels in supporting hippocampal synaptic transmission. Science 264:107-111.
Wu X, Xue L, Mohan R, Paradiso K, Gillis K, Wu L (2007) The origin of quantal size variation: vesicular glutamate concentration plays a significant role. The Journal of Neuroscience 27:3046-3056.
Xu J, Pang ZP, Shin OH, Sudhof TC (2009a) Synaptotagmin-1 functions as a Ca2+ sensor for spontaneous release. Nat Neurosci 12:759-766.
Xu J, Pang ZP, Shin OH, Sudhof TC (2009b) Synaptitagmin-1 functions as a Ca2+ sensor for spontaneous release. Nature Neuroscience 12:759-766.
Yamasaki M, Hashimoto K, Kano M (2006) Miniature synaptic events elicited by presynaptic Ca2+ rise are selectively suppressed by cannabinoid receptor activation in cerebellar Purkinje cells. The Journal of Neuroscience 26:86-95.
Yu Y, Maureira C, Liu X, McCormick D (2010) P/Q and N channels control baseline and spike-triggered calcium levels in neocortical axons and synaptic boutons. The Journal of Neuroscience 30:11858-11869.